PV in the built environment: Module Level Power Management

Final Project Report 2015

Abstract: We are standing at the brink of a huge expansion of installed PV capacity in The Netherlands and worldwide. Most of this newly installed capacity will be realized in the built environment. One of the issues to be dealt with in this respect is the issue of heterogeneous systems. Heterogeneous PV systems are PV systems in which modules differ in performance due to different orientation (for instance East-West systems), different grades of pollution (for instance due to birds' nests) or different shading patterns (very common in the built environment).In this project we bring together Dutch power electronic companies and develop two distinct approaches that may result in more kWh yield of heterogeneous PV systems. One of these approaches is based on module level dc-dc conversion, the other on a micro-inverter. The project will develop the two approaches up to the level of functional prototypes with proven lifetime performance and efficiency. Furthermore the project involves the set-up and execution of a field test with extensive monitoring of the performance of the MLPM systems.

3/31/2016

TKI: Z01005

Project Start: July 2012

Project End: December 2015

Authors and project participants:

Solar Energy Application Centre (ECN Eindhoven): Kostas Sinapis (PM), Menno van den Donker, Wiep Folkerts, Chris Tzikas, Geert Litjens, Tom Rooijackers, Guus Verberne

Energy research Centre of the Netherlands (ECN Petten): Nico Dekker, Mark Janssen

TNO: Dorrit Roosen-Melsen, Henk Hakkesteegt

Hogeschool van Amsterdam: Laura Ramirez Elizondo, Wilbert te Velde, Cruz Barco

Femtogrid: Rob Schaacke

Heliox: Rudi Jonkman, Robert van der Sanden

Mastervolt: Anro van Zwam

Solned: Rudy van der Ven, Marianne van der Ven

Contents

Chapter 1: Introduction to MLPE

Conventional photovoltaic systems are designed for application in ideal circumstances. “Ideal” means that all panels are of the same type and have the same orientation and are not partially shaded by objects in the surroundings.

Typically such a PV system consists of solar modules connected in series and a power inverter which converts DC current to usable AC as shown in figure 1. This installation design is complex and requires special personnel due to lethal DC voltages.

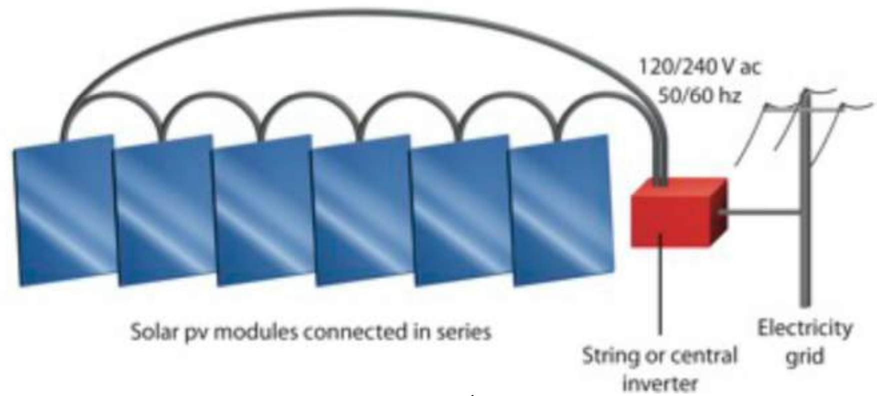

Figure 1.1: Standard PV system configuration[1]

Main disadvantages of the standard system design are:

- Mismatch losses. One of the basic principles of electrical engineering is that in a series connection only one current can flow. This basic principle imposes that in case a solar module performs worse than the rest of the modules, it will reduce the performance of the whole chain reducing the total energy yield. Due to the fact that the current produced in a PV module is proportional to the irradiation, an important problem occurs. Heterogeneous environmental conditions such as shadowing from horizon, obstacles casting shadows at the installation location, dirt or dust accumulating with time unevenly and manufacturing tolerance of power output can significantly reduce energy yield.

- Installation of the PV modules must be performed in the same orientation and inclination angle to assure as much as possible the same irradiation level of the PV modules. Additionally PV modules must be of the same power class and technology.

- The central inverter used in a conventional PV system is a single point of failure. In case the inverter fails the whole system shuts down.
- Monitoring capabilities with conventional PV systems are limited and restricted to string voltage and current, making it difficult to identify faulty PV modules especially in large PV systems

- Safety issues have arisen in recent years because of the penetration of PV systems in the residential sector. Fires have been recorded which probably occurred from high DC voltage sparks.

Several approaches have been proposed to mitigate these disadvantages and to optimize the output of PV systems in non-ideal circumstances. A common feature of these approaches is that power optimization is brought down to the module level. In general we call these approaches Module Level Power Management (MLPM).

We distinguish two different architectures of MLPM:

[1] http://www.enecsys.com/technology/index.php

- Power-Optimizers (DC/DC boost, buck, buck-boost)
- Micro-inverters (DC/AC)

Power optimizers are de-centralized DC/DC converters. They are typically installed to each PV module by the PV system installer. Alternatively, they can be embedded in the junction box by module manufacturers. They are designed to individually tune the Maximum Power Point Tracking (mppt) of a PV module and additionally adjust the output to match the “fixed” voltage of a string inverter.

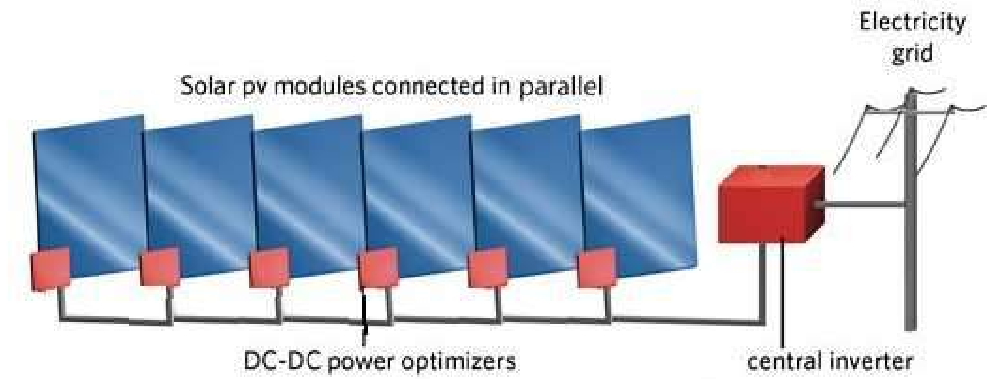

Figure 1.2: PV system configuration with power optimizers in parallel (boost)[2]

Power optimizers come in two configurations. The parallel arrangement is chosen in the solution from the company Femtogrid. The in series configuration by market leader SolarEdge.

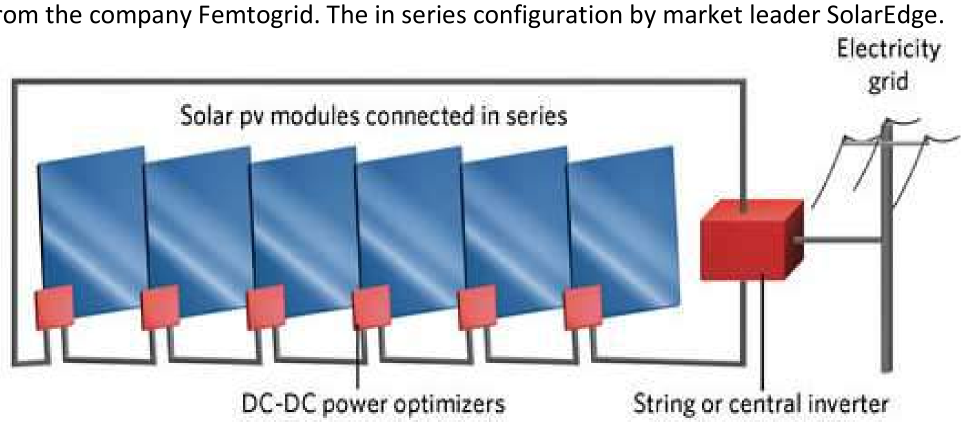

Figure 1.3: PV system configuration with power optimizers in series (buck and buck-boost)[3]

Micro-inverters are de-centralized power electronic converters installed to each or every other PV module. A micro-inverter essentially combines a power optimizer with a small inverter. Every micro-inverter contains a DC/DC and a DC/AC converter.

MLPM elements are a natural evolution in system design and architecture. They offer flexibility in design since now all inclination angles and orientations are suitable and not affecting each other. Different module classes and types can be connected in the same system for example upgrading of an existing system by adding more modules even if the power class of the existing modules has been discontinued. Installation is now easy and standardized because every MLPM device comes with its own wiring.

[2] http://www.enecsys.com/technology/index.php
[3] http://www.enecsys.com/technology/index.php

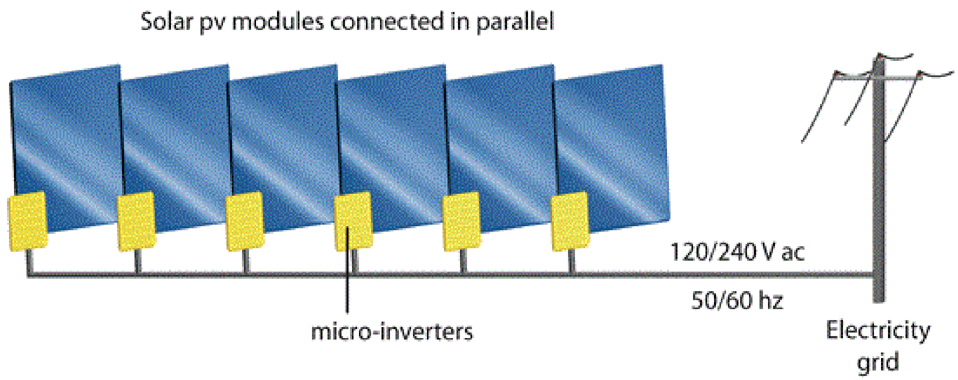

Figure 1.4: PV system configuration with micro-inverters

Additionally hazardous risks are being minimized due to the safety features introduced in MLPM. Spark detectors (mainly for DC/DC power optimizers) and DC shut down mechanisms from the module reduce accident rates of the lethal DC voltages. This feature of the MLPM devices adds value in terms of safety for the home owners-workers-firefighters. Another feature added with MLPM units is the wide monitoring capabilities. Until now monitoring was only possible at string level. Now power output of individual modules can be monitored and assessed. Faulty modules and components can be easily identified and corrected accordingly. This feature reduces the down time of the PV system and thus improves the annual energy yield. Figure 4 shows an example of PV monitoring on the panel side.

Figure 1.5: Screenshot from the enlighten software offered with Enphase micro-inverters

String and central inverters are devices serving the solar PV industry for 3 decades. They have evolved in terms of performance, functionality and reliability. They represent the traditional PV system architecture and they have a big variety of applications and input ranges. Performance and quality of inverters especially from experienced manufacturers has been improved, however there are still remaining problems[4]. Improvement has been done also in the mppt section of the string and central inverters. New algorithms that work faster and more reliable have been introduced by many inverter manufactures[5]. Moreover, traditional inverters have high efficiencies up to 98% making them ideal for large ground mounted applications.

Three-phase string inverters for large ground mounted and roof commercial installations entered the market during 2010. These inverters help to maintain stability of the grid voltage and frequency because they are designed to meet the new “reactive power” and “Medium Voltage Directive”

[4] Evolution of inverters for Grid connected PV systems from 1989 to 2000, H. Haeberlin

[5] OptiTrac Global Peak SMA- www.sma.de

legislations that are introduced in Germany. Additionally utility providers request residential PV installations to have three phase grid feeding to prevent grid imbalances.[6]

Not only the architecture but also the main components of the traditional inverters are changing. Silicon-Carbide diodes are a promising solution to reduce size and cost of the expensive magnetic materials such as copper[7]. Additionally inverters with Si-C diodes have a higher current density making them ideal for high voltage operation thus reducing the BOS. Additionally GaN based power devices represent an excellent choice for improved device performance. GaN power devices reduce losses in all stages of power conversions. The first commercial 600V GaN devices have already been released to the market[8].

As inverter suppliers are under huge pressure to reduce costs there are some interesting examples on how the inverter manufacturers can save overall system costs with new developments:

- Increasing input voltage (Vdc): Longer strings can lead to less BOS costs like cables, fuses, switches etc
- Outdoor rated inverters: Manufacturers are increasing the supply of outdoor rated inverter which they don't need separate housing and thus save infrastructure costs
- Weight reduction: Work hours can be saved by lighter equipment. Installation and replacement are now easier without bulky inverters
- Using small string inverters rather than large central inverter: By offering more Mppt trackers and small three phase inverters, suppliers are targeting in reduction of lifetime system costs by increasing yield and downtime

It is interesting to mention the improvements that are needed from the power optimizer and the micro-inverter devices in order for the devices to penetrate the market faster.

Power Optimizer:

- PV modules are designed to withstand harsh environmental condition for at least 25 years. Specific standards for testing reliability have been successfully implemented the past years. Like in every electronic device reliability starts at the design phase of the product. The selection of components is the other critical factor. The most frequently identified failure mechanism in power optimizers is the capacitor bank. For this reason many manufacturers disqualify electrolytic capacitors which are affected by high temperatures. Alternatives are thin film capacitors or Multilayer ceramic capacitors.
- The use of Application Specific Integrated Circuits (ASIC) helps to improve reliability as well, because the required number of components can be reduced.
- Power-optimizers must have a small and flexible size. Junction box embedded power optimizers have been developed in cooperation with module producers and are already in the market today.
- Another important success factor is the cost per watt. Because of the usage of the string inverter (even the simplified version of it without mppt), power optimizers will always add extra costs to the PV system. A more easy system design and more straightforward installation process partly compensates the cost of the power optimizer.
- Adaptation of power optimizers is popular in Europe. Probably this is based on the fact that power optimizers are still using a string inverter which is the common practice at the

[6] The World Market for PV Micro-inverters and Power Optimizers 2012 IMS research
[7] Si-c make solar power systems more efficient, Michael Oneil, Cree Inc
[8] Latest in PV Inverter & Trends , Baumgartner- Vezzini

traditional European PV systems. The fact that power optimizers can be utilized at problematic modules only increases the penetration and adaptation of power optimizers.

Micro-inverter:

- The inverter in a PV system has been identified as the dominant failure mechanism. Usually inverters have to be replaced at least once during the lifetime of a PV system. Because of their mounting nature, micro-inverters need to be able to withstand harsh environmental conditions and deliver at least 25 years of fault free operation. The dominant wear-out failure mode is the electrolytic capacitor. This single component can reduce the lifetime and Mean Time Between Failures (MTBF) of the device. New capacitors which can withstand higher temperatures must be used for the micro-inverter industry. Companies already are using thin film capacitors which are known to be temperature tolerant.
- Efficiency of the micro-inverters is still lacking behind the string inverters which can reach up to 98%. The fact that string inverters are using transformer-less topologies boosts their efficiency and simplicity.
- Size of the micro-inverters must also be reduced in order to fit at the junction box without temperature problems. Micro-inverters that are small and reliable enough can be embedded in the junction box of the PV module. Modules with their micro-inverter embedded are commonly referred to as “AC modules”. There are many development efforts towards these AC modules going on worldwide, but still there is no reliable solution.
- The cost of the micro-inverters is still high and the general approach of the industry is to add a premium price on top of the reference string inverter. In this way the micro-inverter will always be more expensive than the string inverter.
- Due to the fact that PV is becoming a significant percentage of some countries’ energy mix, grid stability and requirements change. For example in Germany the Low Voltage Directive introduced recently commands reactive power feeding requirements from the solar inverters. At this moment there is no micro-inverter with tunable power factor and thus installation of these devices is blocked in the German market for the moment.

In general the use of MLPM devices is based on a “spend more, get more“ philosophy which makes them ideal for problematic installation but not yet ideal for big roof commercial and ground mounted PV power plants. Simplified devices with low cost and high reliability will be the key developments that both the approaches must adopt. MLPM devices have started very dynamically and are claiming a part of the inverter market. Additional developments have to be made to increase penetration in market segments that are still dominated by more traditional solutions.

Chapter 2: Industrial Development and Benchmarking

2.1 Benchmark Report MLPE

The PV market is highly associated with governmental subsidies and incentives. Currently the attractiveness of PV systems is determined by 4 major factors:

- Cost of PV equipment
- Governmental incentives
- Retail electricity price of the country
- Irradiation levels

Volumes and capacities are growing going hand in hand with remarkable price reductions worldwide. Subsidies are still leading the PV market even now that grid parity can be reached in many countries. 2011 was a mixed year for the inverter industry. Even if shipments grew by a third the revenues stayed on the levels of 2010[9]. 2012 was a year that started with a rush in many traditional markets because of the annually FIT reductions scheduled and the total shipments slightly rise from 2011 to 2012. 2013 was a harsh year for the industry having severe impacts in module and inverters shipments. In figure 6 the GWp of shipments in EMEA region can be seen.

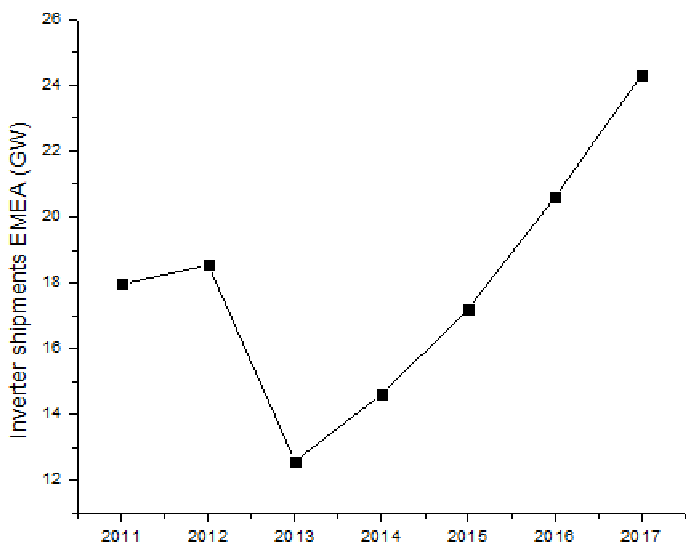

Figure 2.1: Historical and predicted inverter shipments in EMEA region [10]

Regional demand in inverters has also shifted. In the first half of 2013 EMEA accounted for nearly the half of inverter demands driven by large inverter markets like Germany. In the second half demand fell rapidly due to the EU anti-dumping tariffs. The demand for inverters shifted to Asia for the second half of 2013 which means that inverter suppliers have to align their operations and businesses to capitalize from demand because there could be big impact on lead times if there is not a local presence in the countries where demand forecast is high.

It is estimated that the inverter accounts for up to 15% of the total PV installation cost and it is considered the second most expensive component of a PV system after the solar modules. However the inverter cost as a percentage of the total PV system cost is projected to increase. In an effort to follow the cost reduction of PV systems, many major inverter suppliers announced price discounts.

---

[9] iSuppli Topical Report : PV Microinverters and Optimizers: Can Moore's Law be Disruptive Again?
[10] The World market for micro-inverters and power optimizers, 2013 edition IHS

Chinese suppliers continue to price competitively. For high power inverters bigger than 250kW western pricing was 43% higher than Chinese while lower power inverters are still cheaper by 40%. Chinese suppliers mostly ship their products in the local market which is rising. Huawei is developing low power inverters (<35kW) which could result in even cheaper inverter prices.
Many agree that price reductions must come in-line with the FIT reductions which in some countries are very high. In figure 6 the average €/Wp can be seen.

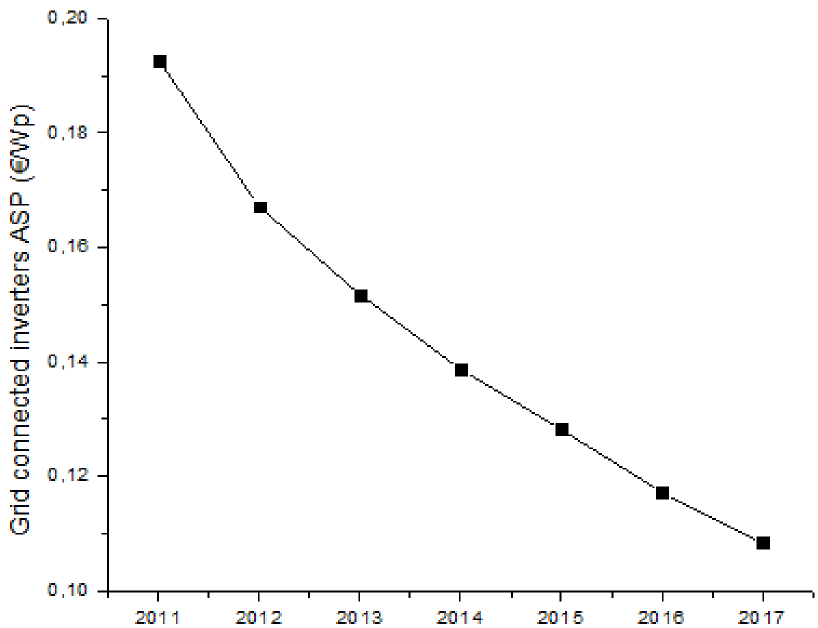

Figure 2.2: Predicted factory-gate selling prices of inverters[11]

Another major change in the inverter industry is the new Low Voltage legislation recently introduced in Germany[12] (VDE-AR-N 4105). More than 80% of the installations in Germany are connected to the Low Voltage grid. With the penetration of PV in the energy mix, stability of the grid has become an important issue. In order to be able to provide reliability of the grid in the long term, inverters must execute functions contributing to ensuring grid stability in the future. The directive introduced in Germany will soon be adopted by other countries with increased solar activity to ensure grid stability. In figure 8 the predicted change of traditional inverters to new "smart" inverters in EMEA region can be seen. The graph represents the change in inverter functionality for all the markets of EMEA excluding Germany because of the already existing law which forbids interconnection of inverters without reactive power management in the Low Voltage grid.

[11] The World market for micro-inverters and power optimizers, 2012 edition IMS
[12] http://www.vde.com/de/fnn/arbeitsgebiete/seiten/n4105.aspx

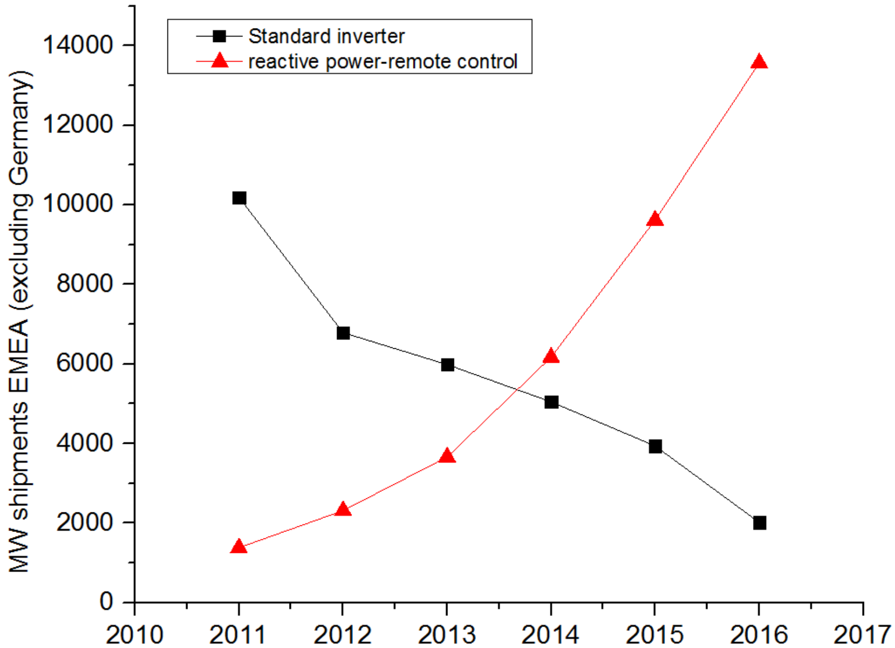

Figure 2.3: Predicted inverter shipments by type in EMEA region excluding Germany[13]

The evolution of PV architecture with the introduction of MLPM devices will play an important role for the development of traditional inverters. The fact that MLPM technologies can work together with a traditional inverter, simplified inverter or even eliminate the need for a central inverter may and will change the inverter market. For this to happen a higher penetration rate in the traditional markets has to be achieved.

Possible target markets for micro-inverters and power optimizers are residential and small commercial installations. The fact that small installations have usually more expensive inverters per Wp will lead to an easier closing of the price gap between string and micro-inverters. Additionally small installations are the ones affected by shadowing and thus MLPM solutions can increase yield by using panel-level mppt. Power optimizers will probably have a higher penetration than micro-inverters because of the similar topology with the traditional systems and the fact that power optimizers can be equipped at panels who are under shady conditions than in the whole array.

The MLPM market is projected to grow even during 2012-2013 which are considered two of the “black years” of the PV industry. Shipments are expected to rise significantly after 2013 and peaking at 2016 at an astonishing 7GW and 1.2B€. revenues[14]. In figure 9 the historical and shipment forecast can be seen for power optimizers. In figure 10 the historical and forecast shipments for micro-inverters can be seen.

[13,15] The World market for micro-inverters and power optimizers, 2012-2103 edition IMS/IHS

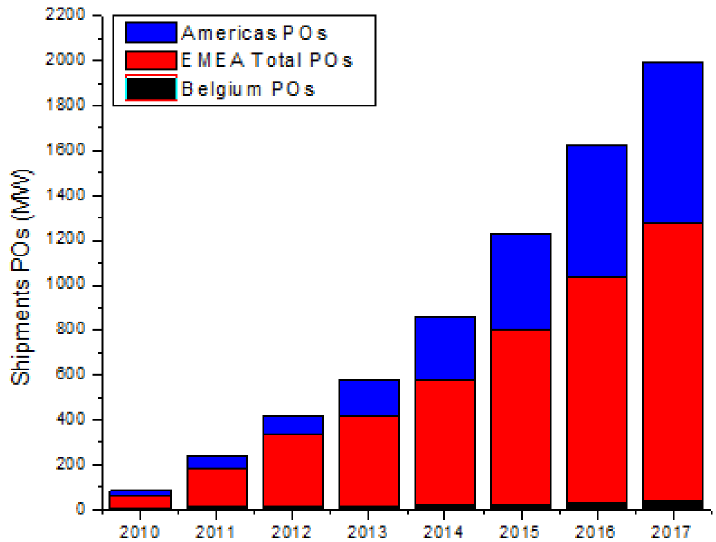

Figure 2.4: PO shipment forecast[15]

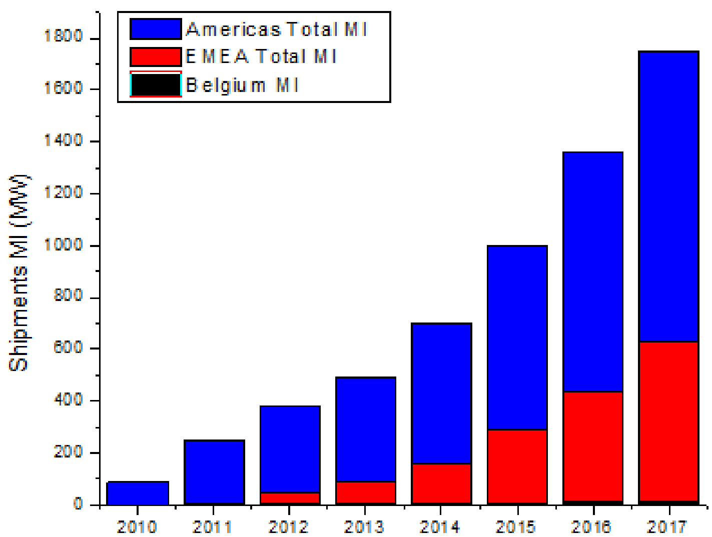

Figure 2.5: MI shipment forecast[16]

[15,17] The World market for micro-inverters and power optimizers, 2013 edition IHS

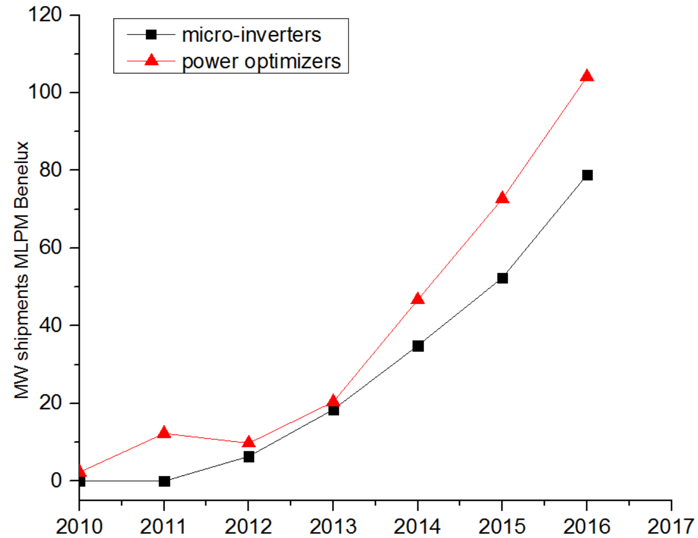

Figure 2.6: MLPM shipment forecast in Benelux[17]

Penetration in traditional markets is never easy. MLPLM solutions must overcome two major obstacles, reliability and pricing. Even if they are still in an infancy stage, there is high acceptance especially from residential markets. It is very interesting to notice in figure 11 that the average penetration rate in EMEA on 2016 for micro-inverters and power optimizers is 3.5 % and 9 % respectively while in Benelux region there is a remarkable 10 % and 14%.

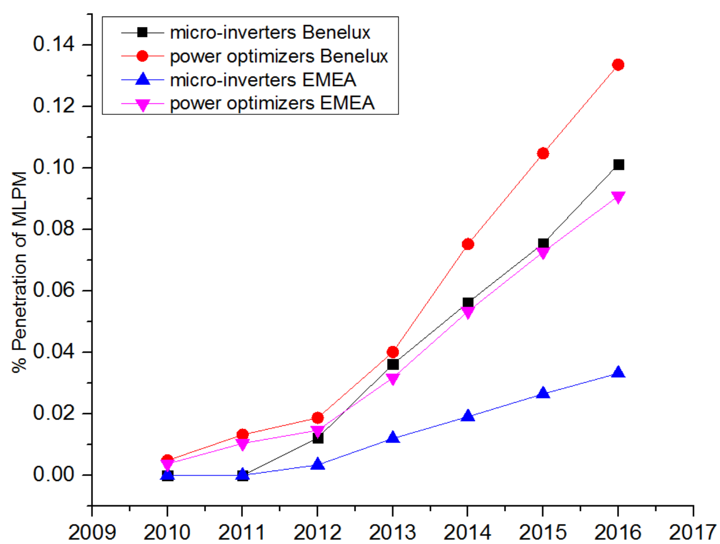

Figure 2.7: Penetration rate forecast of MLPM solutions in EMEA and Benelux[18]

Most micro-inverter and power optimizer suppliers are currently highly focused on developing strategic partnerships with module manufacturers. For example Enphase started a partnership with Centrosolar while Solaredge and Tigo are both moving towards this trajectory with Renesola, Upsolar and Trina Solar. The main benefit of this route to market is that the micro-inverter and power

[17] The World market for micro-inverters and power optimizers, 2012 edition IMS

optimizer suppliers can take advantage of the module manufacturer existing sales channels and open up new opportunities in new markets.

Finally in figure 12,13 the price per watt forecasts can be seen. It can be observed that the 2017 prices for power optimizers and micro-inverters are 0.08€ / Watt and 0.25€ / Watt respectively. Note that the power optimizer prices do not include the string inverter. In general MLPM solutions are priced with a premium on top of the reference inverter brands. The current price for a string inverter in the Benelux is in the order of 15-16 € cents while a micro-inverter solution will cost almost double. Further price reductions have to be achieved for a wider penetration of MLPM devices.

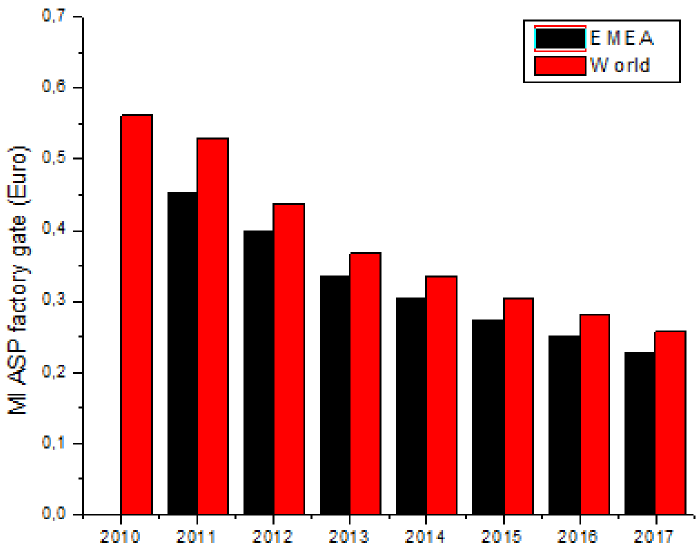

Figure 2.8: Factory gate price per watt forecasts for micro-inverters[19]

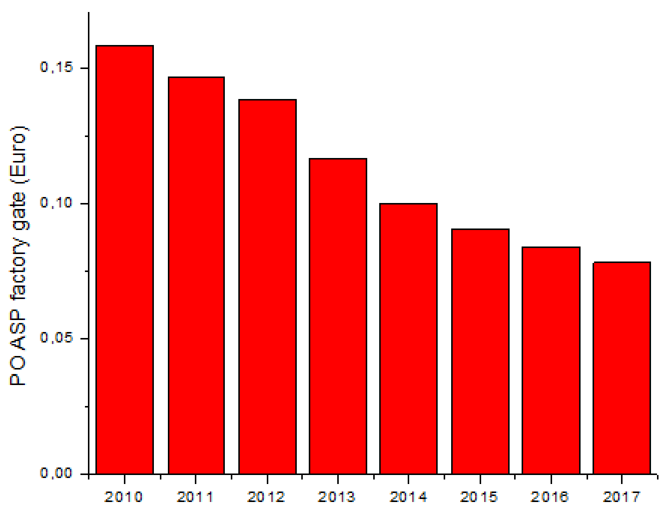

Figure 2.9: Factory gate price per watt forecast for power optimizers

Another important market segment that has to be taken under consideration is the inverter replacement market. With central and string inverter average lifetimes of 10 years, many PV systems installed during the solar boom of 2007-2008 will soon need inverter replacement. This is an

[19] The World market for micro-inverters and power optimizers, 2013 edition IHS

excellent opportunity for MLPM devices to increase their penetration. In figure 14 the inverter size in MW that need replacement can be seen.

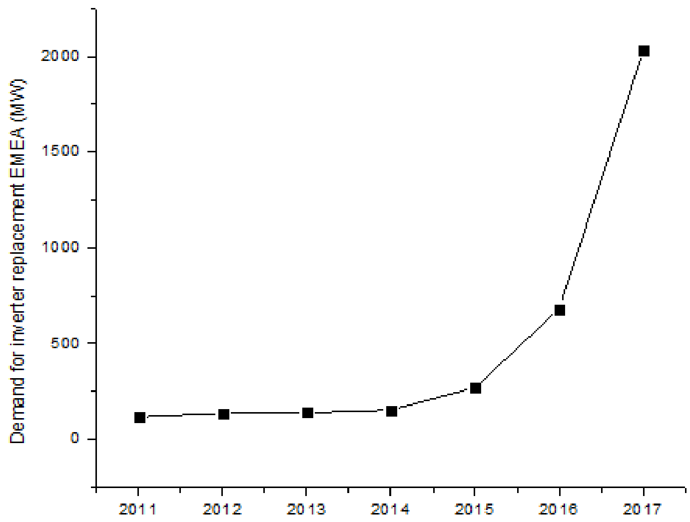

Figure 2.10: Inverter replacement market size in MW

Brands	Model	weighted eff (%)	Mppt range (V)	topology	enclosure	communication	monitoring	power range (W)	warranty (years)	dimensions (mm)	weight (kgr)	Market entry	Estimated shipments (MW)
Apparent Inc	MGI220	91,0	n.a	n.a	IP67	ethernet	Energy Review	100-240	15	203,2 x 127 x 50,8	3,2		
Dorfmuller	DMI 350/35	90,9(Euro)	29-70	electrolytic capacitors	IP65	power line	n.a	300	n.a	385 x 170 x 90	7,3	n.a	n.a
Enecsys	SMI-S240W-60	91,5(Euro)	23-35	thin film capacitors	IP66	wireless	n.a	260	20	262 x 160 x 35	1.8	Q2 2010	< 50
AE Conversion	INV250-45	92,6 (Euro)	20-40	n.a	n.a	power line	n.a	250	n.a	314 x 267 x 66,5	2,5	Q1 2010	n.a
iEnergy	iMicro inverter	93 (CEC)	25-50	n.a	IP66	power line	n.a	240-265	10	232 X 212 X 42,6	2,2	2010	<15
Sparq Systems	S215NA2240	93,1(CEC)	22-40	n.a	IP67	power line	n.a	230	25	195 x 127 x 30	1,36	Q4 2011	< 10
Darfon	MIG300VD00	94 (CEC)	30-50	n.a	n.a	power line	n.a	240	15	220 x 32,5 x 13	n.a	Q2 2012	<7,2
Samil Power	SolarPond 240HF	95 (Euro)	27-40	n.a	IP67	wireless	n.a	250	25	165 x 170 x 32	2	2013	n.a
SolarBridge	P250LV-208/240	95(CEC)	18-37	thin film capacitors	n.a	power line	n.a	235-280	25	273 x 101 x 35	1,6	Q3 2011	< 50
Involar	MAC300	95(CEC)	24-40	n.a	IP65	power line	n.a	210-300	15	230 x 138 x 35	2.4	Q2 2010	< 30
SMA	Sunny boy 240US	95(CEC)	23-32	n.a	IP14	power line	Sunny Portal	250	10	188 x 218 x 43	1,3	Q4 2012	< 10
Altenergy Power Systems	YC250-EU	95,5 (Peak)	22-45	n.a	IP65	power line	n.a	180-280	25	160 x 150 x 29	1,5	Q2 2011	<20
Enphase	M215	96(CEC)	22-36	electrolytic capacitors	IP67	power line	Enlighten software	190-260	25	173 X 164 X 25	1,6	Q2 2008	> 850
Power One	micro-0.25-I-OUTD/240	96(CEC)	25-60	thin film capacitors	IP56	wireless	Aurora CDD	265-320	10	266 x 246 x 35	1,65	Q4 2012	< 20
Heliox	SMI250	94,5(Euro)	16-48	thin film capacitors	IP66	power line	n.a	275	25	264 x 245 x 34	1,65	Q1 2015	n.a
Chilicon Power	CP250	96,09 (CEC)	22-38,5	thin film capacitors	IP66	power line	Cloud monitoring	190-300	10	304,8 x 203,2 x 45,7	1,55	Q32013	<5
Enphase	M250	96,5 (CEC)	27-39	electrolytic capacitors	IP67	power line	Enlighten software	210-300	25	171 X 173 X 30	2	Q2 2013	n.a

Table 1.1: Overview of available micro inverters in the market (Research end 2013)

Brands	model	weighted eff (%)	Mppt range (V)	topology	enclosure	communication	monitoring	power range (W)	warranty (years)	safety	dimensions (mm)	weight (kgr)	Market Entry
Tigo Energy	MM-ES (discontinued)	99,5(Peak)	16-48	impedence matching	IP65	power line	Tigo monitoring portal	350	25	Yes,DC bus deactivation	142 x 142 x 27	n.a	Q2 2009
SolarEdge	P300	98,9(Euro)	8-48	buck-boost	IP67	power line	SolarEdge monitoring portal	300	25	Yes, SafeDC™	125 x 132 x 30	0.8	Q4 2009
Power One	OPTI-0.3TL-OUTD	98,2(Euro)	25-60	buck boost	IP66	wireless	CCD Aurora	350	10	No	203 x 135 x 30	1,5	2013
Azuray technologies	ACM300	97,6(CEC)	20-80	buck boost	IP66	power line	Azuray Gateway	250	25	Yes but optional	136 x 136 x 40	0,97	Q1 2010
eIQ Energy	vBoost250 (discontinued)	97(peak)	20-50	boost	IP66	power line	n.a	250	n.a	No	260 x 127 x 57	2,08	Q3 2009
Femtogrid	P0310	97(Euro)	8-42	boost	IP65	wireless	Femtogrid monitoring portal	310	25	Yes, spark detection	135 x 225 x 50	1	Q32013
Femtogrid	PO300	95,7(Euro)	8-42	boost	IP65	wireless	Femtogrid monitoring portal	300	25	Yes, spark detection	288 x 342 x 51	1,45	Q42011
AMPT	V50-x	99,2(Peak)	17-48	buck-boost	n.a	wireless	optional	320	25	No	150 x 119 x 36	0,3	

Table 1.2: Overview of available power optimizers in the market (end 2013)

The benchmark report was concluded in the beginning of 2014 and forecasted global shipments of around 1GW for micro inverters and 1.2GW of power optimizer shipments. On the meantime the MLPE market grew surpassing even the most positive scenarios of growth and penetration. New industry reports show that the MLPE market will reach 1bn dollars revenue by 2019. Main drive of the growth is the US accounting for 20% of global residential systems. The growth opportunity for MLPE outside the US is also large provided that MLPE suppliers continue expanding to new markets and launch new innovative products that can be coupled with storage solutions. Moreover module manufacturers and suppliers such as LG, Sunpower, Jinko Solar have started to develop their own MLPE or partner with big players of the MLPE industry.

While volumes are increasing MLPE solutions become cheaper. An example is the recent 19% price reduction of Enphase’s micro inverter which was triggered by sustained competition by SolarEdge. For 2015 shipments, SolarEdge has surpassed Enphase for residential installations in the US market.

2.2 Industrial Development Heliox

2.2.1 The micro inverter – connecting the solar panel to the AC mains

To connect a solar panel to the AC mains we have to define an interface to load the solar panel and to source to the AC mains. Each side has a totally different characteristic.

The solar panel:

The solar panel acts as a voltage limited current source. To obtain the maximum output power, we have to maintain a relatively constant voltage across the panel (V_{MPP}) and absorb whatever current flows into that voltage. The voltage is determined by means of a Maximum Power Point tracker.
The advantage of a constant voltage load is that whatever the current from the panel is, not much control is needed to maintain the voltage and thus the maximum power.

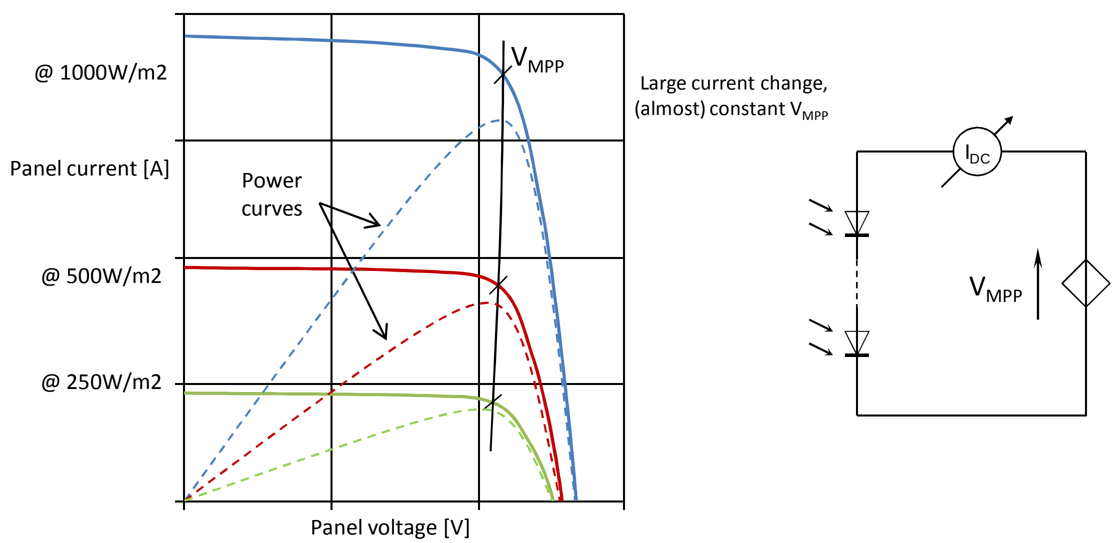

Figure 2.1: IV curve of a typical c-Si solar module

Output to the AC mains:

A Micro Inverter feeds current into an existing voltage on the power grid. Standalone operation is not allowed. The current into the mains is sinusoidal and in phase with the voltage for optimum Power Factor. An inverter topology is used with a current source characteristic, where the current is controlled to follow the sinusoidal shape of the voltage.

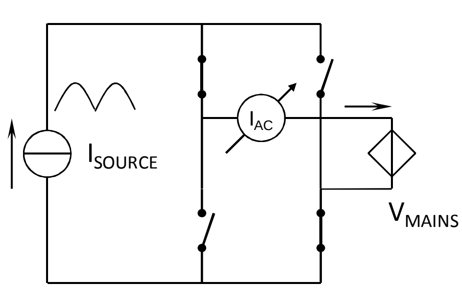

Figure 2.2: Micro inverter topology

2.2.2 Dual Stage Topology

The constant voltage load to the PV module as well as the current source characteristic towards the grid are combined into a dual stage topology.

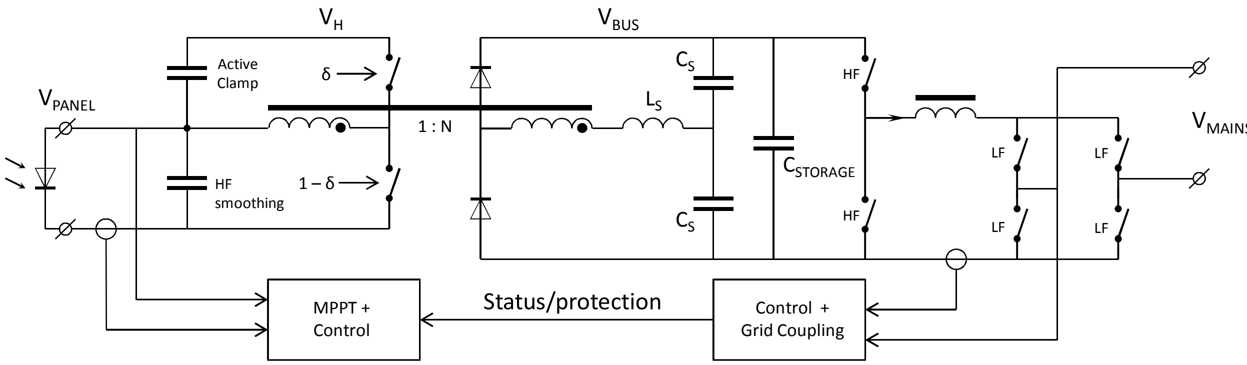

Figure 2.3 Dual stage topology with Zero Voltage and Zero Current switching is used to reduce losses in the converter.

2.2.3 Maximum Power Point Tracker

The micro inverter uses the Perturb and Observe method for finding the optimal working voltage to obtain the maximum power. This method has been modified from the standard version as described in literature, for better performance.

The power is measured at three voltages. The actual voltage and a voltage slightly above and below this value. This determines if there is a need to change the working voltage. This is a continuous process.

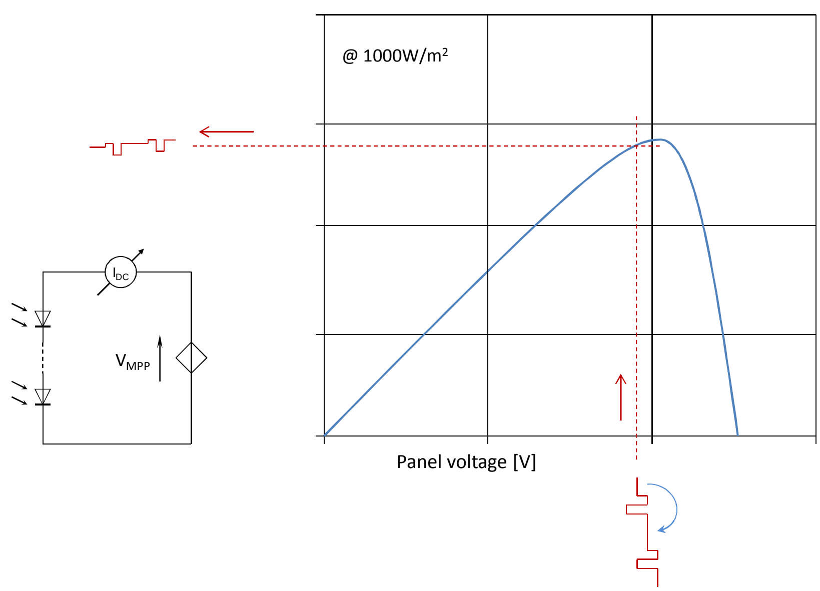

Figure 2.4: Mppt of a typical solar PV module

This method only gives the best working voltage in a local maximum. If there are two maxima (in a shaded situation) the inverter checks for the best global maximum using a voltage sweep over a wider voltage range. These voltage sweeps repeat every 5 minutes.

2.2.4 Electrical Specifications

Input side (PV)

Parameter	Symbol	Min	Typ	Max	Units	Notes
DC Input						
Voltage	$V_{DC,MIN}$		15.0		V	
	$V_{DC,MAX}$		48.0	50.0	V	Voltages in excess of 50V will damage the unit
Rated voltage	$V_{DC,R}$		31.0		V	
MPPT range	$V_{MPP,MIN}$	15.5	16.0		V	
	$V_{MPP,MAX}$			48.0	V	
Start voltage	$V_{DC,START}$		24.0		V	
Current	$I_{DC,MIN}$	0.05	0.1		A	
	$I_{DC,MAX}$		9.0	9.7	A	
	I_{SC}			9.7	A	
Rated power	$P_{DC,R}$		260		W	
Max. power	$P_{DC,MAX}$			300	W	@ $V_{DC,R}$ and $I_{DC,MAX}$ and T_{AMB} < 50°C

Output side (Grid)

Parameter	Symbol	Min	Typ	Max	Units	Notes
AC Output						
Voltage	$V_{AC,MIN}$		198		V_{RMS}	
	$V_{AC,MAX}$		253		V_{RMS}	Operational
Voltage withstand	$V_{AC,MAX}$			264	V_{RMS}	Non-operational
Rated voltage	$V_{AC,R}$		230		V_{RMS}	
Current	$I_{AC,MAX}$		1.3		A_{RMS}	
Rated power	$P_{AC,R}$		250		W_{RMS}	
Max. power	$P_{AC,MAX}$			285	W_{RMS}	@ $V_{DC,R}$ and $I_{DC,MAX}$ and T_{AMB} < 50°C
Frequency	f_{MIN}		48.0		Hz	
	f_{MAX}		52.0		Hz	
Rated frequency	f_R		50.0		Hz	
Rated cosϕ	$cosphi_{AC,R}$		±0.99	±0.998		

Night-time power consumption

Parameter	Symbol	Min	Typ	Max	Units	Notes
Night-time consumption						
Power	P_{NIGHT}		35		mW_{RMS}	

2.2.5 Performance Monitoring

The inverter measures several parameters like voltages, currents, internal temperature and a couple of status flags. These parameters can be monitored via an RF Z-Wave communication with a web-based portal.

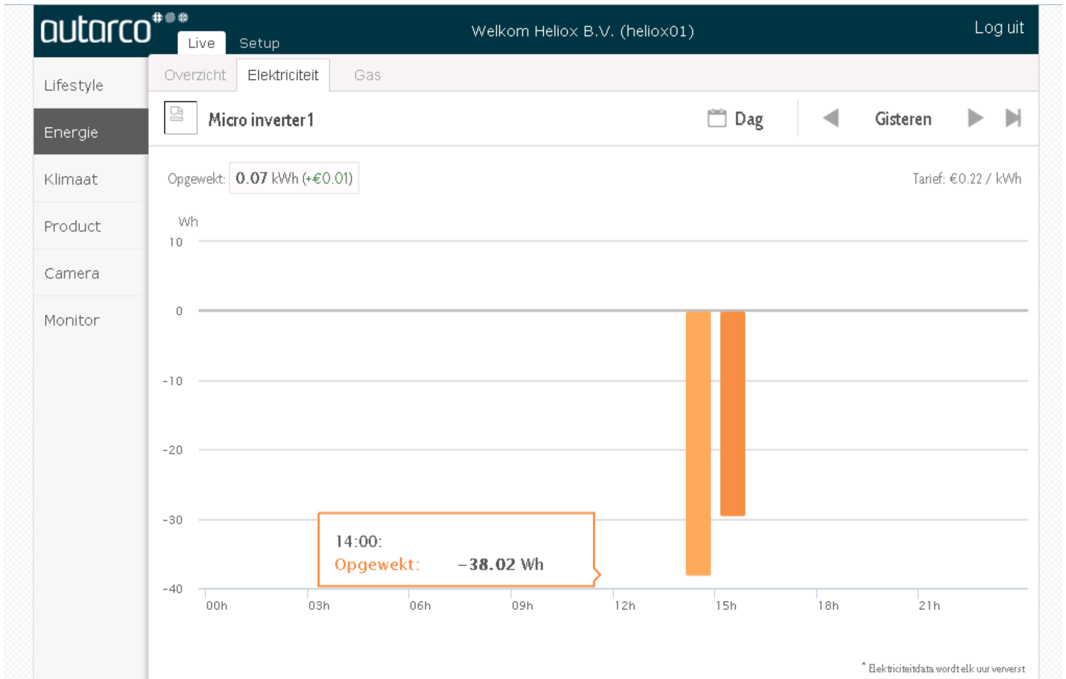

Figure 2.5: Web based monitoring portal developed for the Heliox SMI300 from Autarco

The AC power is not measured accurately. For the monitoring the AC power is calculated from the DC (input) power by using an estimation of the losses in the inverter. A mathematic model of the losses as a function of DC input voltage and current has been determined by SEAC, based on more than a full year of measurement data. This loss model is incorporated inside the micro inverter to calculate the AC output power. The model is more accurate than the tolerances on measured voltages and currents. As such the model is sufficiently accurate for its purpose.

2.2.6 Quality Tests performed in-house

Following quality tests have been performed by Heliox during the development of the inverter.

1) Functional			
101	Output Requirements V / I	OK	
106	Power Consumption & Efficiëncy	OK	see EN50530:2010
108	Peak Inrush Current	OK	
110	Elcap-Lifetime	OK	
111	OVP	OK	see D105.101 (grid codes)
130	Elcap discharge time	OK	
	Fuse derating and breaking capacity	OK	
	Inrush peak current	OK	
2) EMC			
201	Emission Conducted	OK	
202	Emission Radiated	OK	
203	Immunity	OK	see Crei Ven approval report
210	Surge	OK	

212	Burst	OK	
213	ESD	OK	see Crei Ven approval report
214	Mains harmonics	OK	pass for IEC 61000 and UK83/2
215	DC Injection	OK	UK83/2 PASS
3) Quality			
301	Four Corner Test	OK	see D105.101
302	Fault Condition Test	OK	
305	Humidity Test (DH/Hum Freeze/Temp cycle)	OK	
306	Vibration / Bump / Drop	OK	
307	Thermal shock	OK	
308	Cold start	OK	low temperature lockout below –35°C
310	Hi-Pot/leakage resistance	OK	

2.2.7 Expected Market Penetration and commercial activities

This micro inverter is targeted for use in residential areas where circumstances are less ideal for application of PV-solar systems. In particular when dealing with shading conditions and where the investment based upon module level power managements pays off.

As a B2B supplier Heliox doesn’t sell directly to end users. Heliox has contracted an established sales and service channel for the marketing and installation of the micro inverter. This party sells and installs complete PV systems to end users, including PV modules and mounting material.

The first order has been placed and Heliox is currently starting up manufacturing to produce the first batch of products. The potential of the building integrated PV-market is huge and is another area of interest for further market expansion.

2.3 Industrial Development Femtogrid

PV Module Level Power Management (MLPM project)

Everything we see is **DC** powered, so generate and distribute **DC**.

Version: Final report MLPM -Version 0.1
Project: MLPM- PV in the Built environment Module level Power Management
Project number :TKIZ01005- WP **1: Development of a second generation power optimizer**

femtogrid energy solutions

A small introduction in Femtogrid POs

Femtogrid is a smart DC grid. It is a 3-wire, 350-400 Vdc, bi-directional, self-stabilizing, decentralized network designed to distribute DC power and data. A patented safety wire concept keeps the user free of the consequences of arcs, electrical shocks, fire, sustainable energy balancing issues, black/grey start issues and decreases the number of components , copper usage and standby power compared with AC networks and provides high speed (PLC) ethernet out of a tap. This DC grid, the Femtogrid, distributes sustainable energy and data at home, small and medium enterprises buildings and street grids..

Marketing name: PO (Power Optimizer) in fact a micro-converter to connect solar module to a dc grid)

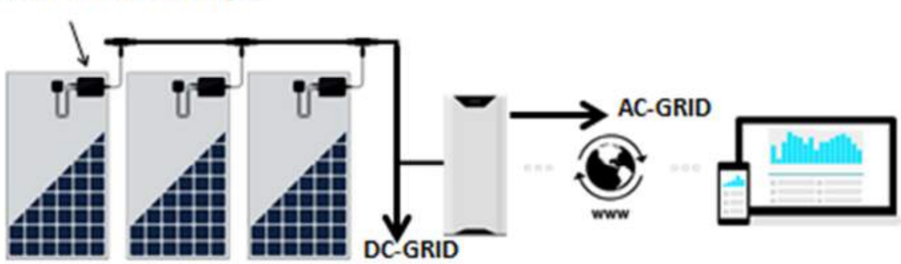

December 2015 page 3

femtogrid energy solutions

MLPM deliverables overview

- Design of a PV module integrated power optimizer (PO4xx)
- 25 years lifetime behind solar module
- 50 % of the volume of the PO310
- Support all other project partners with products, software, test setups
- Reduce the price of the electronics.

MLPM deliverables MLCC

- Design of a PV module integrated power optimizer (PO4xx)
- 25 years lifetime behind solar module
- 50 % of the volume of the PO310
- Support all other project partners with products, software, test setups
- Reduce the price of the electronics.

PO410 test model with MLCC capacitors

MLPM deliverables : Functionality

- Design of a PV module integrated power optimizer (PO4xx)
- **25 years lifetime behind solar module- Technical solutions**
- 50 % of the volume of the PO310
- Support all other project partners with products, software, test setups
- Reduce the price of the electronics.

Functionality: new variables, new monitoring data, alerts, warnings
and new complete functions.

Functions designed, implemented and tested:

a- diode test, estimation of diode dissipation
b- Isc and Voc measurement
c- active IV curve tracking
d- theft control (also at night)
e- smart derating
f- soft starts, dark start, response to DC network disturbances,
g- smart warnings and alerts.
h-remote control of full sweep/ auto sweep.
I- adjustable MPPT method.
j- weak and firm DC grid interface
h- class 1 kW(h) measurement calibration

December 2015 page 6

femtogrid energy solutions

MLPM deliverables : Long lifetime

- Design of a PV module integrated power optimizer (PO4xx)
- **25 years lifetime behind solar module- Technical solutions**
- 50 % of the volume of the PO310
- Support all other project partners with products, software, test setups
- Reduce the price of the electronics.

Femtogrid tests and improvements to increase lifetime and technical performance :

Issue: pass the extended (2000hr + damp/heat test 85/85 *with load*)
Result: changing measurement values
Solution: several coatings tested. (damp/heat), new coating selected.

Issue : Input Capacitor derating: high temp/moisture. Many tests done.
Result: Lifetime extended to 25 Years.
Solution: new brand capacitor, new coating, new soldering technology,
new PCB lay out, new glue, new current control mechanisme.
Issue: connector wear out.
Connector technology: MC4
Mechanics: new connectors (material), gaskets, kit, heat conductive material,

Reduce size/weight

Electronics: new capacitors, ferrite and switching devices.

December 2015 page 7

femtogrid energy solutions

MLPM deliverables : 50 %

- Design of a PV module integrated power optimizer (PO4xx)
- 25 years lifetime behind solar module
- **50 % of the volume of the PO310**
- Support all other project partners with products, software, test setups
- Reduce the price of the electronics.

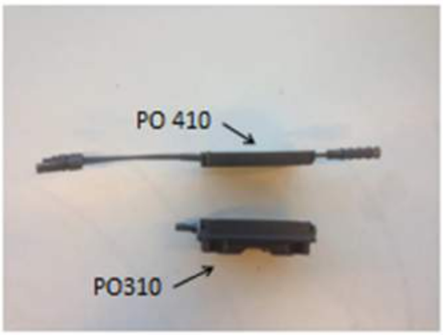

Project target achieved:
50% of volume by new technology

Succeeded:
-new capacitors, integrated coils, new heatspreader and new connection technology, remains class2 (isolated from earth product), new potting material

December 2015 page 8

femtogrid
energy solutions

MLPM deliverables to other Partners

- Support other project partners with products, software, prototypes, tests ,setup

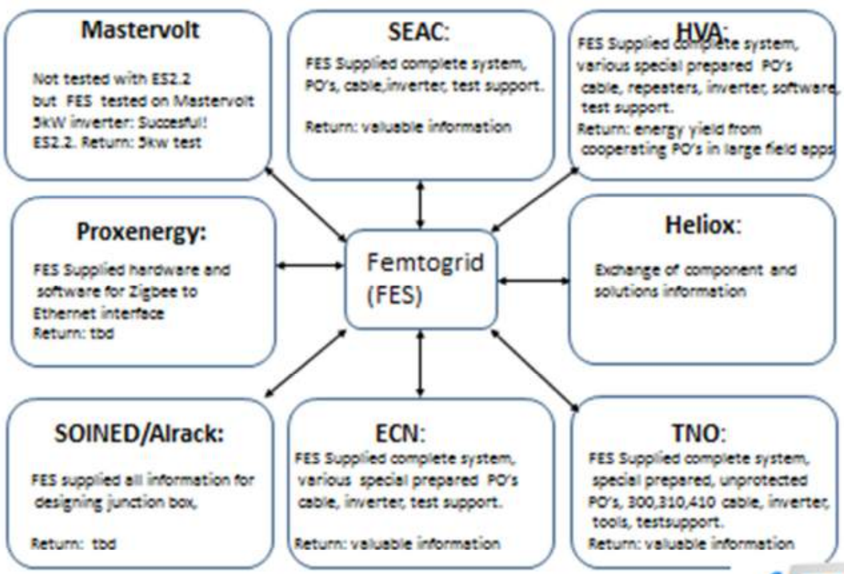

December 2015 page 9

femtogrid
energy solutions

MLPM deliverables
Marketing and technical advantages

A -micro converter (from solar module to DC grid) has the highest energy yield
B- Wide input MPPT tracking increases yield
C- a micro converter to DC grid has less components, so longer lifetime then micro inverters
D- Micro converters are cost effective. (less components)
E- central inverter coupling to AC grid is simple for network operators
F- Enabling local use of DC power, easy islanding (autarkic) or single or multiple AC grid connection.
G- easy to integrate new cell, module technology with higher efficiency
H- easy interface with smart grids & kathodic protection of structures.
I- Day and night monitoring of the system
J- A patented safety wire concept keeps the user free of the consequences of arcs, electrical shocks, fire, fireman safety, sustainable energy balancing issues, black/grey start issues and decreases the number of components , copper usage and standby power compared with AC networks and provides high speed PLC).
H- Future proof system, new PV module technology seemless integration, old or defect solarmodules can be replaced without influencing the system.

December 2015 page 10

femtogrid
energy solutions

Business Model of Femtogrid 2012

Business model to 1 jan 2014

December 2015 page 11

femtogrid
energy solutions

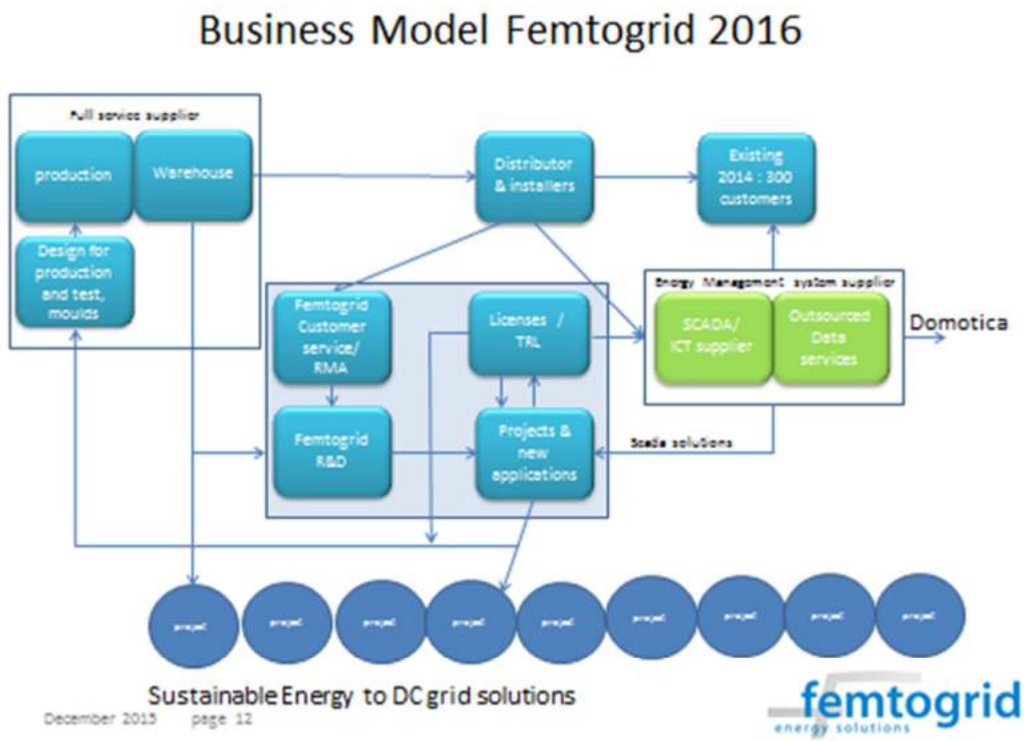

Business Model Femtogrid 2016
Full service supplier
production
Warehouse
Design for production and test, moulds
Distributor & installers
Existing 2014 : 300 customers
Femtogrid Customer service/ RMA
Licenses / TRL
Femtogrid R&D
Projects & new applications
Energy Management system supplier
SCADA/ ICT supplier
Outsourced Data services
Domotica
Scada solutions
Sustainable Energy to DC grid solutions
December 2015 page 12
femtogrid
energy solutions

Femtogrid Solar Power Optimizer PO310 Module Add-On
femtogrid
energy solutions
Maximum Solar Energy using Femtogrid Solar Power Optimizers
December 2015 page 13


femtogrid
energy solutions
Femtogrid Solar Power Optimizer PO330
Module Add-On
Maximum Solar Energy using Femtogrid Solar Power Optimizers
femtogrid
energy solutions
December 2015 page 14
femtogrid
energy solutions

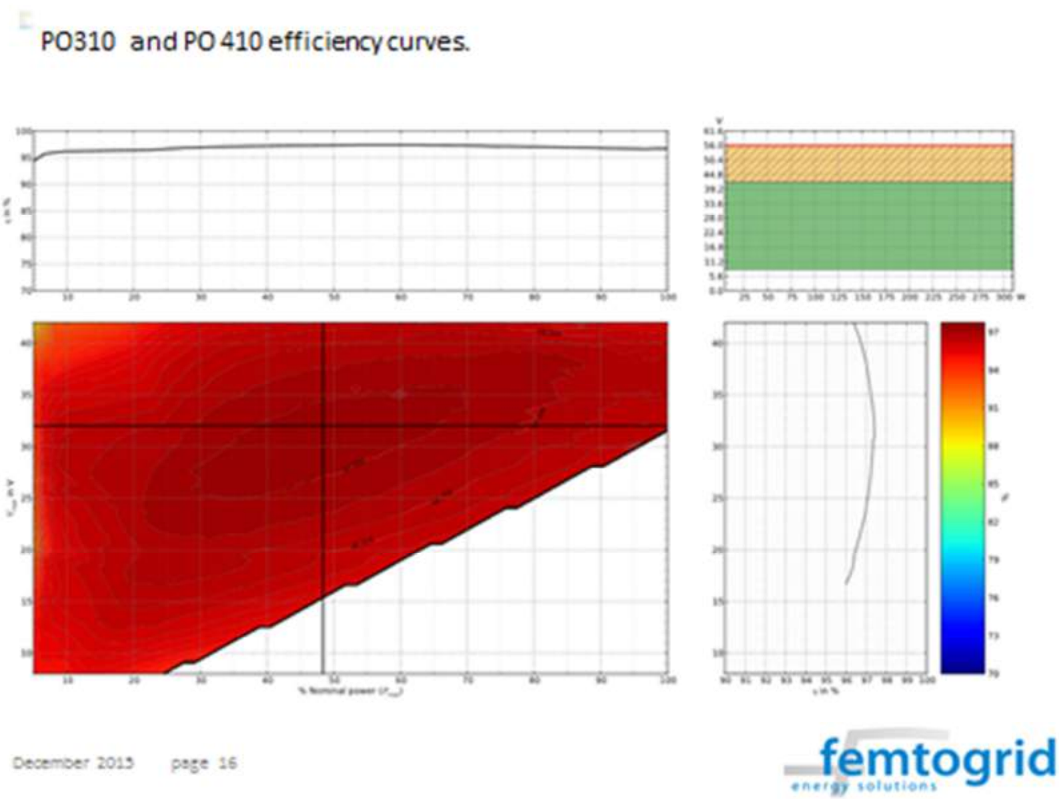
PO310 and PO 410 efficiency curves.
December 2015 page 16
femtogrid
energy solutions

PO330 and PO 430 efficiency curves.

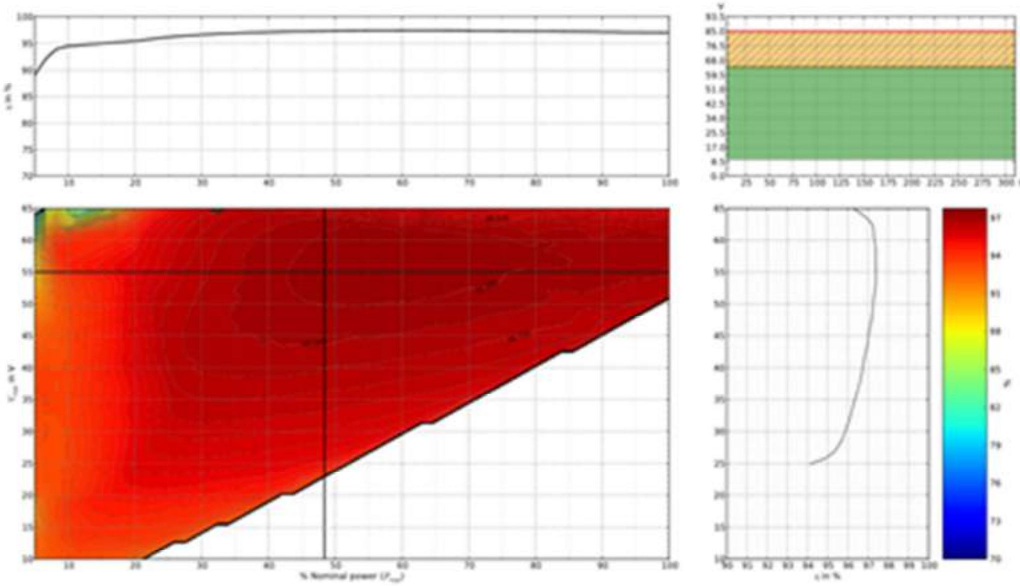

December 2015 page 15

femtogrid energy solutions

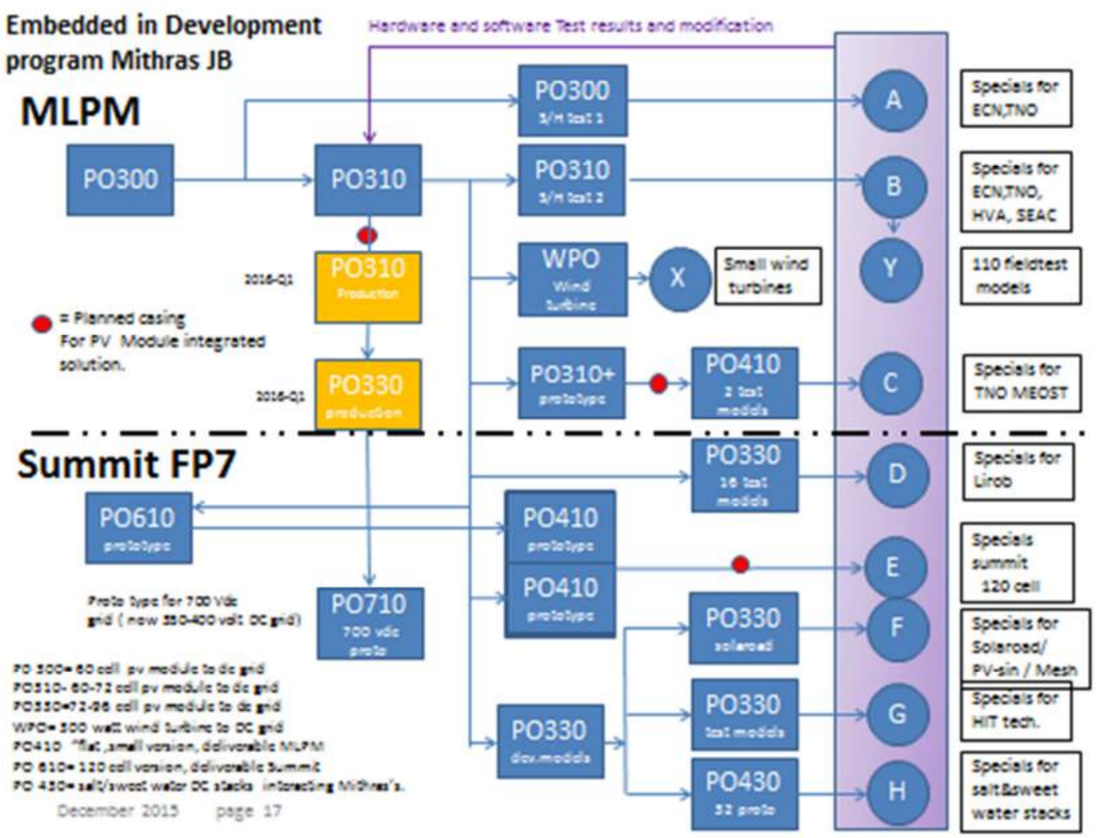

December 2015 page 17

Project Summary MLPM:

General

1- Good cooperation with the project partners, valuable knowledge shared.

2- Most commercial PV companies suffered from economical crisis, low cell prices, low inverter prices, and bankruptcy European module production companies.

3-Femtogrid , even as some other partners, also in heavy weather, obliged to change business model.

4- Received subsidy about 20 % of project costs.

Deliverables

-Technical positive results : design module integrated version ready, all technical issued solved except design of housing.

-Shows the advantages of a DC grid.

-Enforced new business model.

-proves safety, efficiency , elegance of DC grid with safety wire technology

To our partners: Sustainable energy for all!
Regards, Rob Schaacke

December 2015 page 18

2.4 Industrial Development Mastervolt

In the MLPM project Mastervolt verified The Mastervolt Shadow tracker MPPT algorithm.
Based on the Intelliweb monitoring data of the shadowing-experiment in the one year field trial we verified and more important optimized the shadow tracker MPPT algorithm.
The performance of the shadow Tracker is independently tested by SEAC/Kostas. The shadow tracker has been compared with the standard MV MPPT tracker. Our conclusion is that from a techno-economic perspective the Mastervolt Shadow Tracking MPPT algorithm as used in the Mastervolt string inverters eliminates the use/need of Module Level Power electronics. The results are concussive and the extra cost from the MLPE does not offset the extra cost.
The second ambition for Mastervolt in the MLPM project was the independent assessment of the accuracy, reliability and fairness/honesty of the monitoring functions in other suppliers of conversion technology did not come to a conclusion. The monitoring data provided by Mastervolts Intelliweb compared with the Yokogawa-readings shows that (probably due to filtering) the Mastervolt Data is very conservative. The other suppliers of the conversion hardware did not reach a point in the project where reliable online monitoring data was made available for a comparison with the available Yokogawa-power analyser data. Unfortunately during this project the project leader Arno van Zwam left the company and with him all the background and a lot of the knowledge of this project.

Chapter 3: Field Testing

3.1. Field Testing at HTC5

3.1.1 Design and specifications

The aim of our field test is to compare three different PV system architectures under identical operation conditions. For this purpose PV systems with 30 degrees inclination angle and 165 degrees azimuth (South-East) have been built. The field-test site is situated 40 meters above sea level at 51.4 degrees northern latitude and 5.48 degrees eastern longitude. Every system consists of the same installed capacity (1.59 kWp) with solar panels of the same power class and manufacturer installed at two successive rows per system as seen in the Figure 3.1.

Figure 3.1: Impression of the field test.

For the field test the Yingli Panda 265 Wp modules have been selected for their high efficiency and absence of Light Induced Degradation. The panels consist of 60 series connected mono-crystalline n-type cells. Every sub-module of 20 cells is assigned to one by-pass diode connected anti-parallel. Flash data of the solar panels was available from the manufacturer, however, the modules were additionally flashed by a PASAN IIIB solar simulator. On average the maximum power was 98.4 % of the provided rate power capacity (Pmax) by the manufacturer. Note that the solar panels have been distributed randomly throughout the field test.

The string inverter system has been fitted with a commercially active inverter from Mastervolt (Soladin 1500 Web). The string inverter has a nominal AC output of 1500 W and is fitted with a high frequency transformer. The micro inverter system consists of 6 micro inverter prototypes from Heliox rated at 300 W AC while the power optimizer system consists of 6 power optimizers with nominal power of 310 W and an inverter of 2.4 kW with fixed voltage input of 380 V. The power optimizer system including the inverter is supplied by Femtogrid Energy Solutions.

The front rows of the PV systems are shaded during winter months by a wall situated at the south side of the plant while on these months there is also partial shadowing from row to row. Additionally neighboring buildings are situated on the east and west side of the PV systems further reducing the horizon view and thus the available irradiation. Since the goal of the field test is to make a direct and absolute comparison of the three PV systems, a shading analysis was done to determine which parts of the day there is uncontrolled shade.

For this purpose the Suneye from Solmetric[20]has been used. By means of a fisheye camera with integrated compass and a global positioning system (GPS), one can determine the exact time and date that a specific point of the PV system is shaded. Several skyline pictures have been taken from all the module sub strings of the systems and superimposed to the sun path in order to determine which part of the PV generator is shaded and when this happens. An average solar access of 84 % has been calculated for the specific location. The solar access is defined as the ratio of the available insolation including shade in a specific location, to the available insolation without shade at the same location. In this way a "clean measurement time" has been determined where shadeless operation takes place.

[20] http://www.solmetric.com/buy210.html

Three poles have been positioned on the south side of the front row of each system blocking direct irradiance. This results in shading of cells in different substrings of modules. The poles have been positioned at the exact same height, length and width from the setups to provide equal shading among the three systems. The pole dimensions are: 146 cm height, 12.5 cm diameter and have been positioned 69 cm away from the middle solar module of the front row.

Figure 3.2 : Impression of the shading poles

DC and AC electrical parameters are monitored with high accuracy power analyzers from Yokogawa (WT-1800). In total 7 power analyzers with 6 inputs per device have been used. Through a wired network the power analyzers are synchronized providing data capture simultaneously for all channels. The data logging interval is one second for all inputs to assure detection of even the fastest transient phenomena. T-type thermocouples from Rossel are used to measure module and ambient temperature while 2 ISO secondary standard pyranometers from Kipp & Zonen (CMP21) measure in-plane irradiance. Logging of the temperatures and irradiance is via a MW100 data logger that is also synchronized with the power analyzers. All measuring equipment is housed in weatherproof cabinets including the devices under test. All in all more than 130 parameters with 1 second resolution are monitored in order to evaluate system performance.

3.1.2 Device Characterization under operating conditions

String inverter :The string inverter chosen for the task is a new generation low power inverter fitted with a high frequency transformer. It includes a so called “shadow function” which can be switched on using the internal settings of the device. Note that the inverter is supplied with the shadow function deactivated by default from the manufacturer. Experiments with a pole shadow have been performed both with the shadow function activated and deactivated.

In Figure 19 results from the experiments with the string inverter are shown. The relation of input voltage and relative AC power output, with color coded efficiency is presented for unshaded and partially shaded operation. The voltage input range is between 150 V on warm days and up to 200 V during cold mornings. The efficiency of the inverter ranges from 92% up to almost 95.4%. The peak efficiency is observed at around 25% of the nominal power output and it is ideal for central European climate with a lot of overcast days throughout the year.

By introducing shade with a pole to the PV system (Figure 3.3b) a wider voltage range can be observed. In the case where the shadow function is deactivated the inverter operates the PV string at a high voltage and closer to the V_{oc}. This indicates that the MPPT has chosen a local maxima point from the lumpy P-V curve. When the shadow function is activated the PV string is operated at a significantly lower voltage and higher power. By using frequent P-V scans the MPPT can locate and track the global maximum point of the curve and thus by-pass the shade affected groups of solar cells in the string. As a result the available DC power harvested by the inverter is significantly higher.

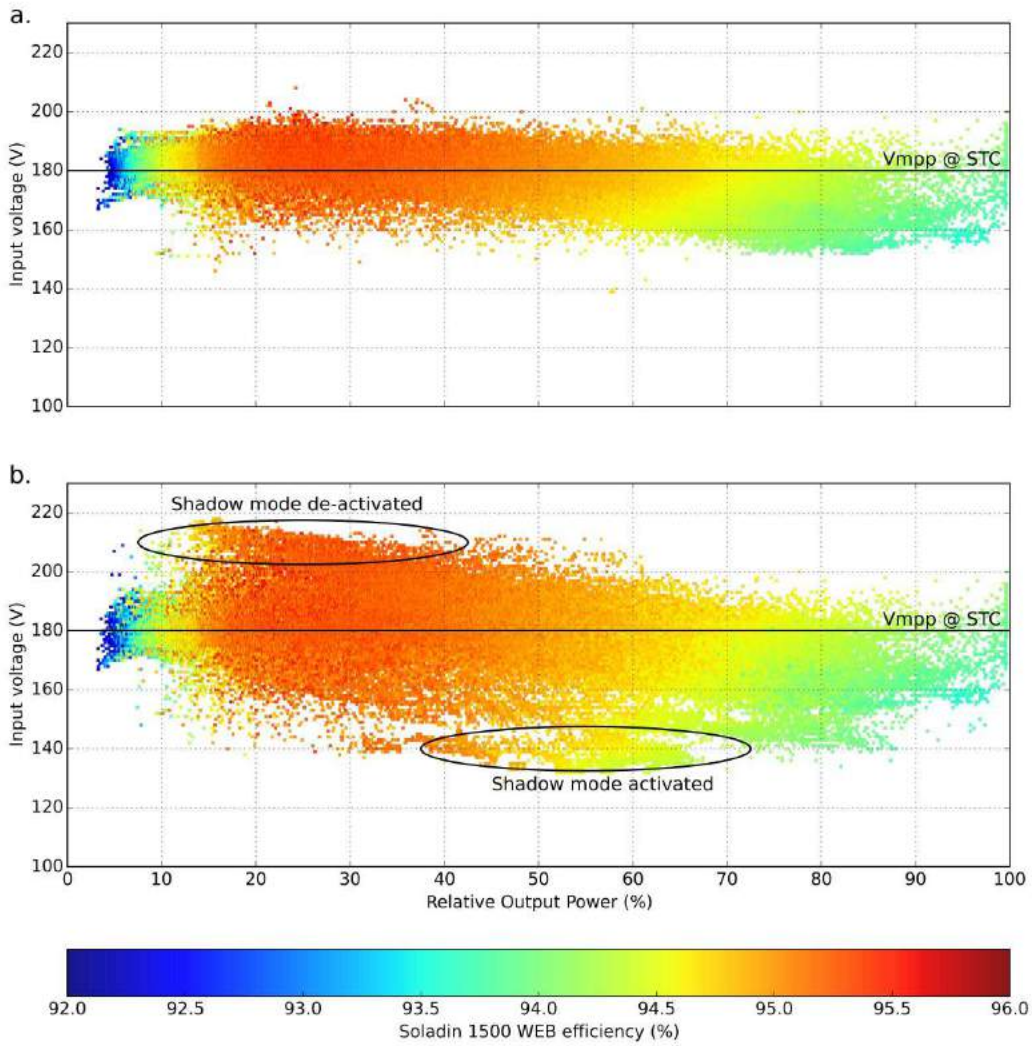

Figure 3.3: Relation of input voltage with efficiency and power output during 5 months of operation under clear (a) and partially shaded conditions (b)

Depending on the system size and the shading conditions and due to the operation of the shadow mode, the inverter can easily fall below the MPPT voltage range specified by the manufacturer occurring in additional energy harvesting losses.

Micro inverter system: The system consists of six micro inverter prototypes supplied by Heliox rated at 250 W AC. The micro inverter has a wide range of MPPT voltage (16-48 V) and in combination with frequent P-V scans can track the global maximum point under certain conditions in a similar way like the string inverter's shadow function. In Figure 3.4a the operation of the micro inverter can be seen under unshaded conditions. Peak efficiency is achieved at 40 % of the relative power output while momentarily the micro inverter can supply 110 % of the nominal output. It should be also noted that the PV module under certain conditions such as cloud enhancement[21] can deliver much more power than STC rating. In the case of the micro inverter the PV module has delivered for short time over 290 W of DC power which has been utilized and successfully converted to usable AC power.

When shade by a pole is introduced to the micro inverter system (Figure 3.4b) the global MPP can still be tracked and the shade-affected substring of solar cells can be by-passed. A voltage

[21] Yordanov G.H., Midtgard O.M., Saetre T.O, Nielsen H.K., 'Overirradiance (Cloud Enhancement) Events at High Latitudes' IEEE Journal of Photovoltaics 3 (2013) 271-277

dependency in the efficiency can be observed. A total absolute reduction in efficiency of approximately 1.5-2 % can be seen for operation between 18-22 V. When the shade covers more than a substring of solar cells and the global maximum is below 16 V, the micro inverter will operate on a local MPP and thus not harvest all the available power from the PV module.

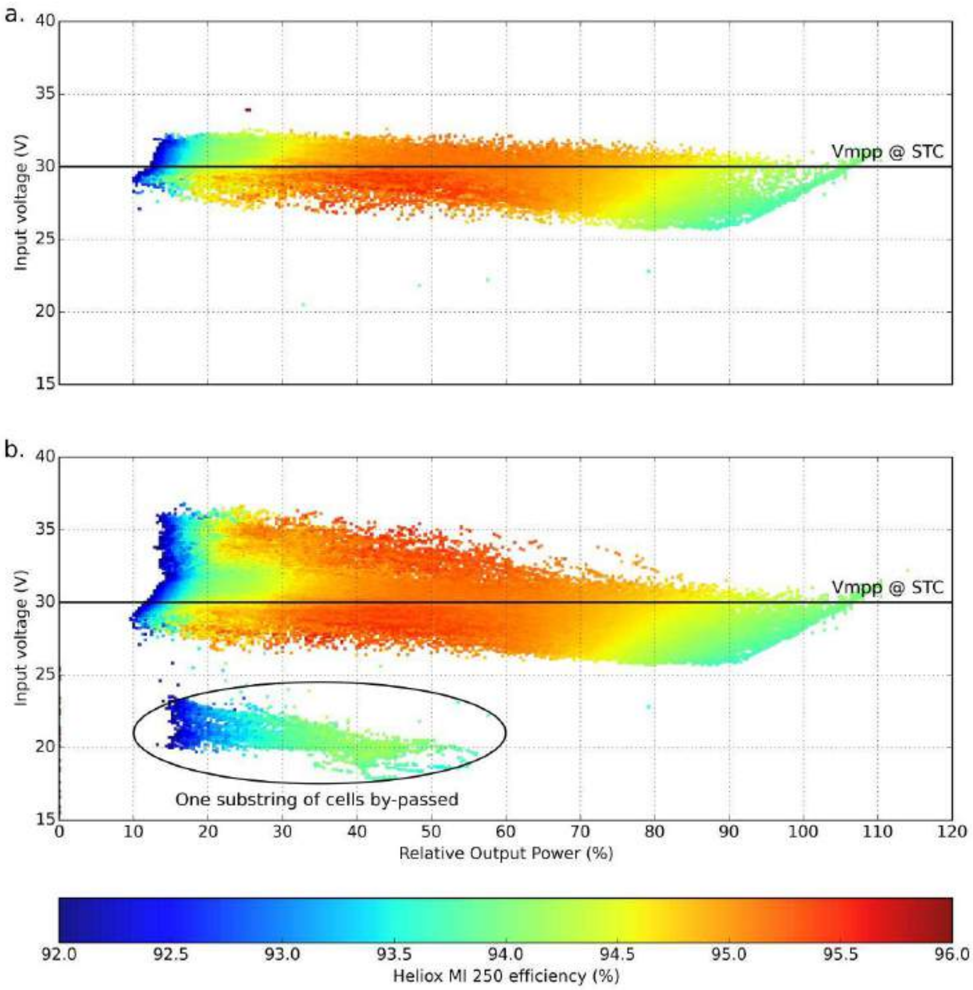

Figure 3.4: Relation of input voltage with efficiency and relative power output during 5 months of operation under clear (a) and partially shaded (b) conditions

Power optimizer system: The power optimizer is rated at 310 W DC output and performs MPPT on a module level. The system utilizes a central inverter with fixed voltage input (380 V). The benefit of the power optimizer system is the wide voltage operation range and the hybrid P&O MPPT which is similar to the string's inverter shadow function and the hybrid MPPT of the micro inverter. The boost converter used at the Femtogrid system can operate from as low as 8 V input with its maximum MPPT efficiency. In Figure 21a the operation of the power optimizer under unshaded conditions can be seen. The PO310 achieves peak efficiency of 97.5 % at 40 % of the nominal output power while the European efficiency is 96.7 %.
By introducing shade by a pole to the power optimizer system (Figure 3.5b) the MPP can be tracked even under extreme shading conditions covering up to 2 of the 3 substrings of solar cells of a typical crystalline solar module. However, the efficiency of the boost converter drops from 97.5 % to 96 % for by-passing one substring and further down to 95 % when two substrings of solar cells are by-passed

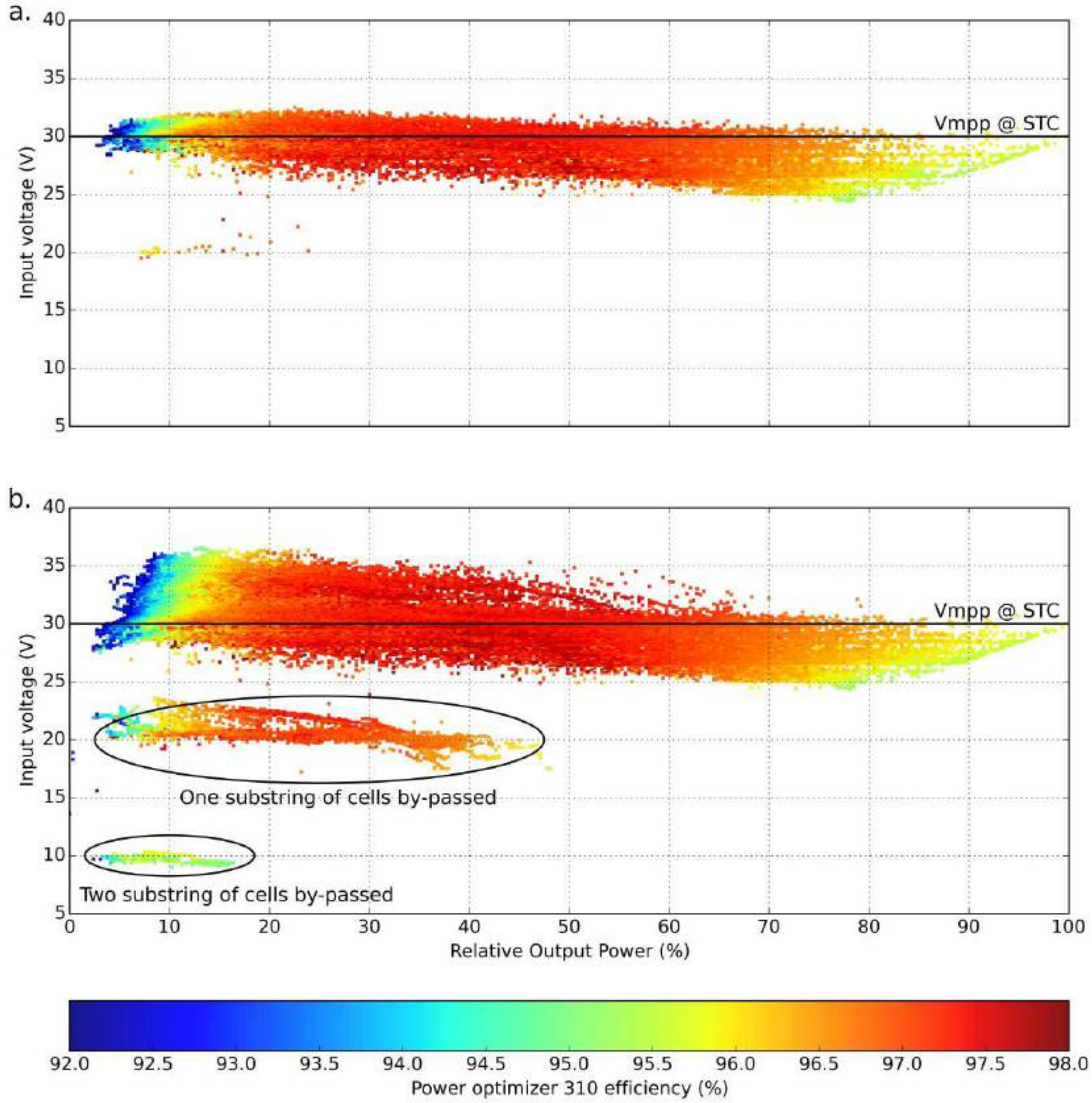

Figure 3.5: Relation of input voltage with efficiency and power output during 5 months of operation under clear (a) and partially shaded (b) conditions

Table 3.1: Calculated and measured parameters of the three systems

Device	Voltage range	Max power measured	$n_{Euromeasured}$	$n_{CECmeasured}$	n_{Max}	n_{Max} @ power %	n_{Euro} datasheet	n_{Max} datasheet
Femtogrid PO310	30 ± 0.2	293 DC	96.56	96.67	97.5	39.93	97	>97
Soladin 1500 WEB	180±0.2	1568 AC	94.74	94.65	95.4	25.38	95	95.6
Heliox SMI250	30 ± 0.2	270 AC	94.33	94.65	95.2	40.37	94.5	95.5

3.1.3 Performance Ratio analysis

The PR of the three systems is calculated daily for the clean measurement time. Moreover, the clearness index (k_t) is calculated daily based on global horizontal irradiance measurements by an additional secondary standard pyranometer in close proximity of the field test. The clearness index is defined as the ratio of the measured horizontal global irradiance on earth and the extraterrestrial irradiance available outside the atmosphere. Weather classification can be done based on the clearness index as follows: k_t<0.2 overcast, k_t=0.2-0.6 partly cloudy and k_t>0.6 clear[22]

Figure 3.6 shows the PR for the three systems as a function of k_t for the unshaded and pole shading cases. On days with overcast weather where the largest part of the light consists of diffuse irradiance, the pole has obviously no effect on the PR of the three systems. PR values of more than 100% can be seen due to lower temperatures from STC conditions. However, when k_t increases, the benefit of distributed MPP tracking under partial shading can be seen.

With the shadow mode of the string inverter deactivated, there is an absolute 35% improvement under certain shading conditions on the PR (k_t=0.74) for the MLPE. The string inverter MPP tracker follows a local maximum point of the I-V curve, while the micro inverters and power optimizers operate the unshaded parts of the system at MPP and electrical mismatch losses are restricted to the affected module only. However, when the shadow mode of the string inverter is activated and the MPP tracker of the inverter tracks the global maximum the difference between the string inverter and MLPE on absolute PR is almost 5% in favor of the MLPE. Thus, it is recommended to activate the shadow function (if any) of the string inverter when partial shading is expected. The fine-tuning and optimization of the MPP tracker scan intervals during shadow mode needs to be further investigated.

During unshaded conditions differences in DC ratio are minimal among the three systems while they are clearer for the PR. The multiple conversion stages (DC/DC and DC/AC) in the case of the power optimizer system and the low efficiency under low power input of the micro inverter lead to additional losses in power production when electrical mismatch losses are minimal. These losses can be better seen with low k_t values (0.1-0.3) resulting in significantly lower PR compared to the string inverter system.

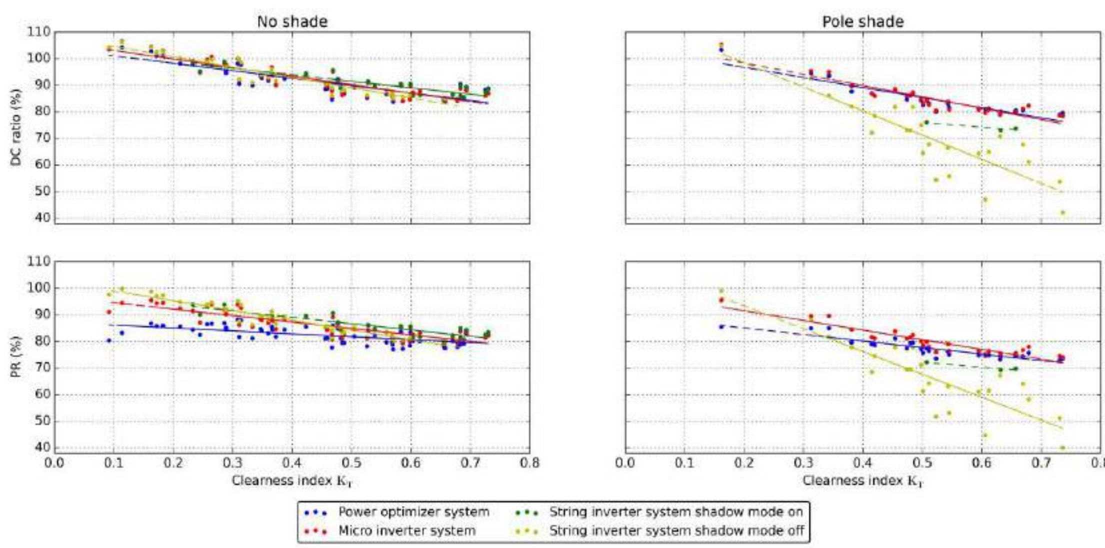

Figure 3.6: Daily calculated PR and DC ratio versus average clearness index of the day for unshaded and

[22] Reindl D.T., Beckman W.A., Duffie J.A. 'Diffuse Fraction Correlations' Solar Energy Vol 45 No1, pp 1-7, 1990

partially shaded operation of the three systems with a pole shading 1-2 % of the total PV system surface. Data presented at the graph are calculated during spring and summer months.

3.1.4 One year outdoor Field Testing

In order to assess the performance of the three systems , a full year (4 seasons) of outdoor field testing took place in HTC5. In total 9 different shading and unshaded periods were tested starting from 18th November 2014 until 17 November 2015. In the graph below the PR for the DC and AC power can be seen for all periods. Notice that due to malfunctions in the Heliox micro inverters some days of measurements have been excluded from the calculations. Additionally a “clean measurement “time has been defined and was taken into account in the final calculations.

Days not taken into account (due to either H1, H2, H3 malfunctioning):

- All days from 30 Dec 2014 up to and including 7 Jan 2015
- 31 Mar 2015
- 19 Apr 2015
- All days from 8 May 2015 up to and including 13 May 2015
- 28 Jun 2015
- All days from 1 Jul 2015 up to and including 13 Jul 2015

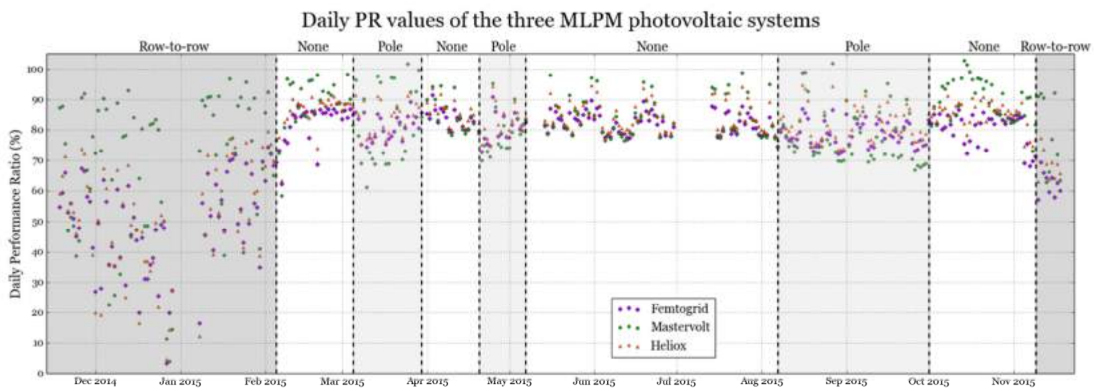

Femtogrid DC	**60.58%**	88.13%	**84.12%**	87.16%	**83.01%**	85.07%	**81.14%**	88.33%	75.45%	**82.85%**
Mastervolt DC	57.25%	**89.36%**	79.15%	**88.18%**	81.14%	**86.56%**	78.94%	**90.48%**	**78.14%**	82.48%
Femtogrid AC	51.18%	82.22%	78.96%	82.88%	78.84%	80.69%	76.67%	82.44%	63.76%	77.88%
Mastervolt AC	52.91%	84.47%	74.90%	83.29%	76.66%	81.72%	74.71%	**85.68%**	**73.18%**	77.87%
Heliox AC	**52.97%**	**84.95%**	**81.08%**	**84.58%**	**80.69%**	**82.74%**	**79.41%**	85.52%	69.22%	**80.14%**

Figure 3.7: PR calculations for one year in the outdoor set-up

Overall the systems performed very well throughout the year. The benefit of MLPE architectures is especially visible during shaded periods. The micro inverter system overall performed 2.3 % better from the PO and string inverter system. In terms of DC power output which is very relevant especially for the PO system which can accommodate smart grids, the Femtogrid system scored around 0.5% better than the string inverter. Notice that the DC output of the POs is measured after DC/DC conversions while the string inverter system does not include any power conversion. Taking into account the 97% efficiency of the POs the Femtogrid system has significantly harvested more DC energy than the string inverter system, making the Femtogrid system ideal to combine with a DC 380V smart grid.

3.2 Testing the Surface Gradient Algorithm

3.2.1 Scope of the test

The goal of the test is to check whether there is significant increase in performance if modules are subject to a modified sweeping regime compared to a fixed sweeping regime when both modules are under partial shading conditions. Under partial shading conditions more than one maximum power point could occur, where the sweeps have the objective to detect whether the modules are operating in a local or in the global maximum power point. Most standard maximum power tracking software performs sweeps at regular intervals. A drawback of the method of sweeping is that whilst a sweep takes place, the power output is not optimal, so a little energy is lost. The gradient method (Cruz Barco, 20140519 Report V6, 2014) saves energy by reducing the frequency of sweeps at fixed interval, whilst at the same time the necessity of a sweep is assessed by comparing the output of adjacent modules. If differences are detected, an algorithm calculates whether an additional sweep, the 'gradient sweep' should take place.

According to previous simulations (Cruz Barco, 20140519 Report V6, 2014), "in average it is possible to increase up to ~0.17-0.19% of the daily energy yield, with the minimum being 0.05% and the maximum is 0.95%". The gradient method should be able to recover up to 40 % of these losses due to operation in the wrong maximum power point. Simultaneously, every avoided sweep due to the lower fixed sweep frequency of the gradient method, saves the energy that would have been lost during sweeping.

The modules are of the type Yingli Panda YL255C-30b. They are mounted in landscape format on an Ubbink Solar Console 4.2 under an angle of 25° with the horizontal plane heading 152° (Southeast)

The power optimiser is of the type Femtogrid PO310, which was introduced in 2014. All sweeping intelligence in these power optimizers has been switched off. The modules were able to be swept by command according to the gradient method.

The modules are numbered as follows:

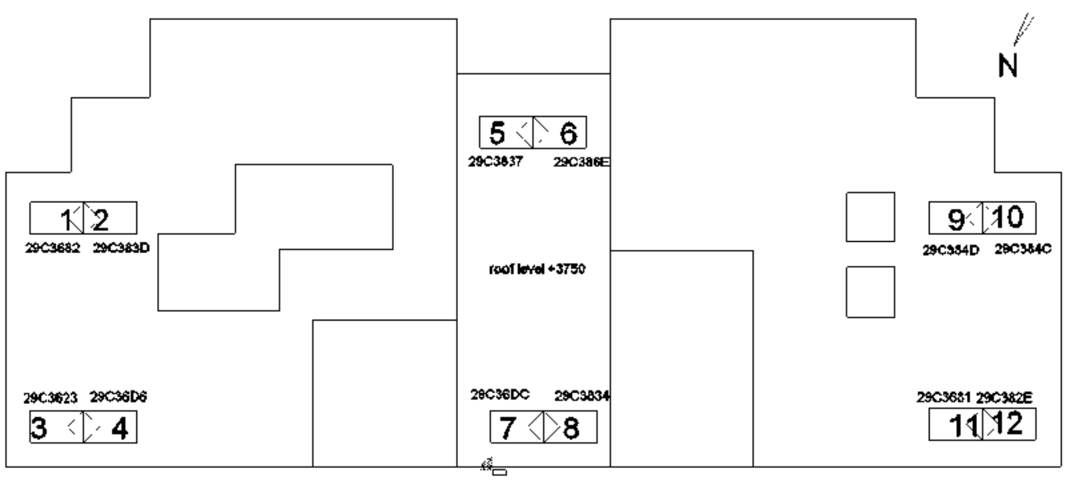

Figure 3.8 Roof layout of Tafelbergweg (not to scale). Module numbers and MAC addresses are shown.

Figure 3.9 An overview of the test modules. Left picture: 3-4 in the foreground, 1-2 in the background. Middle picture: 5-6. Right picture: 11-12 in the foreground, 9-10 in the background.

3.2.2 Testing Methodology

In the experiments the *test* and *reference* modules are swept as follows:

- The six *reference modules* are swept at a constant interval of 5 minutes, all at the same time.
- The six *test modules* are swept according to the gradient method (Cruz Barco, 20140519 Report V6, 2014). If no sweep has taken place after 8 minutes, a sweep is induced. Test modules are swept one after the other

In the summer of 2015 it was found out that the Femtogrid Power Optimizers had been commissioned in the standard mode. See section **Error! Reference source not found.** for a more detailed description hereof. As a result, all tests from October 2014 till late September 2015 were not suitable to evaluate the gradient method, and therefore can only be used as reference. From the 28th of September 2015 onwards the proper tests were carried out on as many week days as possible. Due to agenda restrictions most of these tests could not be manned continuously. On weekend days the test location could not be accessed, and for safety reasons only vertical pole measurements were done.

Not all modules were involved in the test performed between September and October 2015. Early summer 2015 a new airco unit was placed in front of modules 5 and 6. At the end of September 2015, the shade of this airco unit covered the bottom part of the modules, therefore these modules were not used for tests. In terms of shadows, modules 9 through 12 were in good condition for the testing, however now and then, they had data transmission interruptions –in spite of a Zigbee repeater on the edge of the higher roof-, so these modules were not used for the tests. After further evaluation, it turned out that most of the time the data to and from module 9 was transmitted well, therefore the unshaded module 9 is used as the unshaded reference module. Modules 7 and 8 were not used for testing in the morning before 10.30 h, because a new anemometer pole was placed to the Southeast of them.

Figure 3.10 Module 7 with anemometer mast shadow at 9.45 on September 23rd

Modules 1 through 4 were best for testing. Even at the end of September they receive sun from 8.00 h onwards, and the sun disappears after 17.00 h.
There are four software versions for data collection: #8a, #8c, #8d and #8e.
In these software versions the pairing of test and corresponding reference module is as follows:

Table 3.2 #8a and #8c allocation.

#8A software version			#8C software version	
Test module	Corresponding reference module		Test module	Corresponding reference module
1	2		2	1
3	4		4	3
5	6		6	5
7	8		8	7
9	10		10	9
11	12		12	11

Table 3.2b #8d and #8e allocation.

Test module	Corresponding reference module		Test module	Corresponding reference module
1+2	3+4		3+4	1+2
5+6	7+8		7+8	5+6
9+10	11+12		11+12	9+10

3.2.3 Measurement, data collection and data logging

The insolation is measured with a Kipp en Zonen CMP 11 pyranometer attached to module 5 in plane with the module and logged with an interval of 10 s through a Labjack U12. The recorded measurement is the instantaneous value.
The logging of the data from the solar modules is based on the functionality of Femtogrid, where at an irregular interval of every 10 to 20 s instantaneous data from each module is sent to the Femtogrid EAP (Ethernet Access Point), where it can be accessed on a local HTML-page. Part of this information is also sent by GSM to the web monitoring server of Femtogrid, but that data cannot be accessed.

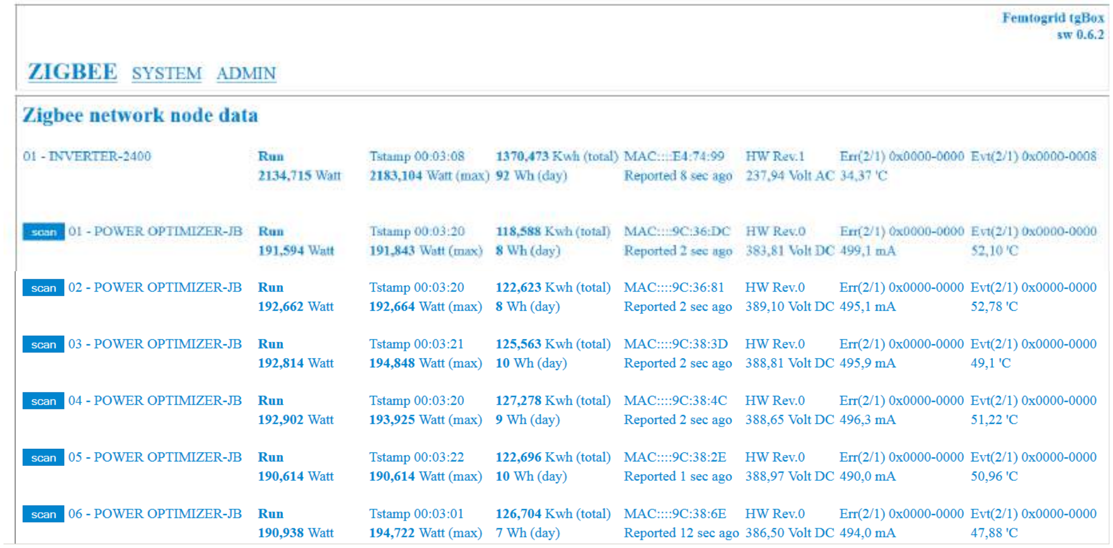

Femtogrid tgBox
sw 0.6.2

ZIGBEE SYSTEM ADMIN

Zigbee network node data

01 - INVERTER-2400	Run 2134,715 Watt	Tstamp 00:03:08 2183,104 Watt (max)	1370,473 Kwh (total) 92 Wh (day)	MAC::::E4:74:99 Reported 8 sec ago	HW Rev.1 237,94 Volt AC	Err(2/1) 0x0000-0000 34,37 'C	Evt(2/1) 0x0000-0008
scan 01 - POWER OPTIMIZER-JB	Run 191,594 Watt	Tstamp 00:03:20 191,843 Watt (max)	118,588 Kwh (total) 8 Wh (day)	MAC::::9C:36:DC Reported 2 sec ago	HW Rev.0 383,81 Volt DC	Err(2/1) 0x0000-0000 499,1 mA	Evt(2/1) 0x0000-0000 52,10 'C
scan 02 - POWER OPTIMIZER-JB	Run 192,662 Watt	Tstamp 00:03:20 192,664 Watt (max)	122,623 Kwh (total) 8 Wh (day)	MAC::::9C:36:81 Reported 2 sec ago	HW Rev.0 389,10 Volt DC	Err(2/1) 0x0000-0000 495,1 mA	Evt(2/1) 0x0000-0000 52,78 'C
scan 03 - POWER OPTIMIZER-JB	Run 192,814 Watt	Tstamp 00:03:21 194,848 Watt (max)	125,563 Kwh (total) 10 Wh (day)	MAC::::9C:38:3D Reported 2 sec ago	HW Rev.0 388,81 Volt DC	Err(2/1) 0x0000-0000 495,9 mA	Evt(2/1) 0x0000-0000 49,1 'C
scan 04 - POWER OPTIMIZER-JB	Run 192,902 Watt	Tstamp 00:03:20 193,925 Watt (max)	127,278 Kwh (total) 9 Wh (day)	MAC::::9C:38:4C Reported 2 sec ago	HW Rev.0 388,65 Volt DC	Err(2/1) 0x0000-0000 496,3 mA	Evt(2/1) 0x0000-0000 51,22 'C
scan 05 - POWER OPTIMIZER-JB	Run 190,614 Watt	Tstamp 00:03:22 190,614 Watt (max)	122,696 Kwh (total) 10 Wh (day)	MAC::::9C:38:2E Reported 1 sec ago	HW Rev.0 388,97 Volt DC	Err(2/1) 0x0000-0000 490,0 mA	Evt(2/1) 0x0000-0000 50,96 'C
scan 06 - POWER OPTIMIZER-JB	Run 190,938 Watt	Tstamp 00:03:01 194,722 Watt (max)	126,704 Kwh (total) 7 Wh (day)	MAC::::9C:38:6E Reported 12 sec ago	HW Rev.0 386,50 Volt DC	Err(2/1) 0x0000-0000 494,0 mA	Evt(2/1) 0x0000-0000 47,88 'C

Figure 3.11 Print screen of HTML-page by Femtogrid

The data displayed by the local Femtogrid HTML-page is shown in 3.11. On the left hand side, the 'scan'-button is shown, which can be clicked to invoke a 'sweep'-command on the corresponding module. The HTML-page should be read from left to right, line after line. It shows the following for each module:

1. Scan-button
2. number and assigned name of power optimizer
3. Run
4. Time stamp
5. Total energy production of module since commission
6. MAC: the MAC-address of the power optimizer
7. HWRev – unknown
8. Err-unknown
9. Evt-unknown
10. 191,594 Watt - the reported power after optimizer [W] (a snapshot of the instantaneous power)
11. 191,843 Watt – the maximum power in the last period [W]
12. 8 Wh (day) – the daily energy yield [Wh]
13. Reported 2 sec ago: the time elapsed since the data was collected and sent to the HTML-page [s]
14. 383,81 Volt: the voltage of the 400 V DC bus [V]
15. 499,1 mA: the current in the 400 V DC bus [mA]
16. 52,1°C recorded temperature of the module or power optimiser

The data however is not stored and therefore the Hogeschool van Amsterdam has added a Java-script for data collecting, sifting and logging. From these sixteen options per module the following are logged as a .csv-file at a fixed interval of 10 seconds:

6. MAC-address
10. Output power (Watt)
13. Time log was reported … seconds ago
14. Voltage (V_{DC})
15. Current (mA)
16. Module temperature Degrees Celsius

A column for the sweep command is added: 0= no sweep; 1=sweep command sent in last interval.
These seven variables are logged for every module, for the central grid inverter, and every line is preceded by a date and time stamp from the computer clock.
On top of the logging functionality the script by Hogeschool van Amsterdam is programmed to give sweep commands at an interval of 5 minutes to the reference panels and to calculate by means of the gradient method whether the test modules should receive a sweep command.

3.2.4 Accuracy of the tests

The following aspects influence the accuracy of the tests:

1. The absolute accuracy of the standard sensors and conversion software used by Femtogrid is under normal tolerances.
2. There are production differences in the Yingli modules (i.e. nameplate differences). The modules were not flashed at the beginning since it was decided to apply relative tests.
3. There are power output differences due to reflected light of structures close by and variable diffuse irradiation.
4. The data collection makes use of instantaneous values, and does not consider the intermediate fluctuations.

The absolute inaccuracies have been evaded by looking at relative outcome, i.e. by comparing modules with each other and with their own performance in other periods. This approach also tackled the production differences, where some trust had to be put in the constant performance in time of all sensors, modules and optimizers.
The instantaneous values should only be a problem on days with fast fluctuations in light such as days with clouds and sunshine alternating quickly. On all other days 10-20 second periods should not show large fluctuations in power.

3.2.5 Accuracy and Calibration of the instruments

Calibration of the pyranometer was done at the factory before delivery. The instrument was checked with a portable pyranometer, type CMP3, and compared to data from a local weather station (http://www.sysanalyser.com/actueel/meteoholendrecht.html). Since the tests are concerned with relative output it is not considered very relevant to further calibrate the pyranometer.
It was decided to use the standard data collection functionality of Femtogrid, which is expected to function with an acceptable relative accuracy. The Yingli module power output tolerances are 0/+5W. Although it is difficult to verify whether there are outliers in the modules, it is expected that the difference will not be significant, there will also be repetition of experiments in order to identify any outlier.
The allocation of the individual modules was verified by subsequent full shading of the respective modules.

3.2.6 Verification of the sweep commands

A special point of attention is the question whether the sweep command actually reaches and is carried out by the power optimizer. Once a sweep command is sent, the Femtogrid Power Optimizer does not provide feedback regarding whether or not it has performed the sweep. The first approach to check whether sweep commands were carried out was by statistical analysis. The November 21st 2014 tests showed a slight increase in energy yield when swept modules were compared with all the other modules at the same moment. For the tests in May to July 2015, a statistical analysis in the Program R showed no significant increase. In August these results were shared with Rob Schaacke of Femtogrid, who proposed a dedicated test that would for certain detect a sweep. After this test was

carried out, it appeared that the software in the Femtogrid Power Optimizers was in the standard mode, with automated sweeps. The proper software for these tests, i.e. with all automated sweeps switched off, was restored early September 2015, after which it could clearly (visually) be detected that sweep commands were actually carried out.
Since much time was wasted in tests with the wrong software, an important recommendation for future tests is to design dedicated tests to detect whether the software is in the right mode.

3.2.7 Test Results for vertical and horizontal shades

Figure 3.12: Location at 10.55 h (left hand picture) and 15.45 h (right hand picture) of the vertical poles relative to modules 7 (right hand module) and 8 (left hand module) from 28th September till 2nd October

The poles cast a shade on their respective module between approximately 10.30 h and 15.00 h. Around 11.45 h the shadow is vertical, which is shown in the graph by the temporary jump in power. This is because for a short period of time, the shade on the strings is minimized.

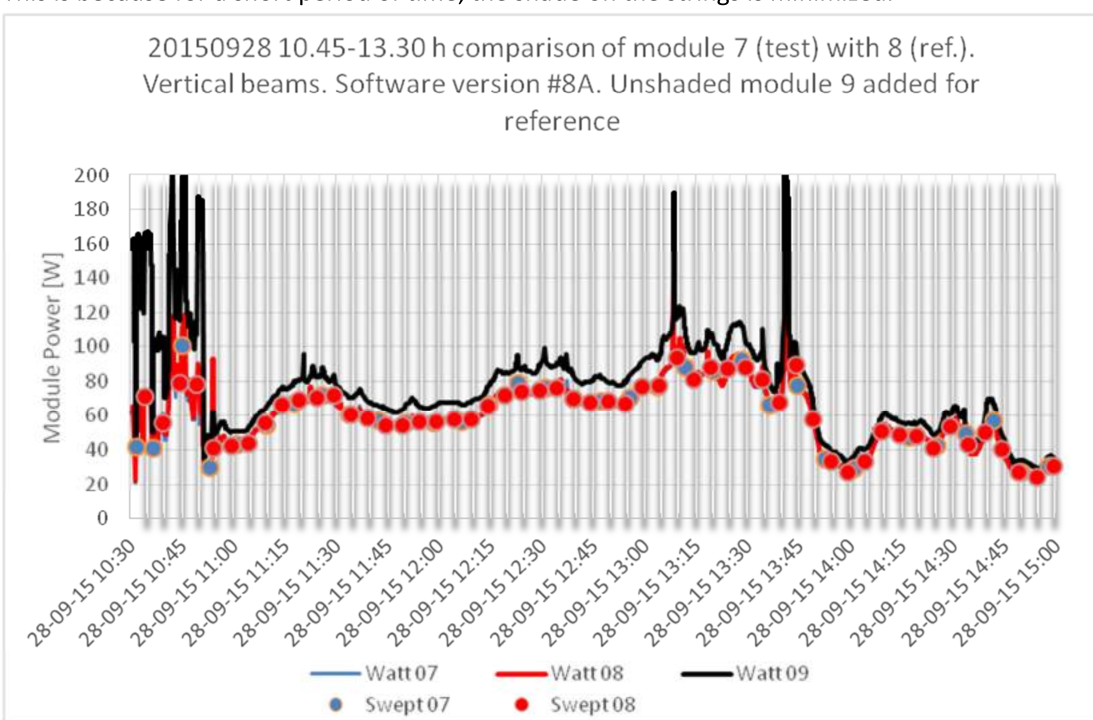

Figure 3.13 Results from 28th September, a day with relatively much diffuse light.

On the 28th September, a mainly cloudy day, the test and reference module have similar outputs so no gradient sweeps are induced. Since the gradient method also saves by reducing the sweeping frequency under uniform irradiation conditions (either direct or diffuse irradiation), an estimate can be made of the energy saved by the gradient method. In this case, from 10:30 – 15:00 the amount of sweeps in the test module is 21 sweeps less than the amount of sweeps in the reference module. Assuming that each of these sweeps causes a loss of approximately 33% power in one second and assuming 70W in average, the method has saved 0.154 Wh/module/day.

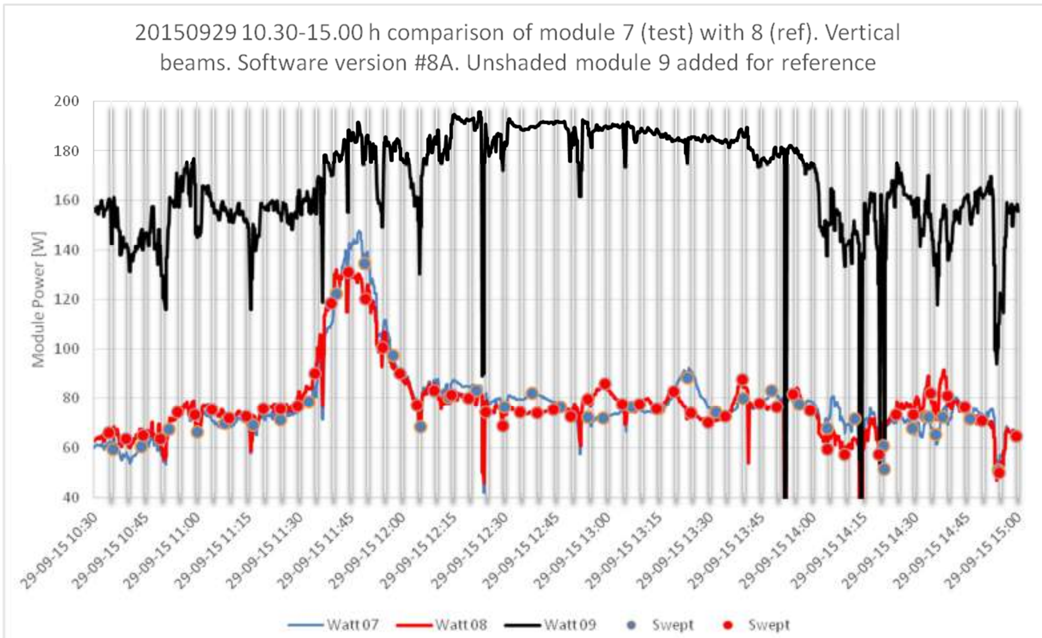

Figure 3.14 On the 29th September the light is more direct.

In figure 3.14, at 13.00 and from 14.20 to 14.40 gradient sweeps can be observed in module 7. The sweep at 13.00 h does not produce a higher module output. The period between 14.20-14.40 is zoomed in below:

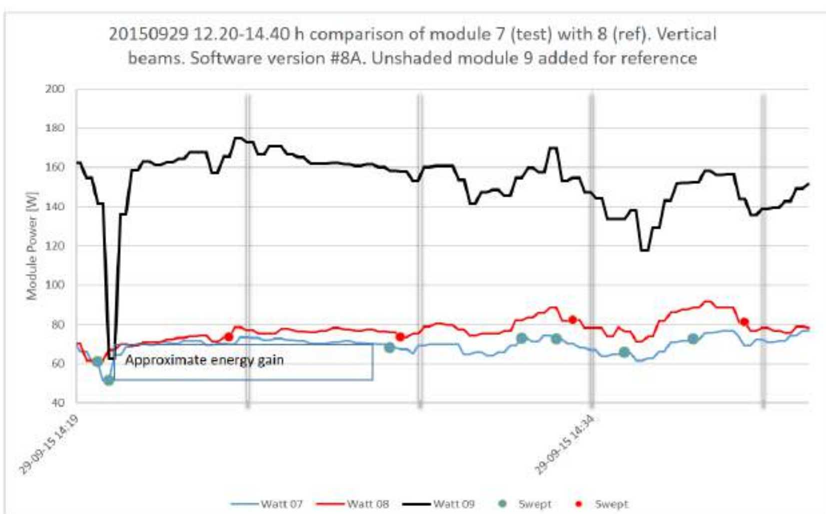

Figure 3.15 zoom from 3.14.

In figure 3.15 the gradient sweep at 14.20 h produces a jump of just under 20 W. The rectangle of a length of 5 minutes and a height of 20 W presents the amount of energy gained by the sweep: approximately 1.67 Wh. The final result is the sum of the energy savings due to less sweeping when not needed (17 saved sweeps equivalent to approx. 0.124 Wh) and due to smart sweeping when is needed (1.67 Wh) giving in total 1.8 Wh.

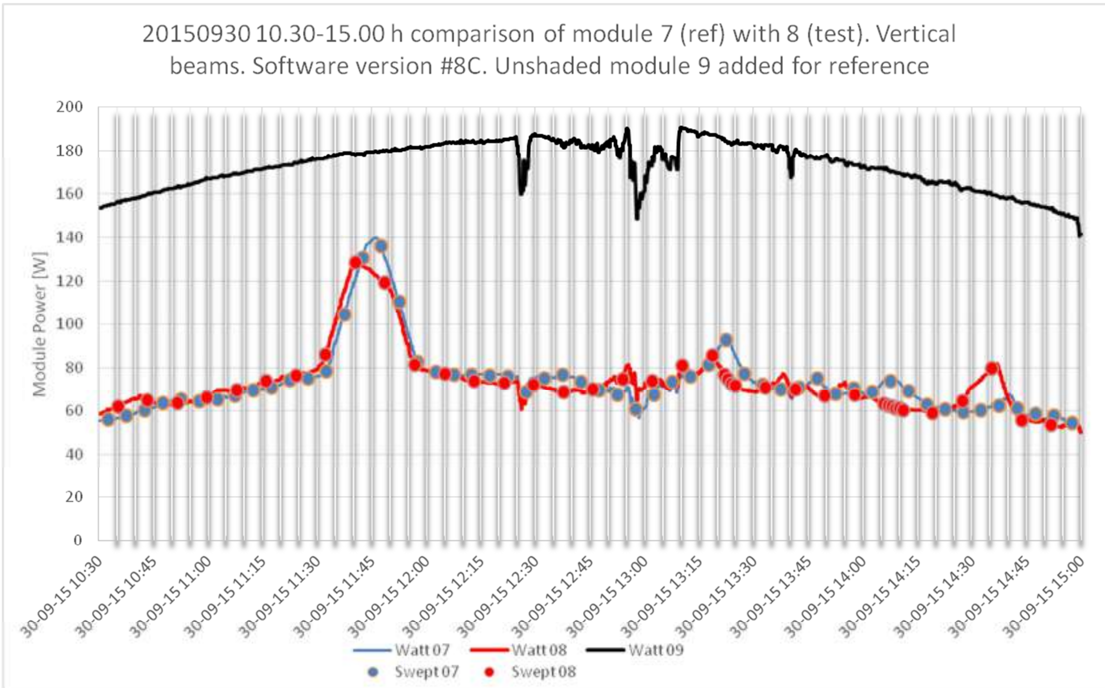

Figure 3.16 On the 30th September the day is strongly sunny.

In figure 3.16 the jump around 11.40 h is observed when the shadows are perpendicular to the strings and thus cover the least area of the cells. Several gradient sweeps can be observed at 13.25 and again at 14.05-14.10. None of these sweeps produce a jump in power, so the gradient method could even be counter-productive if the amount of sweeps would be higher than the amount of reference sweeps, which is not the case here.

Table 3.3 energy yield in test period 28-30 September 10.30-15.00 h, vertical pole tests

Shaded modules, vertical poles	Module 7 [Wh]	Module 8 [Wh]
28th September 2015 10.30-15.00 h Software version #8A	263.02 (test module, 34 sweeps, no gradient sweeps)	276.65 (ref. module, 54 sweeps)
29th September 2015 10.30-15.00 h Software version #8A	350.08 (test module, 37 sweeps of which 3 gradient sweeps)	349.07 (ref. module, 54 sweeps)
30th September 2015 10.30-15.00 h Software version #8C	329.77 (ref. module, 54 sweeps)	328.63 (test module, 41 sweeps of which 7 gradient sweeps)

If the yield of module 7 on 29th September from Table is compared with the previously detected increase in yield of app. 2.64 Wh, the yield increase due to the gradient sweep at 14.20 h is 0.75 % of the total yield during the period between 10.30 and 15.00 h.

The results are insufficient to provide a conclusion regarding the test, and if positive, the increase is low. Possibly a different view appears if the modules are compensated[23] for differences in performance under unshaded conditions on a day with comparable insolation in the same period of the day. This will be assessed below.

For compensation two days after 6th October had to be chosen, because from this day onwards modules 7 and 8 were left unshaded. Unfortunately, days with insolation comparable to 28 – 30 September could only be found nearly a month later.

On the 25th October 2015, a sunny day alternated by clouds, for the period 10.30 – 15.00, module 7 (ref. 54 sweeps) has a 0.993 times lower production than module 8 (ref, 34 sweeps)

On the 29th October 2015, a sunny day, for the period 10.30 – 15.00, module 7 (ref. 54 sweeps) has a 0.997 times lower production than module 8 (test, 54 sweeps).

From these two reference days it is concluded that modules 7 and 8 perform very similarly, so no compensation is needed. It is concluded that the tests on 28 and 30 September cannot be used to verify that the gradient method provides more yield, whilst the test of September 29th shows a light increase in yield of 0.75 % or 2.64 Wh in 6.5 hours due to the gradient method.

On September 30th it was found that the shadow in the previous days covered all three strings of both the test and the reference module at the same time during most of the test period. Therefore, on the October 2nd the poles were put in a new position. Although the author failed to record the exact position of the poles, fortunately, the days were very similar and the data collection software versions were opposed, so the two days can be taken for comparison. With the data from October 1st incomplete, the period that will be compared is from 8.15 h to 10.15 h. The shadow of the anemometer (see 26) hits module 7, but does not influence this test.

[23] The compensation procedure is explained in appendix 1

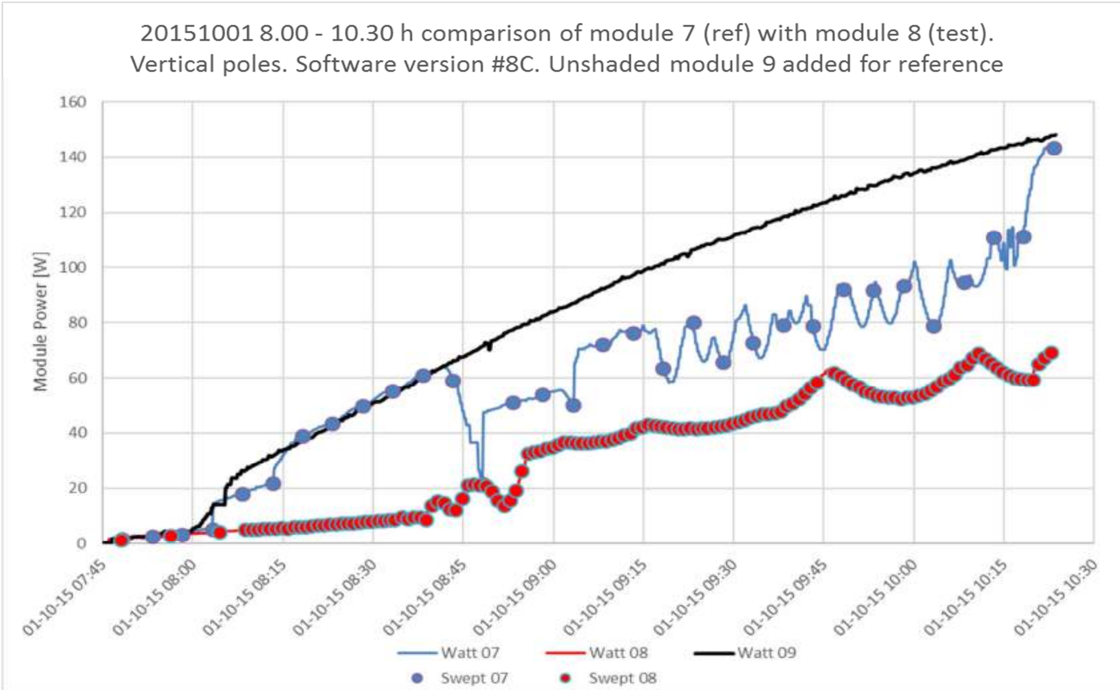

Figure 3.17 On the 1st October the sky was bright. Exact position of the poles not recorded.

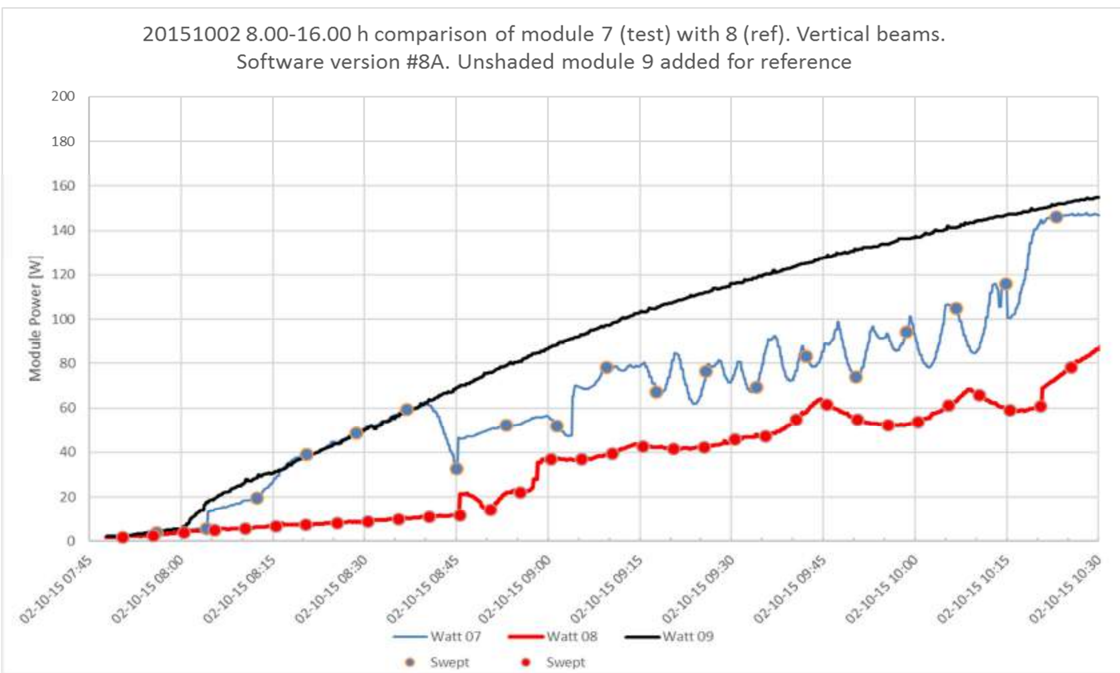

Figure 3.18 On the 2nd October the sky was bright. Exact position of the poles not recorded.

The tests on 1st October show that module 8 performs a gradient sweep every minute, whilst on 2nd October no gradient sweeps occur during the entire period because the power output of test module 7 is always above or equal to the output of reference module 8.

Table 3.4 Energy yield in test period 1-2 October 8.15 - 10.15 h, vertical pole tests

Shaded modules, vertical poles	Module 7 [Wh]	Module 8 [Wh]	Module 7+8 [Wh]	Ratio modules 7 / 8
1st October 2015 8.15-10.15 h	136.98 (ref) 24 sweeps (~ 0.176 Wh[24])	72.23 (test) 118 sweeps (~ 0.437 Wh)	209.21	1.896
2nd October 2015 8.15-10.15 h	137.99 (test) 15 sweeps (~ 0.11 Wh)	72.48 (ref) 24 sweeps (~ 0.088 Wh)	210.47	1.904
Ratio 1st / 2nd October	0.993	0.997	0.994	

Shaded modules summed up	Test modules [Wh]	Reference modules [Wh]
1st and 2nd October 8.15 – 10.15 h	210.22	209.46

Here a mildly higher yield from the test modules is noticed, but this is not due to the gradient sweeps, because the additional yield was made on October 2nd, when module 7 experienced no gradient sweeps at all. On the 1st of October, the Gradient method made extra and unnecessary sweepings: 94 more than the reference panel. This test show that the gradient method does not perform appropriately, as it is constantly sweeping, and in doing so it has wasted approximately 0.35 Wh more when compared to the test on the 2nd of October. However, if the surface were bigger, only the ones in the shadow frontier would be sweeping faster, and the ones in the shadow or direct light would be sweeping at a lower frequency, therefore saving energy for the whole system, but that would be another experiment.

At the end of Friday October 2nd the modules were left in a new position for the weekend days to come, see photo below.

Figure 3.19 Photo from 2nd October 2015 at 15.50 h to show the position of the vertical poles relative to modules 7 (right) and 8 (left)

[24] Assuming 24 sweeps of 1 second; 33% approximate loss of power per sweep; 80 W $P_{Average}$

Saturday the 3rd October was a cloudy day, so the data cannot be used.

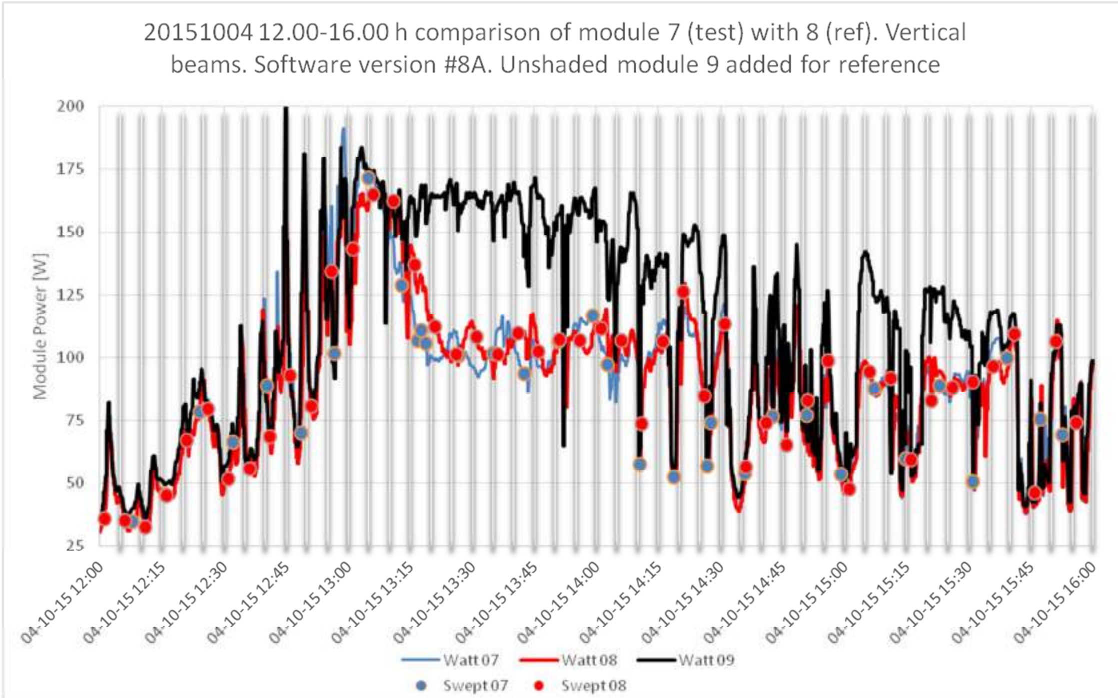

Figure 3.20 Sunday 4th October. Quite a sunny day with occasional clouds.

Each pole only casts a shadow on the respective module from 12.30 h to approximately 15.45 h, therefore this period is usable for analysis. Some high frequency gradient sweeps can be seen between 13.15 h and 13.45 h. This period is zoomed in in the next figure:

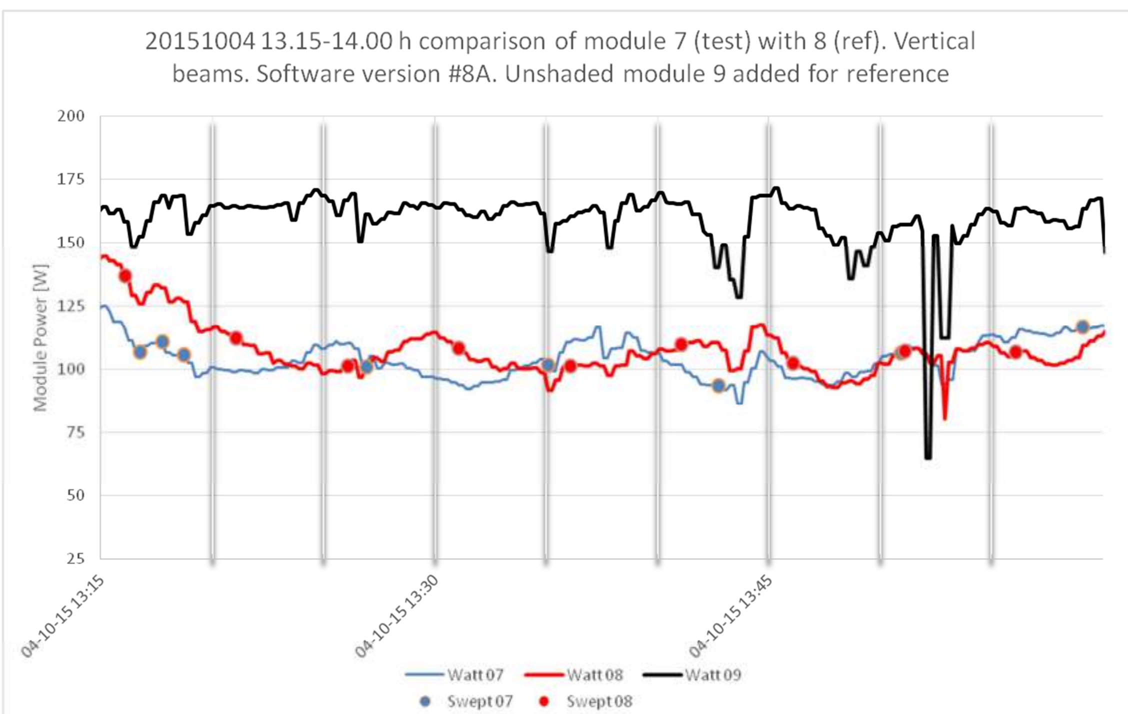

Figure 3.20: Zoom of figure 3.20

In figure 3.20 three gradient sweeps can be seen at 13.17, 13.18 and 13.19. Only the first sweep induced a very small jump in power.

Table 3.5Energy yield on Sunday 4th October 12.30-15.30 h, vertical pole tests

Shaded modules, vertical poles	Module 7 [Wh]	Module 8 [Wh]
4th October 2015 12.30 – 15.30 h	291.87 (test) 26 sweeps of which 3 or 4 high frequency gradient sweeps	292.64 (ref) 36 sweeps

Not much can be concluded from this test, unless the modules are compensated for differences in performance under unshaded conditions on a day with comparable insolation in the same period of the day. Three days with a comparable amount of light are chosen: 25-27 October

On the 25th of October 2015, a sunny day alternated by clouds, for the period 12.30 h – 15.30 h, module 7 (ref. 36 sweeps) has a 1.002274 times higher production than module 8 (ref, 36 sweeps)[25]

On the 26th of October 2015, a sunny day alternated by clouds, for the period 12.30 h – 15.30 h, module 7 (ref. 36 sweeps) has a 1.003712 times higher production than module 8 (ref, 36 sweeps)

On the 29th of October 2015, a sunny day, for the period 12.30 h – 15.30 h, module 7 (ref. 36 sweeps) has a 0.994733 times higher production than module 8 (test, 23 sweeps).

From these two unshaded reference periods it is concluded that modules 7 and 8 perform similarly, and that the tests on October 4th do not show any benefit from the gradient method.

From October 6th to October 11th the vertical pole tests were redirected towards modules 1 and 2, but the test principle did not differ much from the tests on modules 7 and 8 that were described in sections **Error! Reference source not found.** and **Error! Reference source not found.**. The difference is that the poles were set further away from the modules, see photo below.

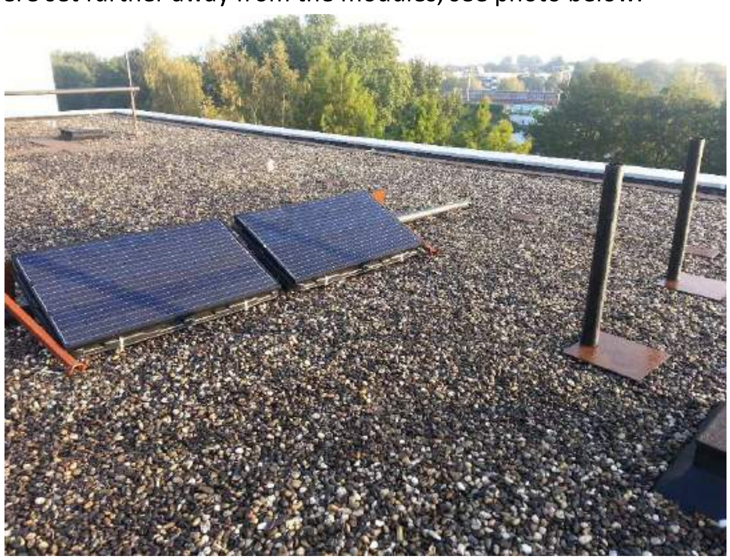

Figure 3.21: 9th October 8.50 h

[25] Both neighbouring modules are reference modules because of the applied (faulty) data collection software #8D and #8E. Since the modules are not shaded, the module power can be used for reference.

Only results from 9th and 11th October from 9.00 h till 10.15 h are useful. Both days were sunny till around 10.45 h, and the tests are mirrored with respect to the data collection software versions used.

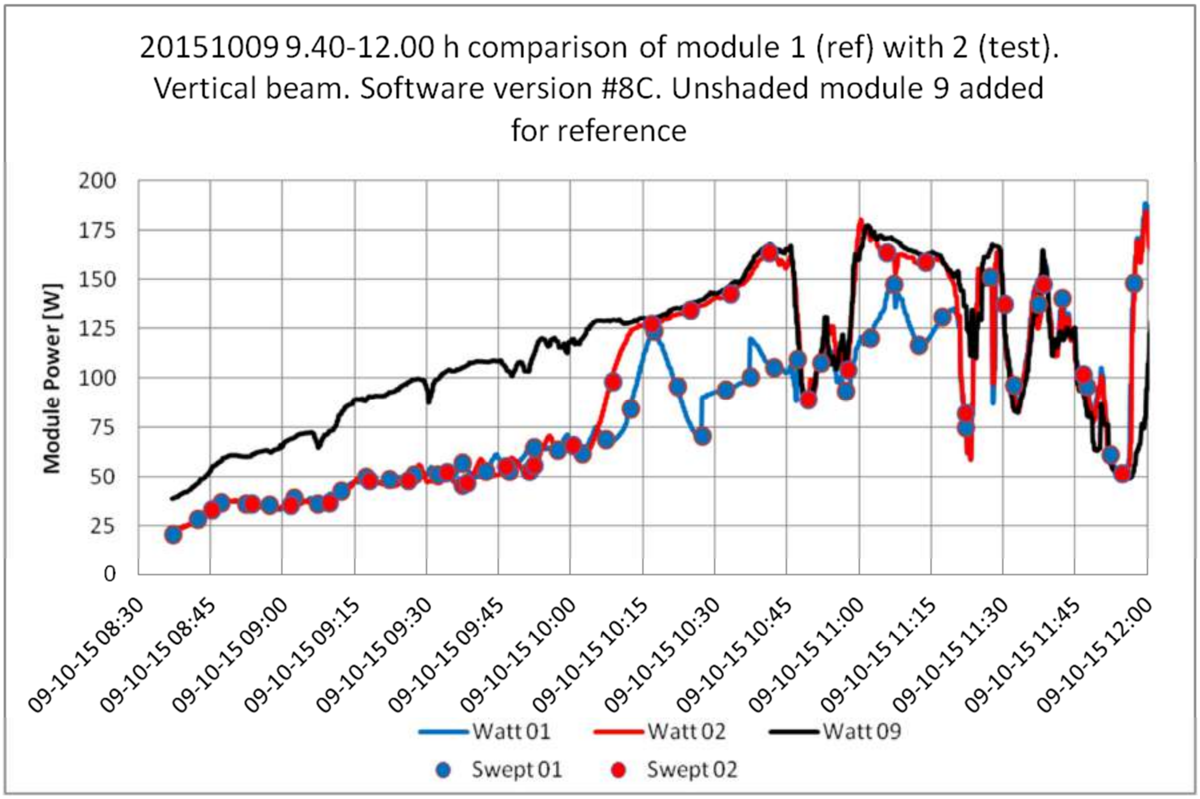

Figure 3.22: 9th October

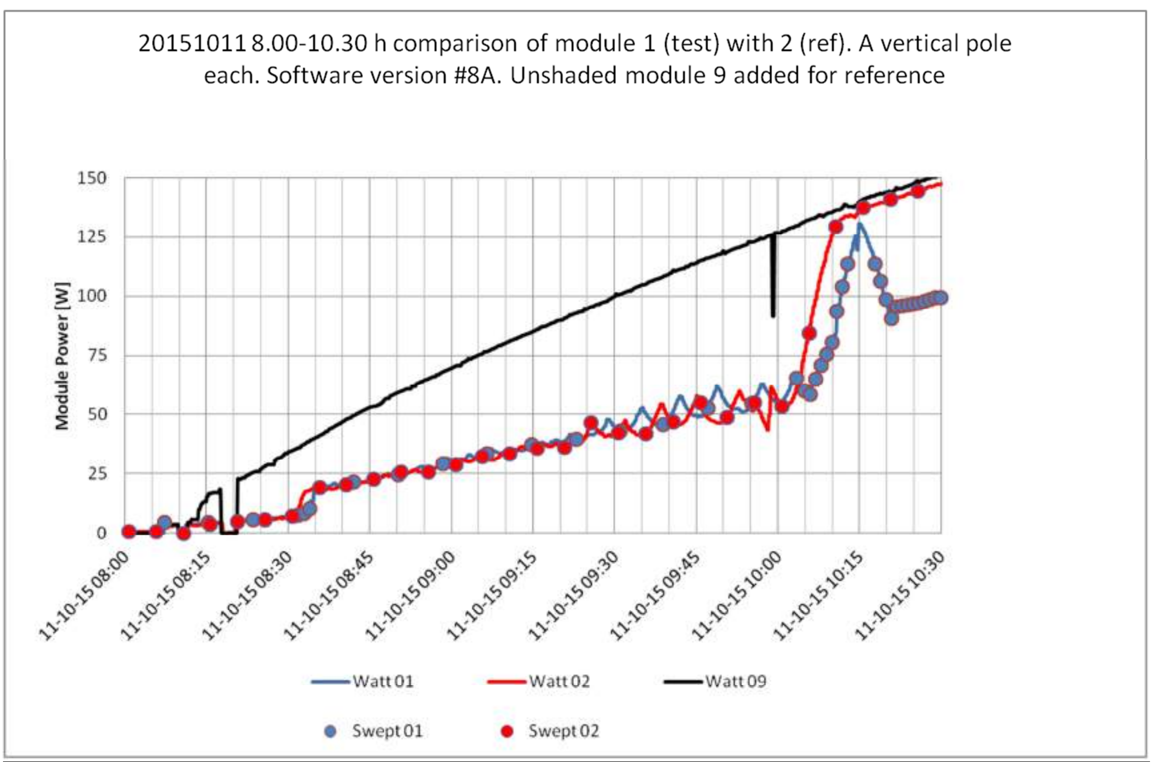

Figure 3.23 11th October

If the period from 8.45 h - 10.45 h is taken for both days, the energy yield of modules 1 and 2 is as follows:

Table 3.6 production results in the test periods

Shaded modules	Module 1 [Wh]	Module 2 [Wh]
9th October 2015 8.45-10.45 h	128.41 (reference)	151.76 (test)
11th October 2015 8.45-10.45 h	122.44 (test)	147.24 (reference)

The tests show a 0.53 % better performance of the two reference modules when compared to the tests modules. Not much can be concluded from this test, unless the modules are compensated for differences in performance under unshaded conditions on a day with comparable insolation in the same period of the day.
The chosen day is Saturday October 3rd 2015. The results are:

Table 3.8

Shaded modules summed up	Test modules [Wh]	Reference modules [Wh]
9th and 11th October 8.45 – 10.45 h	274.20	275.65

The tests on 3rd October show a 2.77 % higher energy yield for module 1 when compared to module 2 in exactly the same period and under the same circumstances. What would happen if the power of module 2 in the shaded tests on the 9th and 10th October were set at 2.77 % higher yield? This is shown in the two next tables.

Table 3.9 performance of test and reference modules after compensation

Modules compensated for unshaded performance	Module 1 [Wh]	Module 2 [Wh]
9th October 2015 8.45-10.45 h	128.41 (reference)	155.96 (test)
11th October 2015 8.45-10.45 h	122.44 (test)	151.31 (reference)

Table 3.10 comparison of test and reference modules after compensation

Shaded compensated modules summed up	Test modules [Wh]	Reference modules [Wh]
9th and 11th October 8.45 – 10.45 h	278.40	279.73

Now the reference modules outperform the test modules by 0.48 %, which is not that different from the non-compensated results.
One pole was placed in front of modules 1 and 2 and another in front of 3 and 4. Adjacent modules were always paired as test and reference module for the gradient method. The vertical pole was placed such that the shadow moves from top left to bottom right across modules 2 and 4, approximately from 8.00 till 10.30 h. The shadow hardly hits the lower left corner of modules 1 and 3 and leaves the surfaces after 10.30 h.

Both on the 28th and 29th it was cloudy until 10.30 h, so the data from those two days is not useful. The data from 30th and 31st October can be used however:

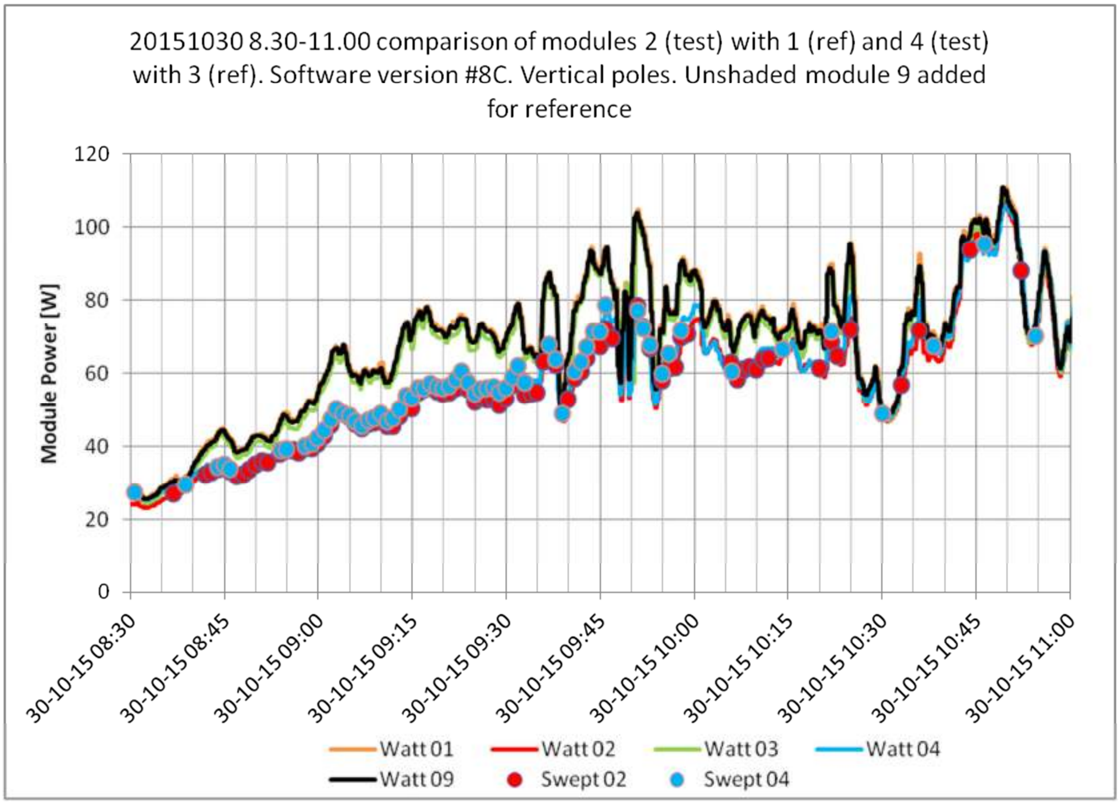

Figure 3.24: 30th October. Sweeps from both test modules are shown. Reference modules were swept every eight minutes.

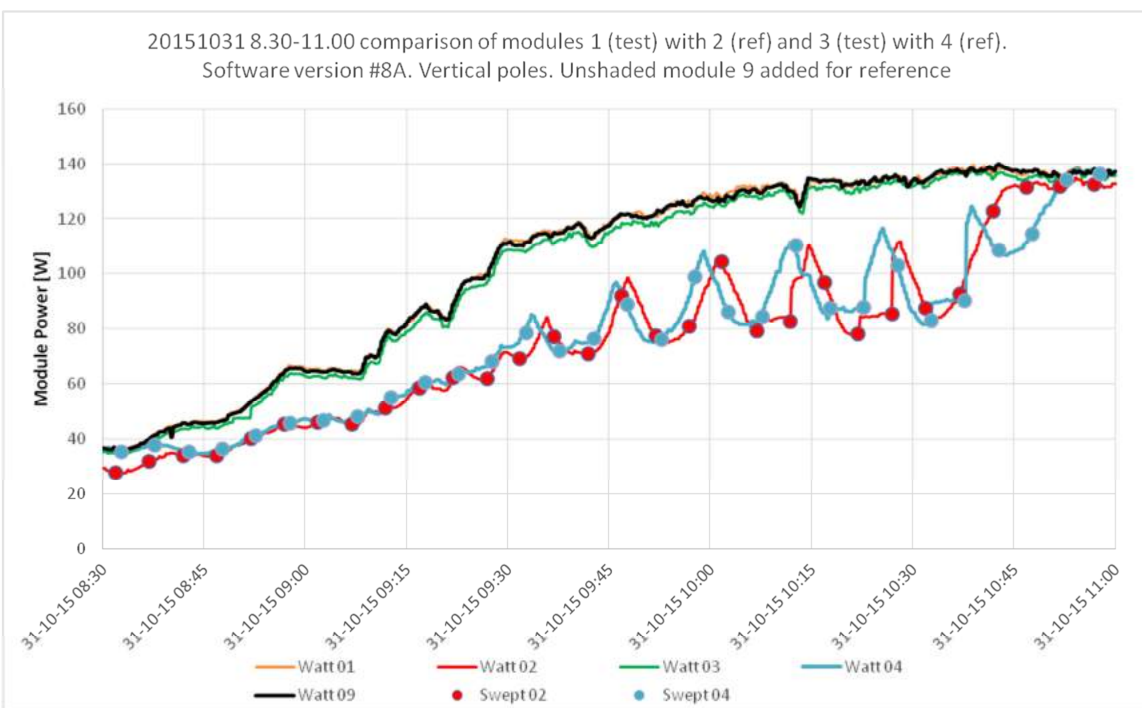

Figure 3.25 31st October. Sweeps from modules 2 and 4 (now both reference modules) are shown, so that the test can be compared with the test on October **30th**

Table 3.11 production results in the test periods

Shaded modules	Module 1 [Wh]	Module 2 [Wh]	Module 3 [Wh]	Module 4 [Wh]
30th October 2015 8.30-10.30 h	130.02 (ref. 24 sweeps)	104.19 (test, 84 sweeps, > 60 gradient sweeps)	124.86 (ref. 24 sweeps)	107.40 (test, 62 sweeps, > 38 gradient sweeps)
31st October 2015 8.30-10.30 h	190.46 (test, 15 sweeps, no gradient sweeps)	130.72 (ref. 24 sweeps)	185.00 (test, 15 sweeps, no gradient sweeps)	135.96 (ref. 24 sweeps)

Since the two days cannot be compared in terms of insolation, a comparison could be to assess the ratio of energy between the paired modules on both days:

Table 3.12 relative performance

Shaded modules	Module 1/Module 2	Module 3/Module 4
30th October 2015 8.30-10.30 h	1.2479	1.1625
31st October 2015 8.30-10.30 h	1.4570	1.3606

This approach does not work because the differences between shaded and unshaded increase with the amount of direct light (which was more abundant on the 31st October). A better idea would have been to place one pole in front of module 1 and the other in front of 4 (instead of 3).

Between September 28th and October 2nd horizontal beams were placed in front of modules 1+2 and in front of modules 3+4. The horizontal beams have challenges: they easily start vibrating in wind and it is difficult to keep them from hanging through, especially when it is hot. This makes it difficult to cast the shade equally on all four modules. The limited length of the beam, app. 6 m, makes that the valid test periods are limited to a part of the day. For safety reasons (fear of wind gusts sending the beams over the edge of the roof) the horizontal beams cannot be left overnight. The exact positioning at renewed setup is difficult, even when supports are left in the same position overnight, which makes exact repeatability of the tests difficult.

Figure 3.26: Beam in front of modules 1 and 2. In the background the beam in front of modules 3 and 4

For a good overview the sweep moments are presented slightly different from the previous tests. First the results from the four testing days is shown, followed by an observation.

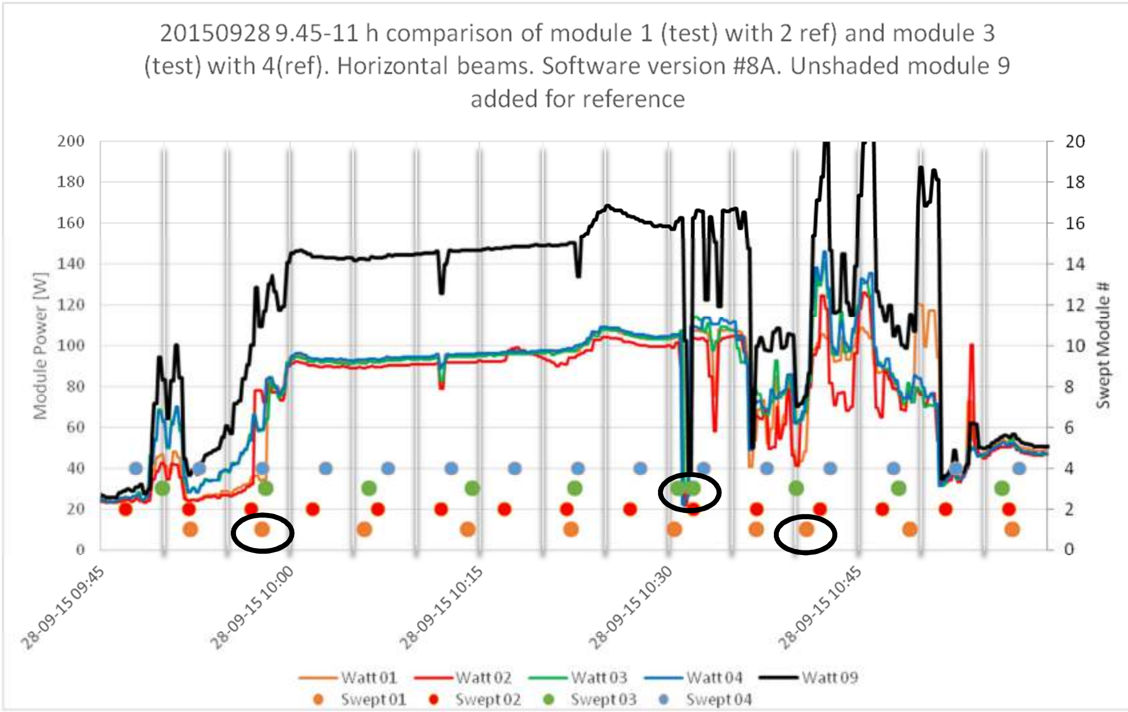

Figure 3.27 28th September 2015 horizontal beam tests

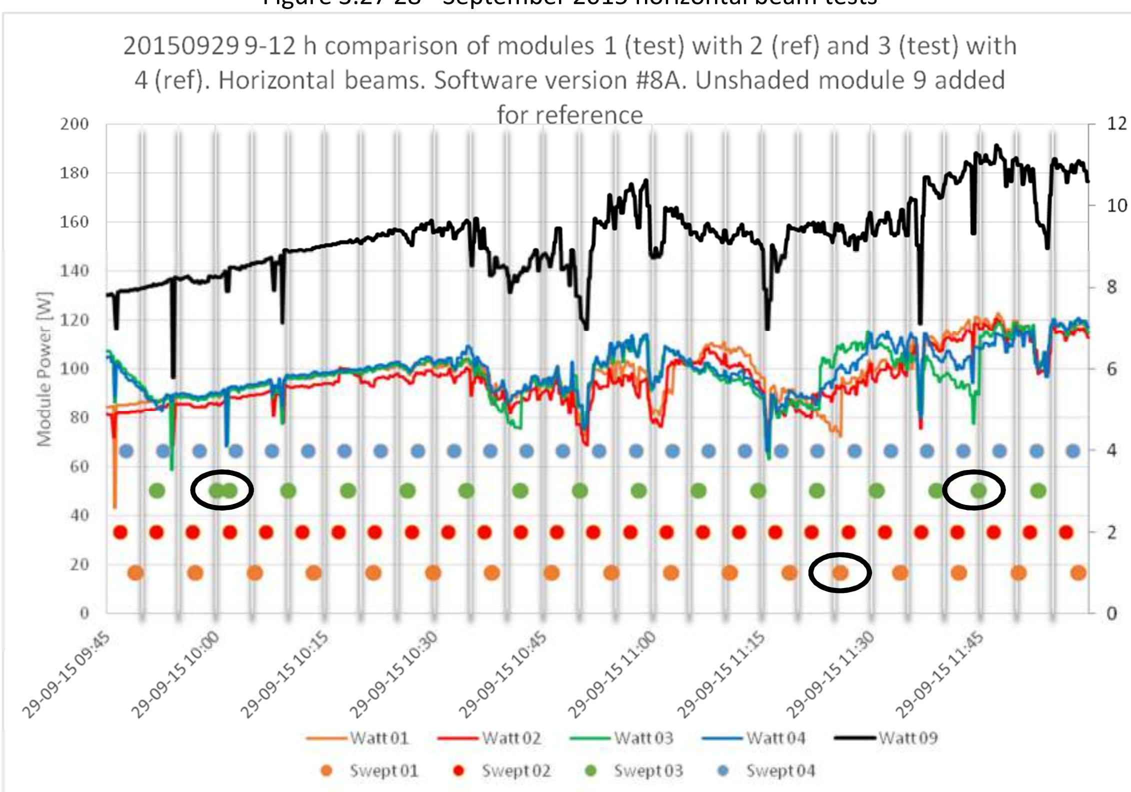

Figure 3.28: 29th September 2015 horizontal beam tests

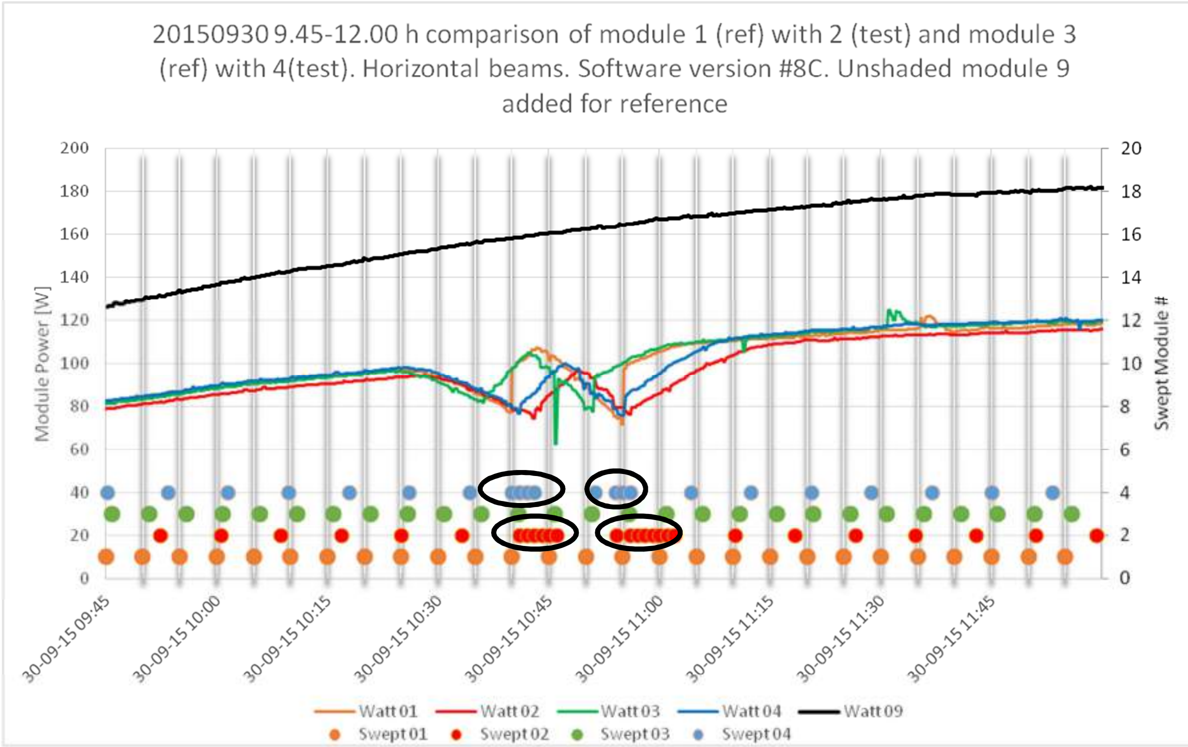

Figure 3.29: 30th September 2015 horizontal beam tests

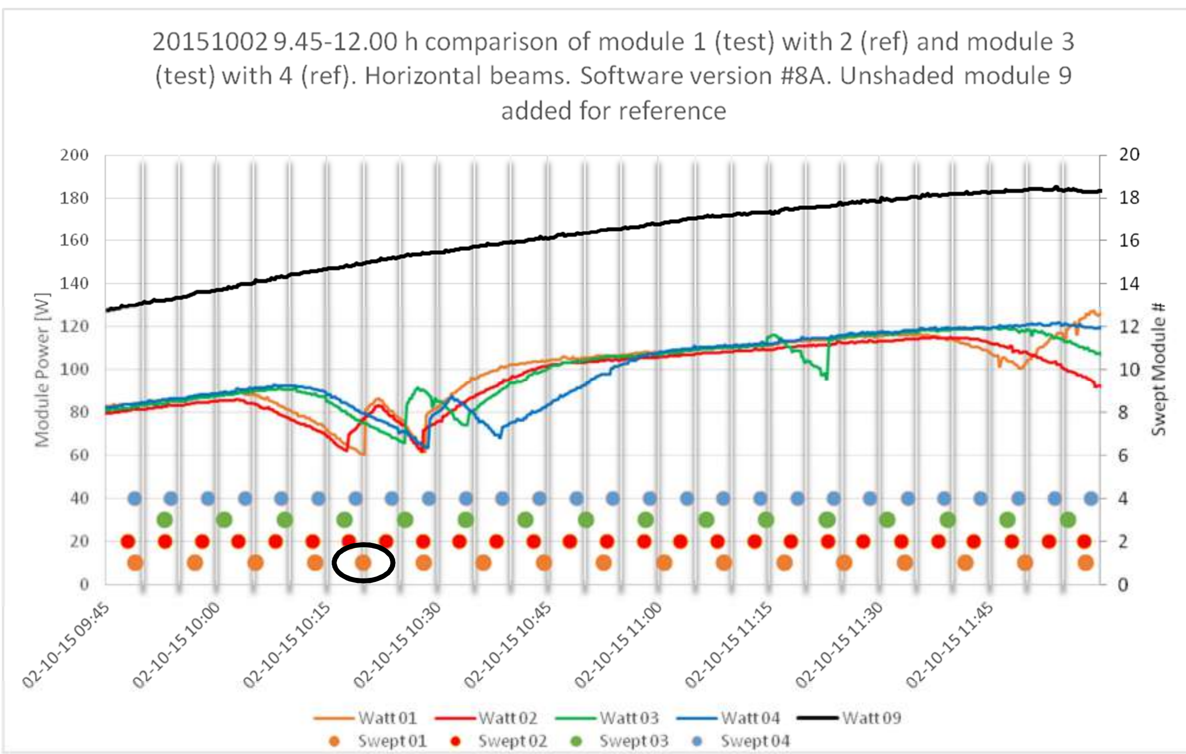

Figure 3.30: 2nd October 2015 horizontal beam tests

Observations from the previous four figures: the gradient sweeps have been circled. These occur at changes due to clouds or when the shades move from one string to the next. In FIGURE 3.29 and 3.30 a slight energy gain due to the gradient method is observed. If 30/09 and 02/10, two days with a very similar insolation pattern, are compared it is seen that the shadows were not placed in the same place.

The period from 9.45 h to 11.30 h the horizontal poles cast a shadow on both neighboring modules simultaneously, whilst the shadows of support poles remain away from the surfaces. This period is chosen for further analysis. First the results in energy will be drawn up.

Table 3.13 energy yield for the shaded modules on the 28th September till the 2nd October

Shaded modules	Module 1 [Wh]	Module 2 [Wh]	Module 3 [Wh]	Module 4 [Wh]
28th September 2015 9.45-11.30 h	130.31 (test, 12 regular sweeps, 2 gradient sweep)	125.07 (ref. 21 sweeps)	131.66 (test, 13 regular sweeps, 1 gradient sweep)	133.12 (ref. 21 sweeps)
29th September 2015 9.45-11.30 h	165.12 (test, 13 regular sweeps, 1 gradient sweep)	159.86 (ref. 21 sweeps)	167.85 (test, 12 regular sweeps, 2 gradient sweeps)	169.48 (ref. 21 sweeps)
30th September 2015 9.45-11.30 h	170.24 (ref. 21 sweeps)	161.11 (test, 12 regular sweeps, 11 gradient sweeps)	170.59 (ref. 21 sweeps)	168.61 (test, 12 regular sweeps, 7 gradient sweeps)
2nd October 2015 9.45-11.30 h	167.95 (test, 12 regular sweeps, 1 gradient sweep)	162.87 (ref. 21 sweeps)	166.93 (test, 13 regular sweeps, no gradient sweeps)	164.15 (ref. 21 sweeps)

The results do not show a consistent improvement in performance of the test modules when compared to the reference modules. A combination of two or more days might give a clue. Since 30 September and 2 October are such similar days, and the test and reference modules are swapped, the ratios of the paired modules are given:

Table 3.14 ratios of energy yield from paired modules

	Ratio module 1/module 2	Ratio module 3/module 4
30th September 2015 9.45-11.30 h	1.057 (ref/test)	1.012 (ref/test)
2nd October 2015 9.45-11.30 h	1.031 (test/ref)	1.017 (test/ref)

The ratios show a lesser performing test module when module 1 is compared to module 2 on the two days, whilst in module 3 and 4 the test module has a better relative performance. It cannot be concluded that this is due to the gradient sweeps because the shadows were not equally placed on the two days.

3.2.8 Conclusions and Recommendations

This report provides an overview of test results intended to evaluate the surface gradient method in an experimental context with a number of setups (horizontal and vertical shadows). The gradient method is meant to recover part of the energy losses from sweeping and suboptimal power points.

Although small increases in energy yield due to gradient sweeps were detected visually from the graphs (apparently the method triggered some jumps in output adequately), the results cannot be reproduced significantly in the numerical summation of the energy. From simulations it is likely that the gradient method improves the result, but in the tests that were carried out this has only partly been proven.
The tests further show that the current sweeping strategies of used power optimizers is relatively effective in minimizing energy losses in shadow casting situations. This was noticed in the first nine months of the tests, when the power optimizers were in standard mode and showed limited losses. As was hypothesized in the simulation model, the gradient method does not provide major improvements in energy yield if at all reproducible.
The results further suggest that further effort to improve energy yield of individual modules through smart sweeping strategies provides limited added value. This may differ in the case of larger solar installations.
The execution of the tests suffered organizational and technical problems. The start of the tests was slow due to low availability of technicians from Femtogrid. Then it took rather long before it was discovered that the sweeping software was not in the testing mode. Other difficulties encountered were that the expected improvement in energy lies below tolerances of the devices and that the irradiance was not always repeatable. Despite these organizational and technical problems, the test results are considered to be sufficiently valid to come to above conclusions.
As a recommendation these tests should be repeated with the modules much closer to each other, because it is expected that in a larger surface (more than 2x2 modules) we could see better improvements.

<u>Learning points next test:</u>

- Make time-lapse images to verify how the shadow moves. Synchronise all clocks before filming.
- Bring thermo-graphic camera and take frontal shots of modules to detect whether a string has been by-passed.

Chapter 4: Performance Simulation Model

4.1 Correlations of shading fracture and power output in c-Si solar modules

A steady state solar simulator[26] was utilized for a series of shading experiments on a solar module with 60 series connected monocrystalline silicon cells. The module consists of 3 groups of 20 cells and each group is connected anti-parallel with a by-pass diode. An IV tracer was recording performance under standard test conditions (25 C, 1000w/m2 irradiance). Artificial shading was applied with two means: a) opaque masking with black cardboard and b) wire meshes with reduced transmittance. The reason of using two shading strategies is to represent field conditions where the beam B irradiance is obstructed and sky diffuse D remains relatively the same.

Measurements were performed for cell shading percentages of: 10, 15, 20, 25, 30, 35, 40, 50, 75 and 100%. Twelve different cells were shaded for every shading fraction giving a total of 120 I-V curves per shading material in order to provide a distribution of the shade effect since the shading response is highly associated with shunt resistance of individual cells [8]. In figure 4.2 the relative power output in correlation with the shading fraction can be seen. As expected the opaque shading is causing the largest drop in power output. It is important to mention that even shading a very small portion of a single solar cell (10%-50%) leads to disproportional losses in power output. When shading as a fraction of a single solar cell's surface exceeds 50% then there is a total reduction of power at that cell's group due to the activation of the by-pass diode. Thus further shading of the specific cell or group of cells will not have any consequence in power output. These results are supported by similar work in the field [7].

From figure 4.3 one can determine the relative effective shading fraction by comparing the power output for the different transmittance materials. For example the power output with the 67% transittance mesh shading 100% of the cell is equivalent to 33% opaque shading. This transition can be better seen in figure 4.3. The results for all the three different transmittance materials fit perfectly leading to equation 1 which describes the effective equivalent irradiance of a partially shaded solar cell.

$$G = (unshaded\ fraction\ \% * global\ irradiance\ in\ plane) \\ + (shaded\ fraction\ \% * diffuse\ irradiance)$$

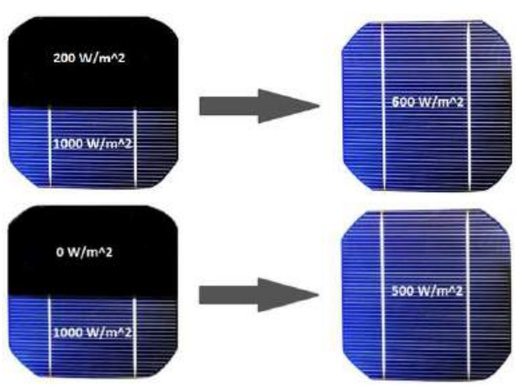

Figure 4.1: Application of the irradiance equivalent equation

[26] http://www.eternalsun.com/products/solar-simulator

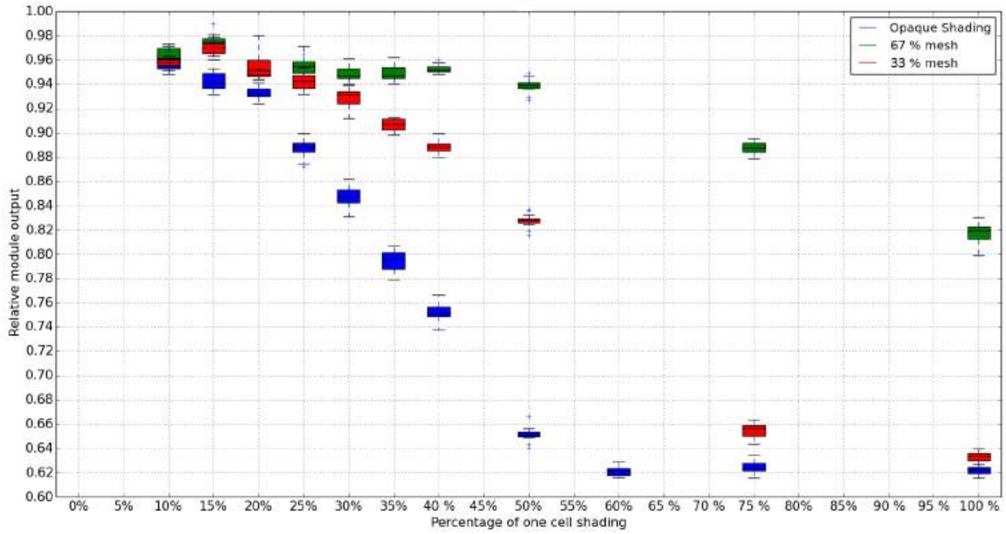

Figure 4.2**:** Relative power output for various shading percentages of a cell by using wire meshes and opaque cardboard

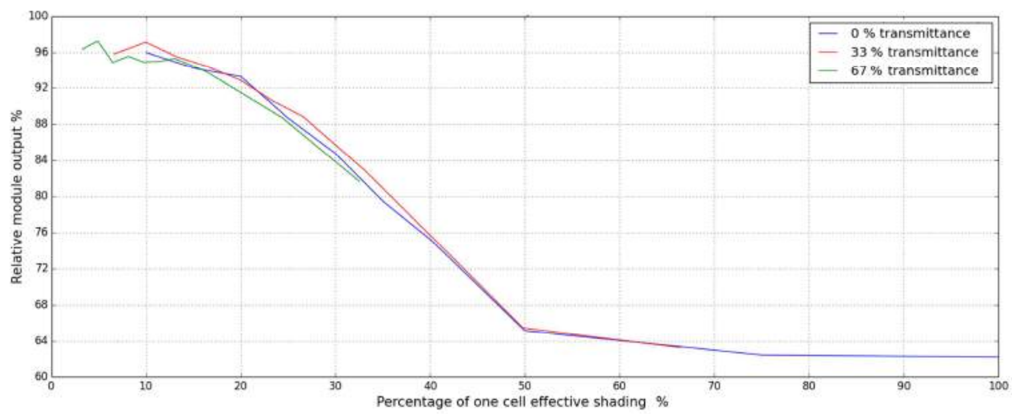

Figure 4.3: Relative effective shading fraction versus power output for three different shading materials

4.2 Building blocks of the model

The complete MLPM yield model includes 5 different models integrated into one. Namely, it includes a 3D SketchUp model, a shading model, a radiation model, a DC and an AC simulation model. All the model inputs used in the complete model and the flow of simulation processes are shown in fig. 4.4. In the following sections, each one of the models will be separately presented along with all its specifics.

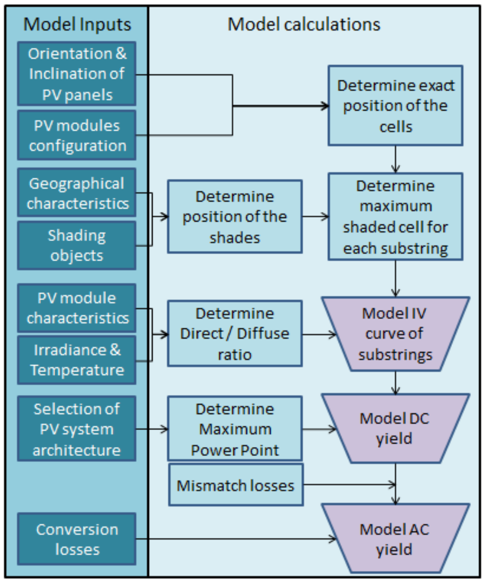

Figure 4.4: Yield model inputs and flow of simulation processes

4.2.1 3D Shading model and determination of shading fraction

To accurately predict the power output and behavior of a partially shaded solar module, the shade coverage of the module's surface has to be known. For this reason, a computer-aided design tool is used to represent the installation site including the PV modules and the obstruction elements which cause the partial shading. There is a big variety of CAD software available in the market but for this study Google SketchUp [9] is used.


Figure 4.5: Impression of the field test (left) and impression of the 3D model (right)

Simulation Procedure:

- Design an accurate representation of the installation including the PV modules and all the obstruction elements (fig 4.5).
- In SketchUp the option is provided of exporting model elements x, y, z coordinates using the point cloud extraction function. This is done by selecting the cells and obstruction elements.
- A Python script is developed to virtually re-create the shading surfaces by using the x, y, z coordinates of the cells and the obstruction elements. Given the azimuth and altitude of the sun which is modeled depending on the location [10] at any particular time, simple trigonometric relationships can determine the relative X and Y offset co-ordinates of shadow points on a flat or inclined plane. Constructing the shadow of a complex 3D object is simply a process of translating each of its vertexes in turn to produce an outline on the ground or at a plane. The output of the model is a look up table with the shading fraction of the cells for any given azimuth and elevation angle of the sun. As a result, these look up tables can be used for various locations.

The shading fraction of each cell in the system is calculated with 0.5 degrees interval of the sun's azimuth and elevation angle. For higher accuracy the look up tables can be constructed with a range of azimuth and elevation intervals with an unavoidable consequence in simulation time. In figure 4.6 a graphic representation of a part of the look up table can be seen. Specifically the shadow extension of a pole situated at the south part of the system for three different times of the day is visible. Subsequently the heaviest shaded solar cell of a substring is determined and is used as an input for the next part of the simulation

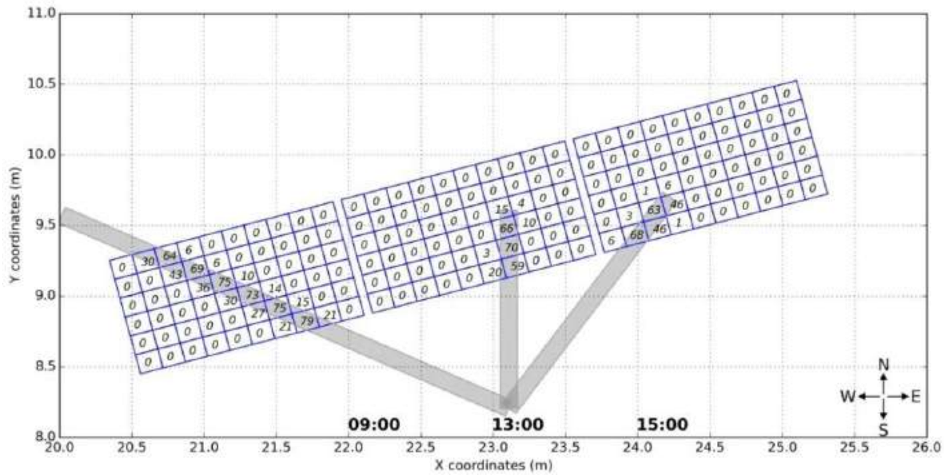

Figure 4.6: Graphic representation of the look up table for specific time and date produced by the shading model

4.2.2 Irradiance model for determination of direct and diffuse light components

After the determination of the shaded fraction of the cell, the diffuse and direct part of the irradiance has to be calculated with an irradiance decomposition model. A comparative review of the various irradiance models and their empirical validation has been presented by Loutzenhiser [11].

For this paper the Reindl 2 model [12] was chosen to estimate the diffuse part of irradiance using as input the clearness index, the global in-plane irradiance and the elevation angle of the sun.

For $0 \leq k_t \leq 0.3$ and $\frac{G_d}{G} \leq 1.0$:

$$\frac{G_d}{G} = 1.02 - 0.254k_t + 0.0123\sin(a) \tag{2}$$

For $0.3 < k_t < 0.78$ and $0.1 \leq \frac{G_d}{G} \leq 0.97$:

$$\frac{G_d}{G} = 1.4 - 1.749k_t + 0.177\sin(a) \tag{3}$$

For $k_t \geq 0.78$ and $\frac{G_d}{G} \geq 0.1$:

$$\frac{G_d}{G} = 0.486k_t - 0.182\sin(a) \tag{4}$$

where:

- G, G_d are the global irradiance and the diffuse part of the irradiance respectively
- k_t is the clearness index
- a is the elevation angle of the sun

4.2.3 PV cell Model

A mono-crystalline cell can be modeled with the equivalent electric circuit of a simplified double diode model developed by Ishaque [13] and shown in figure 4.7.

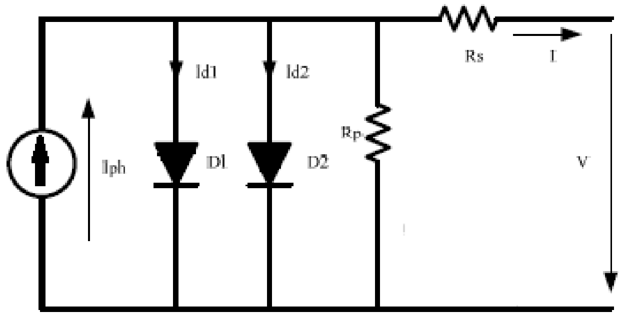

Figure 4.7: Double diode equivalent circuit for a PV cell

The output current of the cell is given by the following equations [14]:

$$I = I_{ph} - I_{D1} - I_{D2} - \left(\frac{V + IR_s}{R_{sh}}\right) \quad (5)$$

with: $I_{D1} = I_{o1}\left[\exp\left(\frac{V+IR_s}{n_1 V_{th}}\right) - 1\right]$ (6)

and $I_{D2} = I_{o2}\left[\exp\left(\frac{V+IR_s}{n_2 V_{th}}\right) - 1\right]$ (7)

$$V_{th} = N_s \frac{kT}{q} \quad (8)$$

where:

- I_{o1}, I_{o2} are the reverse saturation currents of the diodes D_1 and D_2 respectively
- V_{th} is the thermal voltage of the diodes
- n_1, n_2 are their quality factors of the diodes
- R_s, R_{sh} are the series and shunt resistances respectively
- k is the Boltzmann constant
- q is the electron charge
- N_s is the number of cells connected in series
- T is the module temperature

$$I_{ph} = \frac{G}{G_{STC}} I_{ph_{STC}} (1 + K_I \Delta T) \quad (9)$$

where:

- G is the irradiance
- G_{STC} the irradiance under Standard Test Conditions (1000 $\frac{W}{m^2}$)
- $\Delta T = T_c - T_{ref}$ the temperature difference between the solar cell's temperature and the reference temperature (25◦C)

In many papers, researchers are trying to calculate separately the saturation currents of the two diodes in the double-diode cell model, but this procedure is time consuming as it greatly increases the computational time by using an iteration approach [15]. For simplicity reasons, we assume that $I_{o1} = I_{o2} = I_o$ as shown in [13] where the saturation current can be calculated using the equation below. This assumption eliminates the ambiguity of selecting the values n_1 and n_2 as well.

Thus, with some approximations and using the equations presented above, the saturation current can be calculated [16]:

$$I_o = \frac{\frac{I_{sc}(R_s + R_{sh}) - V_{oc}}{R_{sh}}}{\exp\left(\frac{V_{oc}}{n_1 V_{th}}\right) + \exp\left(\frac{V_{oc}}{n_2 V_{th}}\right)} \quad (10)$$

The saturation current increases with temperature as shown by the equation given below [13]:

$$I_o = I_{o_{STC}} \left(\frac{T}{T_{ref}}\right)^3 \exp\left(\frac{q}{N_1 k}\left(\frac{E_g}{T_{ref}} - \frac{E_g(T)}{T}\right)\right) \tag{11}$$

where:

- E_g is the energy band gap of the semiconductor (1.12eV for silicon)
- $T_{ref} = 25$°C and $I_{o_{STC}}$ is the nominal saturation current at STC

The simulated I-V and P-V curves with different irradiance inputs for the whole module are shown in figure 10a. In figure 10b the I-V and P-V curves for inhomogeneous irradiance levels between the cell substrings are shown.

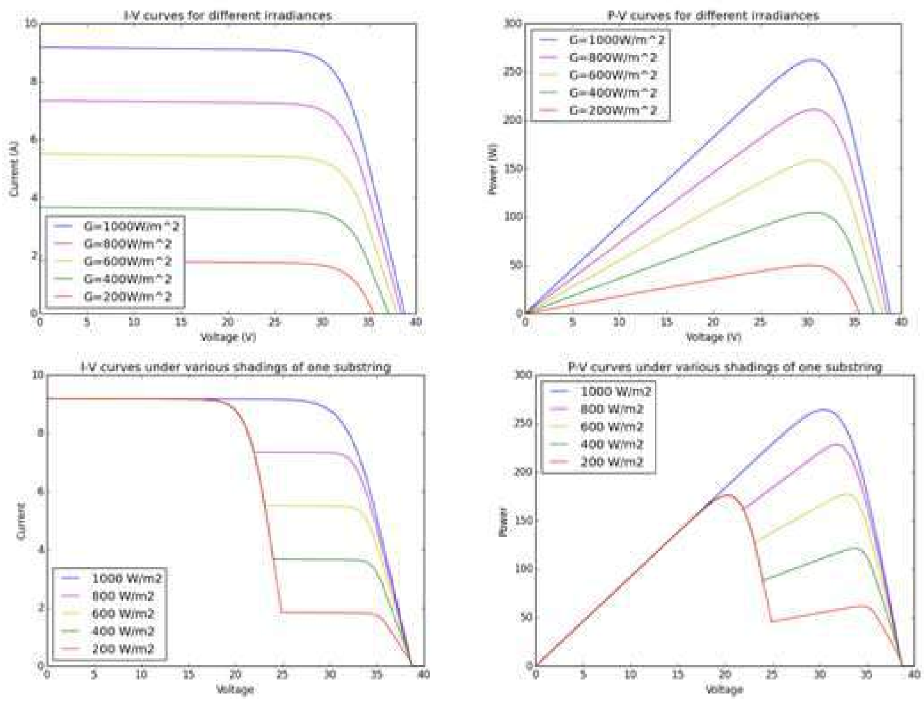

Figure 4.8: Simulated I-V and P-V curves for the solar module for homogeneous (a) and inhomogeneous irradiance levels (b)

By using equation 1 to calculate irradiance input for the solar cell model, a look up table with I-V curves per substring has been created for all possible irradiance and module temperature combinations (1-1500 W/m2 and from 0 – 100 ◦C with 1 W/m2 and 1 ◦C intervals). This way instead of running the script for the PV module which contains complex equations and iterations, the ready-made I-V curves corresponding to the given conditions are called from the look up table in order to build-up the PV module's I-V curve, using the 3 relative I-V curves of the 3 substrings.

5.2.4 MPPT and Power Conversion Model (DC/AC)

Nearly all modern inverters have more than 99% MPPT efficiency. While Perturb and Observe (P&O) is the most used algorithm new hybrid algorithms have been implemented by inverter manufacturers to boost performance at partial shading conditions [17-18]. This is achieved by frequent scans of the P-V curve of the solar modules which ensure that the inverter will detect the MPP even in the case of lumpy P-V curves. In this study the MLPE devices are using the hybrid P&0 algorithm while the string inverter system has the option to activate it. Note that the string inverter is delivered from the manufacturer with the shadow mode deactivated. The model assumes that the

MPP of the solar modules is always found and kept when the hybrid algorithm is used, however the string inverter is modeled with the hypothesis that when the shadow mode is deactivated the solar modules are operated at a local maximum when partial shading is present.
In order to develop the conversion model, real measured data where used [19]. In figure 4.9 the relation of the conversion losses with the current and voltage input can be seen for the string inverter system. By using second degree polynomial fit the loss curves can be calculated based on different voltage and current levels.

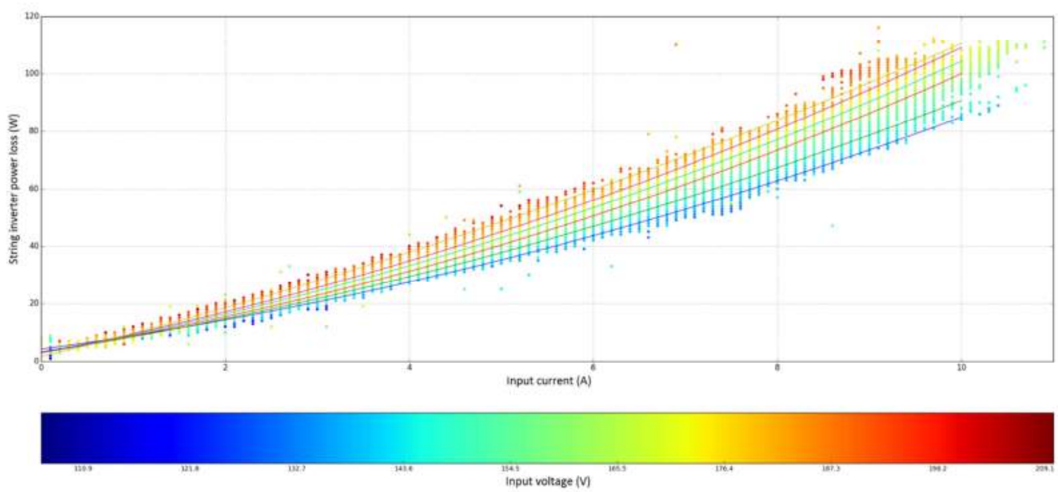

Figure 4.9: Polynomial fit for the power losses of the string inverter for various voltage inputs
The equations of these polynomial fits that were used in the model, along with their conditions are presented below:
For $100 \leq V \leq 145$: $y = 0.3772x^2 + 4.295x + 4.263$
For $145 < V \leq 155$: $y = 0.3668x^2 + 5.096x + 3.068$
For $155 < V \leq 165$: $y = 0.4488x^2 + 5.173x + 3.302$
For $165 < V \leq 175$: $y = 0.4325x^2 + 5.802x + 3.013$
For $175 < V \leq 190$: $y = 0.4419x^2 + 6.189x + 2.945$
For $190 < V \leq 230$: $y = 0.304x^2 + 7.843x + 1.618$

Similar for the power optimizer and micro inverter system polynomial equations based on different voltage inputs have been calculated and used for the simulations. In figure 4.10 the polynomial equations are used to predict the AC yield. The DC measured data from the field test were used as an input to solve the polynomial equations for the micro inverter system. Deviation from measured and simulation were about 0.1% for the unshaded micro inverter while 1% is observed for the shaded micro inverter.

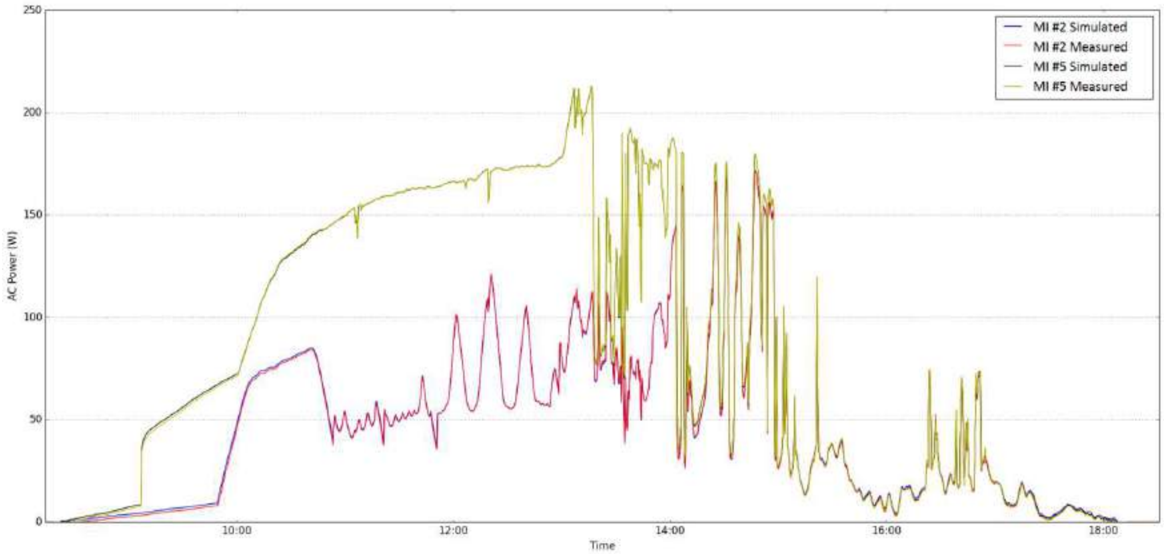

Figure 4.10: Validation of the DC-AC fitting equations for two micro inverters operating with (Heliox 2) and without (Heliox 5) partial shading using real measured and simulated data

5. 3 Model validation by using real measured data

For the validation of the proposed yield model, measurements from 3 systems in Eindhoven [19] are used. The systems are oriented south-east with an inclination angle of 30 degrees. The systems architecture consists of a string inverter system, a power optimizer system and a micro inverter system, all with the same installed power (1.6 KWp). The electrical parameters are continuously monitored before and after every stage of power conversion including in plane global irradiance and module temperatures. For the model validation the measured irradiance from the field test has been used as input after having been decomposed in diffuse and direct components [20]. Moreover, module temperatures have been used by the measured data.

For obstruction shading, three shading scenarios that usually occur in pitched and flat roofs have been defined:

- Pole shading: a pole with 1 m 70 cm height has been positioned on the south side of the systems.
- Row to row shading: A wall situated on the south side of the systems (fig.5.5), homogenously shades all three systems during winter months. Additionally because of the module spacing there is row to row shading.
- Soiling: In central and north European climate, rain is abundant. It is a fact that framed solar modules could build up algae at the bottom part and thus obstruct completely irradiance. The more time the algae remains, the more it builds up. In the scenario investigated at this paper the algae covers 2cm of the bottom of the solar cells.

In figure 4.11 the irradiance, the measured and simulated AC power of the three systems can be seen for a clear day without any shading elements. The simulation measurements follow the measured data with high accuracy except early morning and late evening hours when the irradiance sensor and parts of the PV modules are covered from shade from neighboring buildings. While the system's daily yield is very close for all three systems, the micro inverter seems to outperform the power optimizer and string inverter system by 4.3% and 2.3% respectively. Deviation between measured and simulated daily yield lies below 1% for the power optimizer and micro inverter while it reaches almost 2% for the string inverter system. This occurs partially due to the unavoidable shading late in the evening and because of the increased mismatch losses at high irradiances. When shading is not present hence the mismatch losses are low, the performance of the systems highly depends on the converting efficiency of the power electronics. This issue has been discussed before [19] and results showed that the converting efficiency of the string inverter especially in low power is superior to the MLPE devices examined in this work.

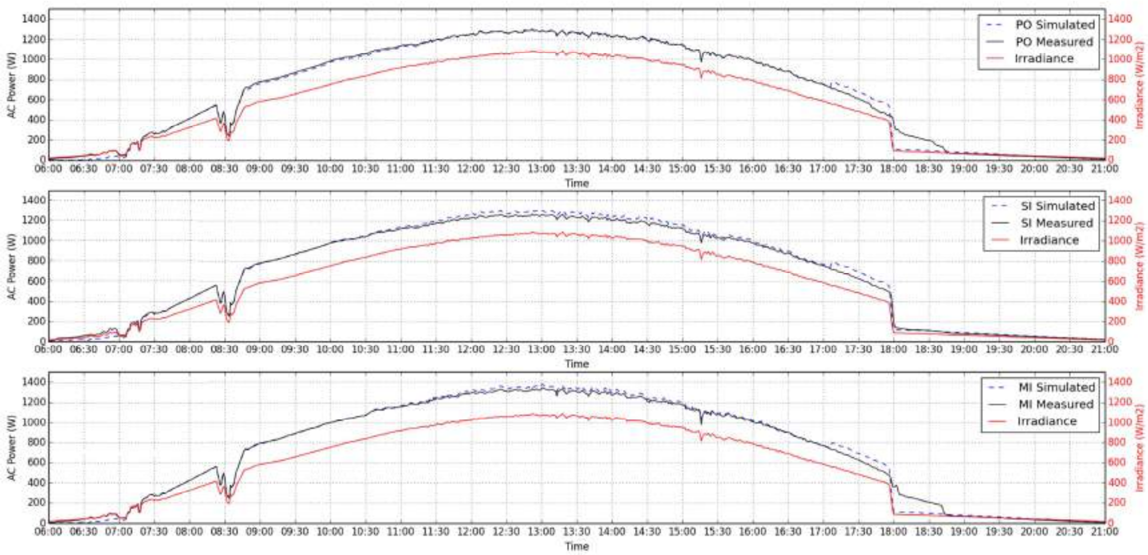

Figure 4.11: Irradiance, measured and simulated AC output of the three systems for a clear day

In figure 4.12 partial shading by a pole has been introduced for the three systems. The simulated and measured AC outputs seem to overlap for the most part of the day. The micro inverter and power optimizer systems outperform the string inverter system both in the measured and simulated daily yield data by 7-9 %. Small variations occur from the measured data due to the shading fraction detection from the 3D model and the MPP tracker. Specifically for the string inverter system, it is visible how the MPPT is losing the global maximum 3 times during the day and thus reducing the system yield. The detection of this behavior from the simulation model is not possible due to the fact that the tracking algorithm is not known. Measured and simulated daily yield has a deviation of 2.5-3.5% for the MLPE and around 6% for the string inverter system.

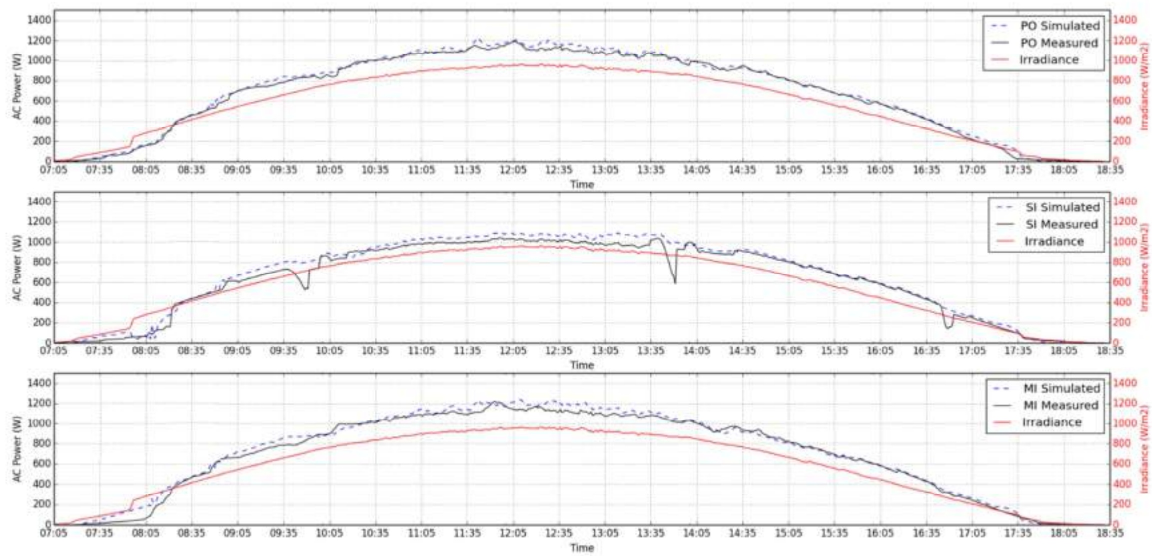

Figure 4.12: Irradiance, measured and simulated AC power for partial shading by a pole

In figure 4.13 the AC output and irradiance during a clear winter day can be seen. During winter months row to row shading is present due to the wall situated at the south of the systems and because of the distance between the two rows of modules. The systems are gradually free of shade with the power optimizer performing better due to the fact that it can detect the global MPP even at low voltage inputs (up to 8V). The string inverter system cannot detect the MPP when the voltage input becomes less that 110-120V and thus operates the PV modules at a local maxima. Therefor the MLPE retrieve 10-11% more energy yield for this specific day. Deviation of simulated and measured data range from 0.5 to 2.5% for the MLPE and around 4% for the string inverter system.

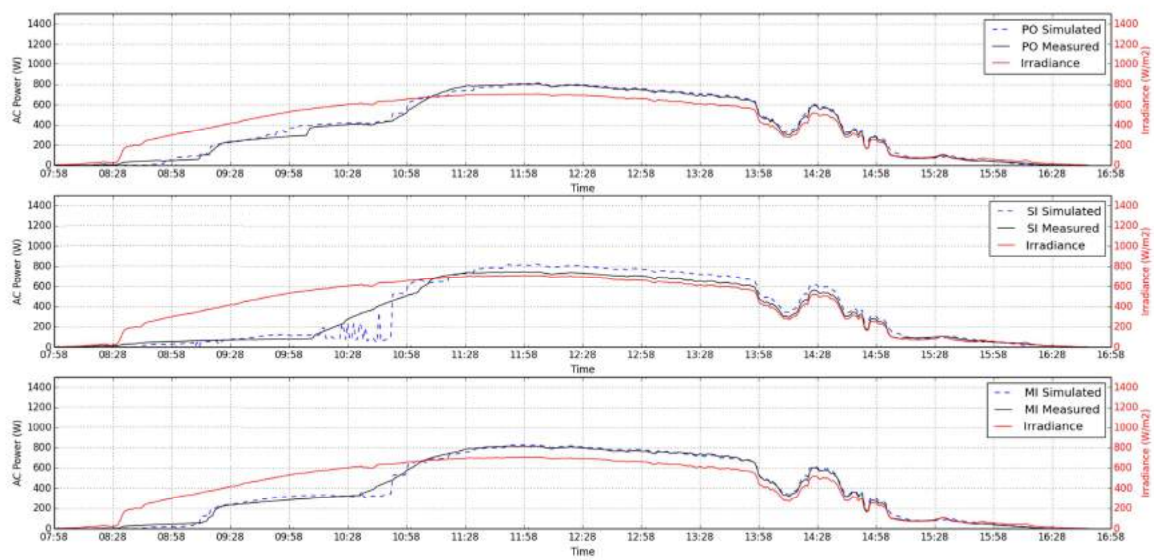

Figure 4.13: Irradiance, measured and simulated AC power for row to row shading

5.4 Simulations of monthly and annual yield for various locations and shade scenarios

By using typical meteorological year**'s** irradiation data by Meteonorm [21], a full year simulation for unshaded and partially shaded scenarios has been performed. Meteonorm provides measured irradiance data for a variety of locations. Moreover, the data can be decomposed and trans-positioned by using known irradiance models. A constant albedo factor of 0.15 has been used for the simulations. In figure 4.14 the monthly simulated losses associated with pole shading can be seen. In this scenario the unshaded yield of the systems serves as reference for the comparison.

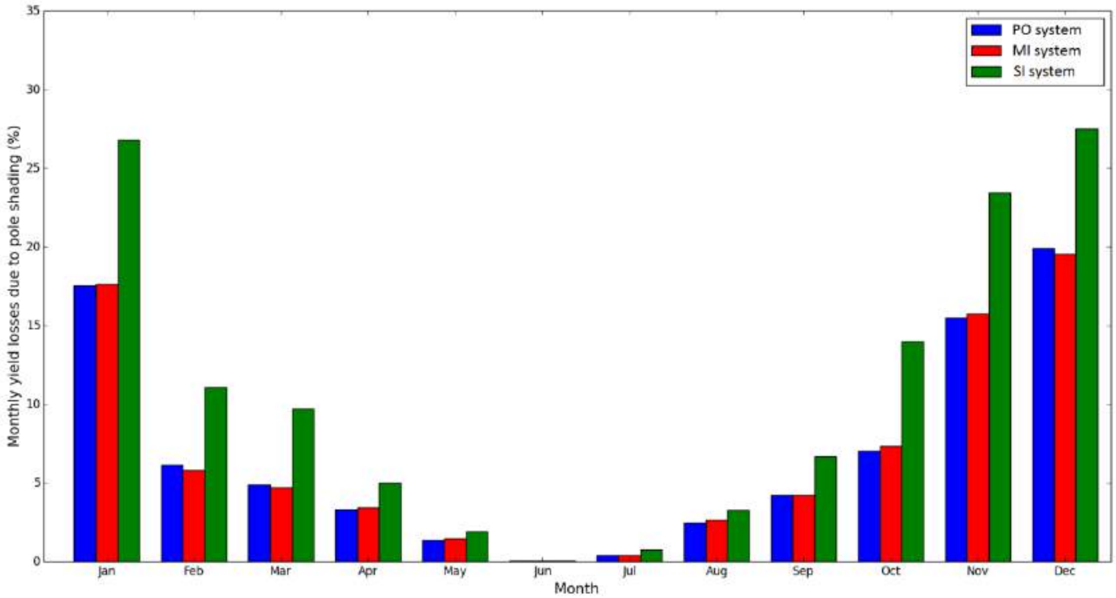

Figure 4.14: Simulated monthly yield losses for the three systems when shaded by a pole

During months when shade extension is long due to the low elevation angle of the sun, MLPE systems retrieve significantly more energy , while on summer months where the sun elevation is high the shade impact is much less for all three systems. Monthly energy losses show that there is a strong seasonal variation of yield but on a yearly basis the differences from unshaded to pole shading are around 4% for the MLPE systems and 6.6% for the string inverter system for Eindhoven (fig 4.15).

In figure 4.15 the AC yield for all shading scenarios and systems can be seen. In the unshaded scenario the string inverter seems to outperform the MLPE systems. This is due to higher operation efficiency of the string inverter system. Surprisingly the string inverter system outperforms MLPE systems at the soiling and row to row shading scenario while the micro inverter system outperforms the rest at the pole shading scenario. While differences of up to 11% on a daily basis have been measured between MLPE and string inverters, on a yearly basis shade impact is modest and especially for central and north European climate which is dominated by low irradiance levels during winter months. However the contribution of summer months in the annual yield has a larger impact than in winter months. As a rule of thumb, system designers and installers evaluate shade extensions and patterns for winter months and avoid installing modules in shade problematic areas. It seems that this approach is very conservative taking into account the results from this study and the current module prices.

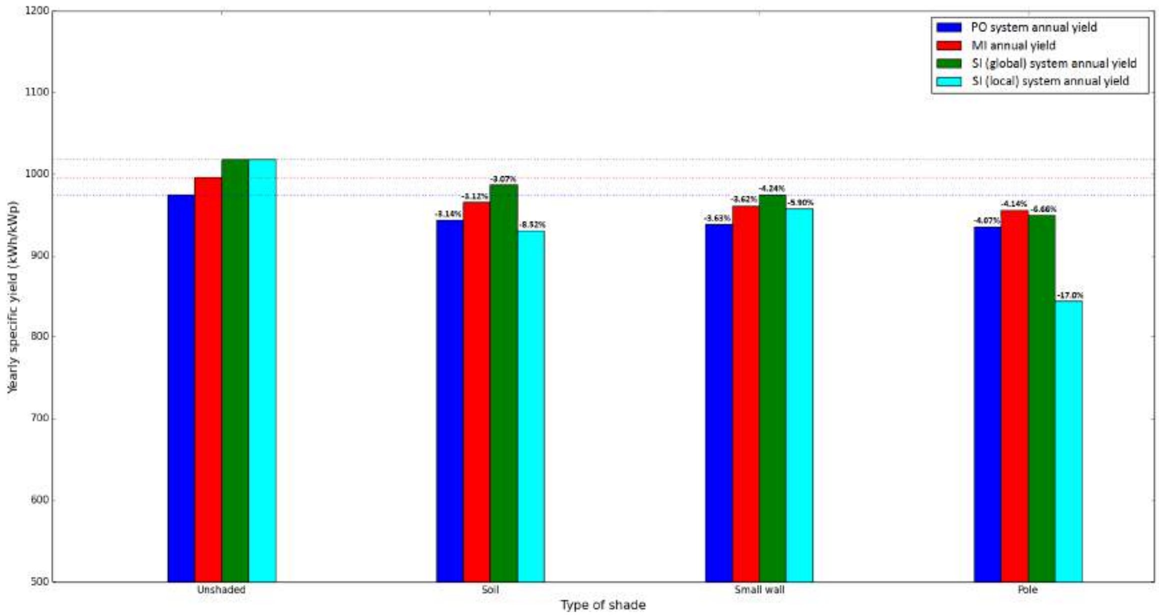

Figure 4.15: Annual yield simulations for three system architectures under three shading scenarios

Simulations with different irradiation profiles give us further insight on the benefit of MLPE when partial shading is present (fig 4.16). Results indicate that the higher the irradiance, the higher the benefit of MLPE systems. MLPE systems are based on a “pay more get more” philosophy. This means that the increased purchase price of MLPE systems should offer more annual yield and thus accelerate the payback period. Therefor potential investors should evaluate the benefit of MLPE system or string inverter system and determine the financial feasibility of such systems.

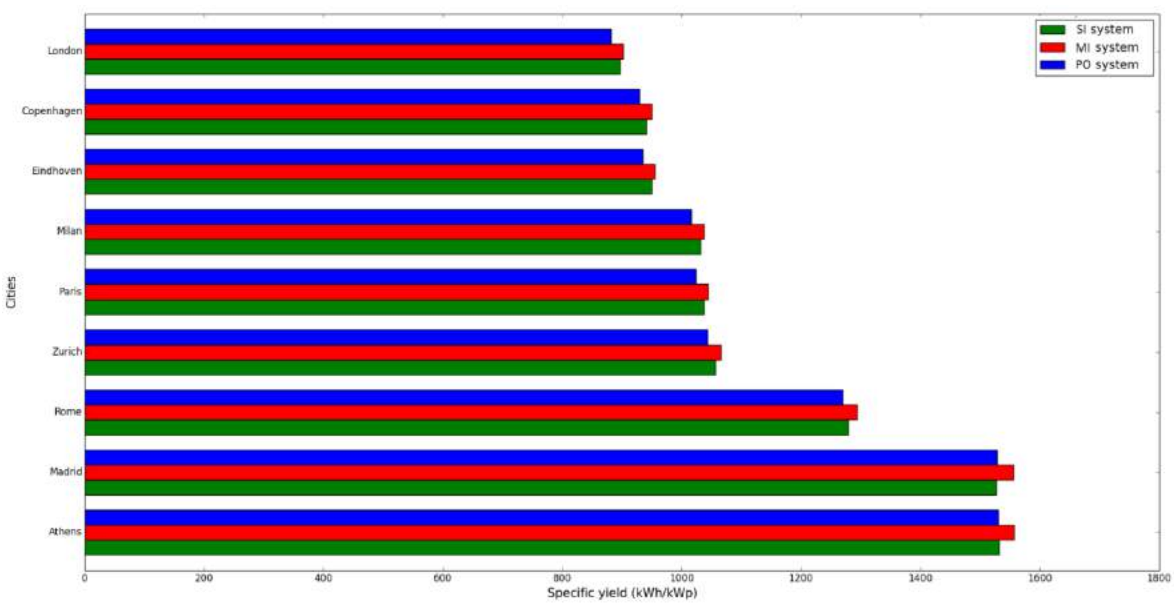

Figure 4.16: Annual yield simulations for major European cities with different irradiance profiles under partial shading

Chapter 5: Techno-Financial Model

5.1 Introduction

This chapter investigates the economic feasibility of the MLPM PV system solutions.

The economic feasibility of a PV system is determined by many external and internal factors. External factors such as net metering regulations, electricity prices, value added tax rates but also the amount of irradiation in a certain area. Internal factors that play a role are the investment cost of PV system, the installation cost, operation and maintenance cost, economic lifetime of a system and installed amount of power. Here the PV system includes all the hardware such as the PV panels, inverter/MPLM, cabling and installation. The choice of hardware has a significant impact on the annual yield of a PV system. In this chapter we focus the economic feasibility of different inverter/ MLPM system topologies under various shading scenarios. The results of the analysis can be used to determine which solution is economically favorable in which shading scenario.

In order to investigate the economic feasibility a techno-financial model has been developed. The techno-financial model includes multiple technical input parameters such as the PV system size, economic lifetime and annual yield combined with financial input such investment cost, electricity prices, inflation level and net metering policy. It determines the net present value (NPV) and the discounted payback period of a complete PV system from an end-user perspective over a pre-defined economic lifetime. The model was used in two distinct modes: a *static* techno-financial analysis for a fixed set of input variables and a *dynamic* techno-financial analysis for a multivariate range of input variables (Monte Carlo method).

Overall, we found that the most influential factors on the net present value (NPV) of the system were the discount rate and the electricity price change, which together accounted for 80% of the NPV variation. The range in investment costs of inverter/MLPM solutions led to NPV differences of up to 16%, although the most important factor here was the inverter/MLPM brand rather than the inverter/MLPM technology. The impact of shading scenarios led to differences in the NPV of up to 5%. The different lifetime/replacement period led to an effect on the NPV of up to 2%. We conclude that the different Inverter/MLPM technology solutions have very similar economic feasibility and the technology is not the most decisive success factor 6.2 The techno financial model

5.2 The techno-financial model

5.2.1 Purpose of the model

The techno-financial model is used to connect specific technologies to key performance indicators. It serves as a tool to evaluate the effects of new and existing solar energy products on economic and technical performance.

The model is used for both *static* and *dynamic* analysis. In the static techno-financial analysis all input parameters have fixed values what results in fixed outcome parameters. This method is simple and easy to apply. It results in a clear overview about which inverter/MLPM solution is most profitable. However, this method has a few pitfalls. The most important one is that it ignores uncertainty. Uncertainty is inseparably related to forecasting. Determining the profitability of a PV system over 25 years involves making assumptions, assumptions which are not certain. To deal with this uncertainty, we incorporated multivariate statistics using a Monte Carlo method. This is hereafter referred to as dynamic techno-financial analysis.

5.2.2 Design of the model

The techno-financial model consists of three main parts. One part holds input that includes technical, financial and a customized scenario input. The second part holds calculations that produce financial outcomes. The last part is the output, which are derived from the calculations and are forecast parameters. Figure 5.1 provides an overview of all the main parameters that are discussed in the model at section 5.3 Building blocks of the model.

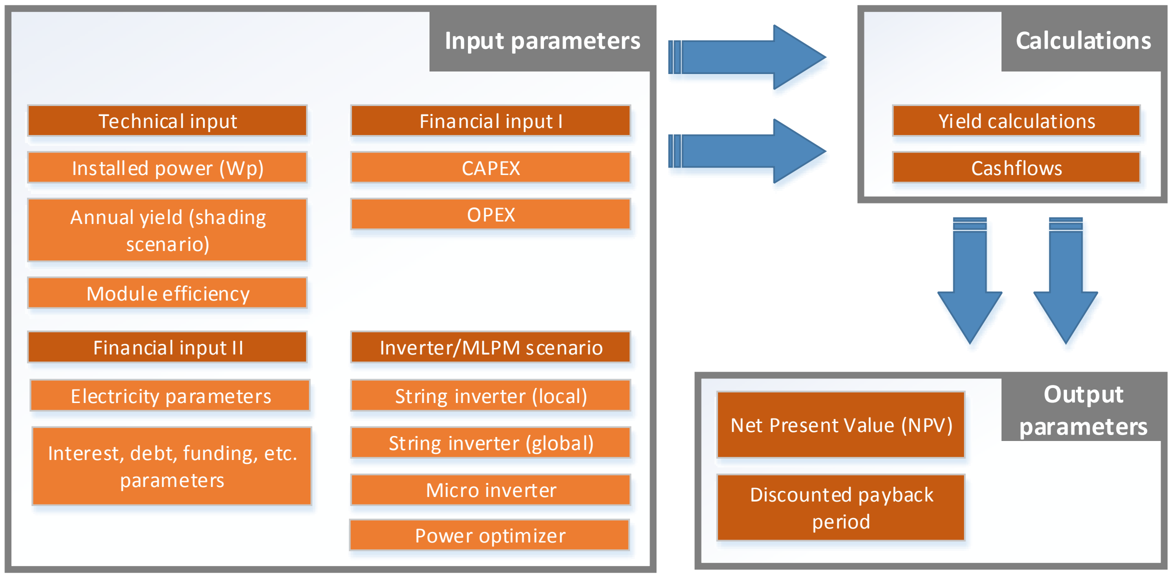

Figure 5.1: Comprehensive overview of the techno-financial model

6.2.3 Definition of the input parameters

Installed power refers to a certain PV system size in kWp.

Annual yield refers to the expected kilowatt-hours per kilowatt-peak installed per year.

Module Degradation refers to the degradation of the PV system and is expressed in %/a of yield loss.

CAPEX (capital expenses) refers to the investment costs for the PV system. In our analysis it is split up in three parts: *Investment cost PV system* for the PV panels and fastening system that are the same for all scenarios, *Investment cost of inverter* that change for each inverter/MLPM scenario and *Installation cost* for the man-hours required for installing the PV panels, fastening system on the roof and electrical equipment.

OPEX (operational expenses) refers to the costs for keeping the PV system in operation. They include *O&M costs* which will annually increase by the *Price inflation*, and *Inverter replacement costs* which refers to the replacement of the inverter after its technical lifetime. In order to calculate the Inverter replacement costs, we assume a certain *Inverter lifetime* and *Inverter price deflation*.

Weighted Average Value of Electricity refers to the value that the generated electricity has. It is calculated from a weighted average of the *feed-in tariff* for electricity fed into the grid and *electricity price* for the self-consumed electricity. Furthermore, it is influenced by the *Electricity value change* which refers to the annual change in the value of electricity. The change is expressed in %/a (annual) and can be chosen differently from the more general *Price inflation*. For full net metering, which is the case for the Dutch residential PV systems sector, the weighed value of electricity equals the electricity price.

The discount rate refers to the percentage by which future cash flows are annually lowered in the cash flow analysis. It is made up of the cost of the investment capital plus a highly situational and sector-specific 'risk percentage'. For consumers investing in a residential PV system the discount rate can be understood as follows. The cost of capital for a consumer equals the interest rate on the bank savings account. However, the PV system should preferably return a bit more than that as incentive for all the organizational burden and financial risks involved in having a PV system on the roof.

5.2.4 Definition of the output parameters

Net Present Value (NPV) is a measure of the PV system's profitability. All future cash flows are calculated into present value using the discount rate *r*. If NPV > 0 it is profitable to invest in the PV system, if NPV < 0 it is not profitable to invest in the PV system.

$$NPV = \sum_{t=0}^{N} \frac{\text{income} - \text{costs}}{(1+r)^t}$$

Discounted payback time is a measure for the time it takes before the break-even point is reached and the investment has earned itself back. The discounted payback time is defined as *N* for which NPV = 0 in the equation above.

Levelised Cost of Electricity (LCOE) is a measure for the cost of the electricity produced by the PV system. It is defined as the weighted average value of electricity for which NPV = 0.

5.3 Simulation settings

6.3.1 Scenario definition

The MLPM scenario is the core of the research question being answered. It refers to the choice of the system topology, each with its own set of input parameters:

- String inverter local mpp tracking (Mastervolt with shadow mode off). This is the historical scenario used in most of the PV systems built before 2010 or so. These string inverters use the conventional 'perturb and observe' algorithm also known as the 'Fraunhofer algorithm'. In this algorithm, the voltage is changed by 2 V every second, and the best of the two datapoints is taken as starting point for the next second. Because steps of only 2 V are taken, this method has the danger of getting stuck in a 'local maximum'.
- String inverter global mpp tracking (Mastervolt with shadow mode on). The recent generation of string inverters is equipped with a global mpp tracking algorithm. When the shadow mode is switched on, the string inverter still employs the perturb and observe algorithm to keep track of the local maximum, but in addition to that performs a broader voltage scan every 10 minutes. The advantage of this method is that it enables bypassing of shaded substrings, limiting the effect of partial shading on the annual yield. The danger of this method is that some solar energy might get lost while performing the voltage scans, although in our case this is estimated to be less than 1 kWh per year.
- Micro inverter (Heliox). A small inverter that is placed outdoors on the mounting rack next to the module. Each panel has its own mpp tracker so even shaded modules do not need to be bypassed and still produce energy.
- Power optimizer (Femtogrid). A dc/dc converter that is placed outdoors on the mounting rack next to the module. Each panel has its own mpp tracker so even shaded modules do not need to be bypassed and still produce energy. The dc/ac conversion is still being done by a string inverter.

In addition to the four MLPM scenarios, we defined four different shading scenarios, each with its own set of annual yield values depending on the MLPM scenario:

- "No shading". Here we assume that the modules are free of shade for the whole year.
- "Pole shading". Here we assume that the system is shaded by a pole-like object, such as a lamp post, chimney pipe, or TV antenna. The pole only blocks direct light and it's effect is more severe in winter than in summer months.
- "Horizon shading". Here we assume that the modules are shaded horizontally in the winter months, corresponding to the shading from a nearby building, wall or row-to-row shading in flat roof mounted PV systems.
- "Soil shading". Here we assume that the modules are to some extent polluted at the edges. We assume algae or dirt covers the first 2 centimeters of the cells around all edges of the module where it blocks all the irradiance, both direct and diffuse, all year round.

Adding both MLPM & shading scenario we end up in a 4x4 matrix of scenarios, each with its own set of input parameters. The exact input values per scenario are given in tables 2-6.

6.3.2 PV System definition

In the analysis, we created a PV system that is equally sized for all the inverter/MLPM solutions. The reference system is based on a typical sized PV system applied to the roof of a Dutch terraced house. The size of the PV system is 3180 Wp. The panels are facing south with an inclination angle of 30°. The costs of the PV system are based on the price benchmark report from SEAC published in January 2015 [1]. Excluded here are the costs for the inverter and cabling because this hardware depends on the type of inverter/MLPM solution. Due to the choice for a residential house, all produced electricity can be net-metered at the retail electricity price. Furthermore, due to the European verdict case C-219/12 all European PV system owners can reclaim a system type dependent part of the VAT on their PV system. In the case of a rooftop PV system, the full VAT can be reclaimed, corresponding to 21% of the total PV system price. However, the VAT reclamation can only take place at the initial investment, not at inverter replacements in a later stage..

6.3.3 Input values for the static techno financial analysis

The input values as used in the static techno-financial analysis are given in Table 1 below.

Table 5.1: Input values used in the static techno-financial analysis.

Quantity	Value	Source
Installed power	3.18 kWp	Section 7.3.2
Annual yield	See table 2	Chapter 6
Module Degradation	0.5%/a	[2]
CAPEX: Investment of PV system	€ 950 per kWp excl. VAT	[1]
CAPEX: Investment cost of inverter	See tables 4-6	Own research
CAPEX: Installation costs	€ 268 per kWp excl. VAT	[1]
OPEX: O&M	0.25% of the CAPEX	
OPEX: Price inflation	2%	CBS
OPEX: Inverter replacement costs	Price deflation of 2%/a See tables 4-6	[8]
Weighted Average Value of Electricity	0.23 €/kWh at current, annual increase 2.8%/a	[5] [6]
Economic lifetime N	25 years	[3], [4]
Discount rate r	2.5%	

The annual yield was taken from the chapter 6 of this report on MLPM modeling. The annual yield depends per MLPM & shading scenario and is given in table 5.2

Table 5.2: Annual yield varying over shadow scenario and inverter/MLPM solution.

Annual yield	no shading (kWh/kWp/a)	pole shading (kWh/kWp/a)	horizon shading (kWh/kWp/a)	soil shading (kWh/kWp/a)
Mastervolt (local tracking)	1018	845	958	931
Mastervolt (global tracking)	1018	950	975	987
Heliox	977	955	961	966
Femtogrid	975	935	939	944

Investment cost of inverter is different for each MLPM scenario. It was difficult to obtain from literature. We decided to execute an own inquiry by asking quotes at various suppliers and in some cases directly at the manufacturer. The investment cost varies strongly per inverter and brand. The average prices excl. VAT found are given in Tables 5.4-6.

The *Inverter replacement costs* also differ for each MLPM scenario. To calculate the costs we used an average price deflation of 2%/a based on scenarios by the Fraunhofer ISE Institute [8]. To estimate the technical lifetime of the inverter after which it needs replacement we first checked datasheets of commercially offered products and found that 10 years is a common guarantee period for string inverters whereas 25 years is common for Power Optimizers and Micro Inverters. As a second check we held an inquiry at technical specialists (MLPM project partners and coleagues) and asked what the expected technical lifetime of the product was. We can say that the average technical specialist is rather skeptical about the 25 years lifetime promised by power optimizer and micro inverter suppliers and expects them to last for 14-18 years only. This poses a dilemma: Which number to use? From an investor's perspective: As long as the 25 years lifetime is guaranteed by an independent financially strong institution such as an insurance company, it is safe to assume the 25 years even though in practice it might not last that long. We therefore decided to use the typically guaranteed lifetimes in the calculation.

Table 5.3: Typical guarantee periods and expected technical lifetime for string inverter, micro inverter and power optimizer products.

	Typical datasheet guarantee (years)	Expected lifetime by technical experts (years)
String inverters	10	12
Micro inverters	25	14
Power Optimizers	25	18

Table 5.4: Cost Mastervolt solution for a 3.18 kWp PV system based on a 25 year economic lifetime.

Mastervolt solution		***Year of investment***				
#	Name product	Year 0	Year 10	Year 20	*total*	*total with VAT reclamation*
3	string inverter	€ 867	€ 725	€ 607		
1	Cabling	€ 226				
	incl VAT	€ 1.093	€ 725	€ 607	€ 2.425	€ 2.235
	excl VAT	€ 903	€ 599	€ 502	€ 2.004	

Table 5.5: Cost Heliox solution for a 3.18 kWp PV system based on a 25 year economic lifetime.

Heliox solution		***Year of investment***			
#	Name product	Year 0	Year 10	Year 20	*total*
12	microinverter	€ 1.920	€ -	€ -	
12	trunk cable	€ 317			
	incl VAT	€ 2.237	€ -	€ -	€ 2.237
	excl VAT	€ 1.849	€ -	€ -	€ 1.849[27]

Table 5.6: Cost Femtogrid solution for a 3.18 kWp PV system based on a 25 year economic lifetime.

Femtogrid solution		***Year of investment***				
#	Name product	Year 0	Year 10	Year 20	*total*	*total with VAT reclamation*
3	string inverter	€ 603	€ 504	€ 422		
12	power optimizer	€ 1.188				
1	trunk cable	€ 79				
12	dropline	€ 62				
	inlc VAT	€ 1,932	€ 504	€ 422	€ 2.858	€ 2.523
	excl VAT	€ 1.597	€ 417	€ 349	€ 2.362	

5.3.4 Input values for the dynamic techno-financial model

A Monte Carlo sensitivity analysis was integrated in the techno-financial model to assess the economic feasibility of a roofing solution with variable input parameters. The results provide new insights regarding the impact of the analyzed parameters on the economic feasibility of the different inverter/MLPM systems.

The effect of the input variables is explained by the contribution to the variance in the forecast parameters. Explaining the variance is also known as a variance-based sensitivity analysis [9]. For this analysis, we started by including all the variable input parameters. After analyzing the initial results, we used only the variable input parameters that had a significant effect on the forecast parameters for the final analysis. The number of iterations for every simulation was set at 10.000, based on the confidence interval and the number of variables used in the simulation.

Where we used the shading condition in the static analysis as the scenario, we now use the technology of the inverter/MLPM system as the scenario. With this method we are able to benchmark the earlier analyzed solutions with its competitors based on price sensitivity. We can distinguish 4 different scenarios: the string inverter (local/global), the micro inverter and the power optimizer scenario. We want to investigate what the impact is of:

- The annual yield of the inverter/MLPM technology based on the shading scenario[28]
- The investment cost of the inverter/MLPM solution?
- The installation cost of the PV system[29]?

[27] For the Heliox solution the total price with the VAT reclamation is €1.849, which is initial price excluding VAT. The VAT reclamation only applies for the initial investment which is the total investment in this case.

[28] Note that we only have simulated annual yield data for the Mastervolt, Heliox and Femtogrid solution. For the competitors in this analysis we use the same annual yield data.

- The operation and maintenance cost?
- The replacement period of the inverter?
- Electricity price changes[30]?
- Deflation price inverter[6]**?**
- The discount rate?

Some of the variable input parameters are the same for all scenarios. These were included in the analysis to put the impact of the inverter/MLPM solution related parameters into perspective 5.3.2 Dynamic Techno financial analysis

5.3.4.1 String inverter sensitivity analysis

In order to get a feeling for the variance in string inverter performance, we assessed datasheets from Mastervolt, SMA and Omnik inverters. Based on the datasheets the next string inverters were selected: the Mastervolt Soladin 3000 web, the SMA sunny boy 3.0 TL-21 and the Omnik omnisol 3.0 K TL Obtained price levels were 329 - € 365 per kWp for Mastervolt, 456 - € 491 per kWp for SMA and 259 - € 314 per kWp for Omnik. Omnik inverters are not able to track the global peak, and as such will suffer a drop in kWh yield in the 'pole shading', 'horizon shading' and 'soil shading' scenarios.

Table 5.7: Annual yield (in Kwh/kWp/a) and turn-key prices of different string inverters (all prices are included VAT)

	Global tracking?	**Yield "no shading"**	**Yield "pole shading"**	**Yield "horizon shading"**	**Yield "soil shading"**	**Assumed price range**	
Mastervolt	No	1018	845	958	931	min	€ 1046
	Yes	1018	950	975	987	max	€ 1160
Omnik	No	1018	845	958	931	min	€ 825
						max	€ 998
SMA	No	1018	845	958	931	min	€ 1451
	Yes	1018	950	975	987	max	€ 1560
String inverter (local)	min		**845**	max	**1018**	**€825 - €1560**	
String inverter (global)			**950**		**1018**	**€825 - €1560**	

Furthermore, we investigated the sensitivity of the financial analysis to the lifetime of the string inverter. Inverter lifetimes are generally assumed to be 10-14 years in literature. It is very difficult to get actual field data on the real lifetime of inverters. In order to get some indication of the lifetime perception a survey was conducted among employees working at the MLPM project partners, see Table 5.3. Using the Monte Carlo method we varied the lifetime between the warranty and the lifetime perception from the survey as shown in Table 5.8. The goal for this range is to investigate the impact of the lifetime on the NPV and discounted payback period.

Table 5.8: Lifetime or Replacement period of the Inverter/MLPM system (warranty vs. expected)

Input variable	Distribution	Range (in years)	
String inverter	Uniform Distribution	10 – 12	Min – Max
Micro inverter	Uniform Distribution	14 – 25	Min – Max

[29] The range used for the installation price is based on an extensive price benchmark study conducted in the Netherlands [1]. For this report we used the Min – Max installation price.

[30] The ranges for these input parameters are already discussed in the static analyses.

Power optimizer, (string inverter)	Uniform Distribution	18 – 25	Min – Max

Table 5.9 provides an overview of the variable input parameters used in the simulation. It includes the parameters for the Mastervolt solution, both with local and global tracking. Between the two shadow modes only the annual yield varies. The ranges as discussed in the table are explained through footnotes and references.

Table 5.9: Variable input parameters for the Mastervolt (local and global) solution

Input variable	Distribution	Range	
Technical parameters			
Annual yield (depends on shading condition) – shadow mode off (local tracking)	Discrete Uniform Distribution	• no shading (1018) • pole shading (845) • horizon shading (958) • soil shading (931)	(custom)
Annual yield (depends on shading condition) – shadow mode on (global tracking)	Discrete Uniform Distribution	• no shading (1018) • pole shading (950) • horizon shading (975) • soil shading (987)	(custom)
CAPEX			
Investment costs total system, excl. inverter, cabling, installation and (excl. VAT)	Uniform Distribution	€ 884 - € 1017 per kWp	Min – Max
Investment cost string inverter (incl. cabling)	Custom Uniform Distribution	Omnik (€ 259 - € 314 per kWp) Mastervolt (€329 - € 365 per kWp) SMA (€ 456 - € 491 per kWp)	Min-Max (custom)
Installation cost, both mechanical and electrical	Uniform Distribution	€ 249 - € 287 per kWp	Min – Max
OPEX			
Operation and Maintenance (OM)	Uniform Distribution	0 - 0,5% [10]	Min – Max
Replacement inverter	Discrete Uniform Distribution	10 – 13 (in years)	Min – Max
Electricity related parameters			
Electricity price change	Normal Distribution	2,8% (plus) (van de Water, 2014)	Std.Dev. 0,5
Additional economic and financial parameters			
Monetary inflation	Normal Distribution	1,76%	Std.Dev. 0,5

The discount rate	Uniform Distribution	2,5% - 5%[31]	Min – Max

6.3.4.2 Micro inverter sensitivity analysis

In order to get a feeling for the variance in cost price and kWh yield for micro inverters, we analyzed the datasheets from Heliox and Enphase. Based on the datasheets the next micro inverters were selected: the Heliox SMI 300 and the Enphase M215. Cost levels obtained were €661-€802 Eur/kWp for Heliox and €508-€570 Eur/kWp for Enphase.

Table 5.10 and Table 5.11 provide an overview of the yield under different shading conditions and the variable input parameters used in the simulation. The ranges as discussed in the table are explained through footnotes and references.

Table 5.10: Annual yield and turn-key prices of different micro inverters (all prices are included VAT)

	Yield shading”	“noYield shading”	“poleYield “horizon shading”	Yield shading”	“soilAssumed price range
Heliox	997	955	961	966	Heliox Min € 2102 Max € 2549 EnphaseMin € 1614 Max € 1812
Micro inverter	min	**955**	Max	**997**	**€1614 - €2549**

Table 5.11: Variable input parameters for the Heliox and Enphase MLPM solution

Input variable	Distribution	Range	
Technical parameters			
Annual yield (depends on shadow condition)	Discrete Uniform Distribution	• no shading (997) • pole shading (955) • horizon shading (961) • soil shading (966)	Min-Max (custom)
CAPEX			
Investment cost MLPM micro inverter (incl. cabling)	Custom Uniform Distribution	Heliox (€ 661 - € 802 per kWp) Enphase (€508 - € 370 per kWp)	Min – Max (custom)
OPEX			
Replacement inverter	Discrete Uniform Distribution	14 – 25 (in years)	Min – Max

[31] The range of discount rate is based on the two factors. The minimum discount rate of 2,5% is the average deposit savings interest calculated over the 10 highest deposit savings rates in the Netherlands at this moment. The maximum discount rate is based on literature about individual discount rates [11].

5.3.4.3 Power optimizer sensitivity analysis

In order to get a feeling for the variance in cost price and kWh yield for micro inverters, we analyzed the datasheets from Femtogrid and Solar Edge. Based on the datasheets the next string inverters and power optimizers were selected: the Femtogrid 2400 and the PO310, and the SolarEdge Se3000 and P300. Obtained price levels were € 558 - € 720 per kWp for the Femtogrid solution and € 488 - € 550 per kWp for the SolarEdge solution.

Table 5.12 and Table 5.13 provide an overview of the yield under different shading conditions and the variable input parameters used in the simulation. The ranges as discussed in the table are explained through footnotes and references.

Table 5.12: Annual yield and turn-key prices of different power optimizers (all prices are included VAT)

	Yield "no shading"	Yield "pole shading"	Yield "horizon shading"	Yield "soil shading"	Assumed price range	
Heliox	997	955	961	966	Heliox	Min € 2102 Max € 2549
					Enphase	Min € 1614 Max € 1812
Micro inverter	min	**955**	Max	**997**	**€1614 - €2549**	

Table 5.13: Variable input parameters for the Femtogrid and Solar edge MLPM solution

Input variable	Distribution	Range	
Technical parameters			
Annual yield (depends on shading condition)	Discrete Uniform Distribution	• no shading (975) • pole shading (935) • horizon shading (939) • soil shading (944)	(custom)
CAPEX			
Investment cost string inverter (incl. cabling)	Custom Uniform Distribution	Femtogrid (€ 171 - € 257 per kWp) Solaredge (€ 314 - € 472 per kWp)	Min – Max (custom)
Investment cost MLPM power optimizer (incl. cabling)	Custom Uniform Distribution	Femtogrid (€ 284 - € 294 per kWp) Solaredge (€ 202 - € 205 per kWp)	Min – Max (custom)
OPEX			
Replacement inverter	Discrete Uniform Distribution	18 – 25 (in years) for the power optimizer 10 – 13 (in years) for the string inverter	Min – Max

** Note that a second and perhaps a third investment is required due to the technical lifetime of the string inverter.*

5.4 Results of the analysis

5.4.1 Static analysis

Using the static method, we have analyzed the three shading scenarios for the 4 inverter/MLPM solutions that were tested in this project. Figure 5.2 shows the NPV and discounted payback period of the 4 different inverter/MLPM solutions under the 'no shading' scenario. The profitability is calculated assuming the economic lifetime of the PV system is 25 years.

Analyzing the figure, we find that both Mastervolt solutions with the shadow mode on (global tracking) or off (local tracking) have the same NPV, which is (€11.975). The annual yield of the system under both modes is equal which explains the equal NPV. The Heliox micro inverter has a NPV of (€10.975) which is about 8% lower than both Mastervolt solutions. The Femtogrid solution has a NPV of (€9.906) which is about 17% lower than both Mastervolt solutions. The discounted payback period of the Mastervolt solution is 7 years where the MLPM solutions have a payback period of 9 years. This can be explained by the initial investment cost of the inverter/MLPM solution. As shown in Table 5.4 the Mastervolt inverter has the lowest investment cost in year 0. Therefore, the payback period for the initial investment is shorter.

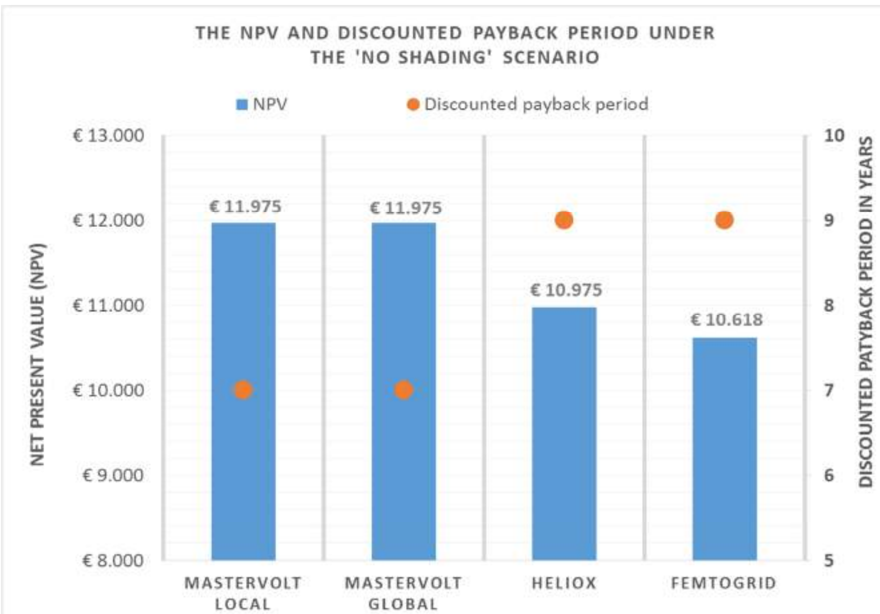

Figure 5.2: The NPV and discounted payback period under the 'no shading' scenario

Figure 5.1 shows the NPV and discounted payback period of the 4 different inverter/MLPM solutions under the pole scenario. Analyzing the figure, we find that the Mastervolt solution with global tracking has the highest NPV (€10.765). With the local tracking mode on the Mastervolt solution has a NPV of €8.869, which is about 18% lower. The Heliox micro inverter has a NPV of €10.584, which is only about 2% (€175) lower than the Mastervolt solution with global tracking. For the Femtogrid solution the difference is somewhat higher (€900) which is about 8%. The discounted payback period is 8 years for the Mastervolt global solution and 9 years for the Femtogrid solution and other Mastervolt solution. The discounted payback period for the Heliox micro inverter under the pole shading condition is 10 years. We see that the shading scenarios increase the differences in NPV between the various system designs.

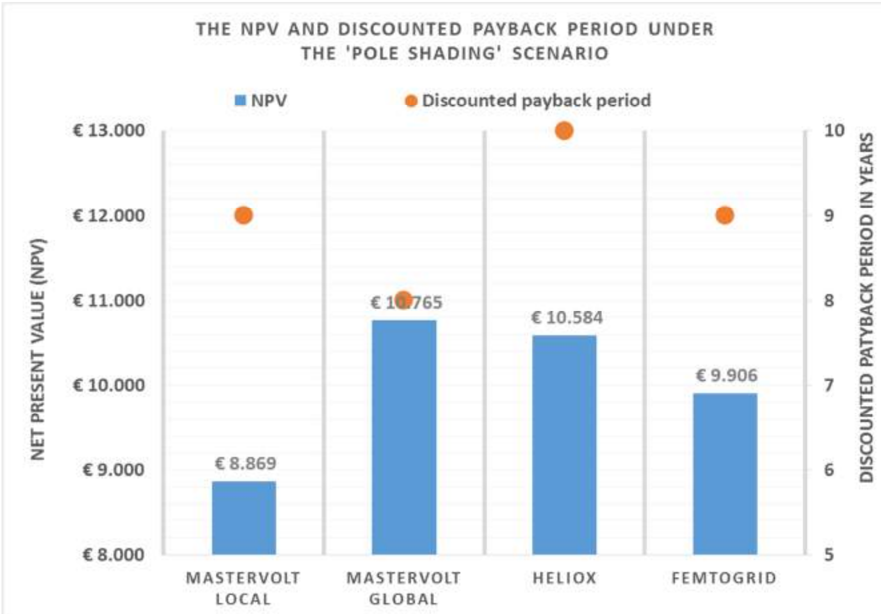

Figure 5.1: The NPV and discounted payback period under the ‘pole shading’ scenario.

Figure 5.2 shows the NPV and discounted payback period of the 4 different inverter/MLPM solutions under the horizon shading scenario. Analyzing the figure, we find that the Mastervolt solution with global tracking has the highest NPV (€11.210). The Heliox micro inverter solution has a NPV of €10.691 which is about 5% lower. The Femtogrid solution has a NPV of € 9.977 which about 11% lower. The discounted payback period is respectively 7 years for the Mastervolt solutions, 10 years for the Heliox solution and 9 for the Femtogrid solution.

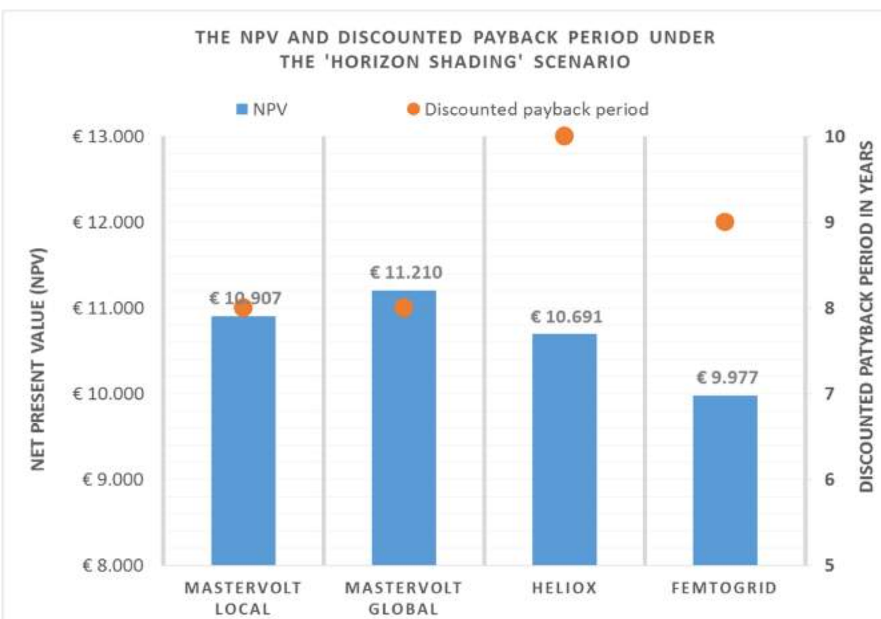

Figure 5.2: The NPV and discounted payback period under the ‘horizon shading’ scenario.

Figure 5.3 shows the NPV and discounted payback period of the 4 different inverter/MLPM solutions under the soil shading scenario. Analyzing the figure, we find that the Mastervolt Global solution has the highest NPV (€ 11.423). The Heliox solution has a NPV of € 10.780 which about 6% lower. The NPV of the Femtogrid solution is about 12% lower than the Mastervolt solution. The discounted payback period is respectively 7 years for the Mastervolt solutions, 10 years for the Heliox solution and 9 years for the Femtogrid solution.

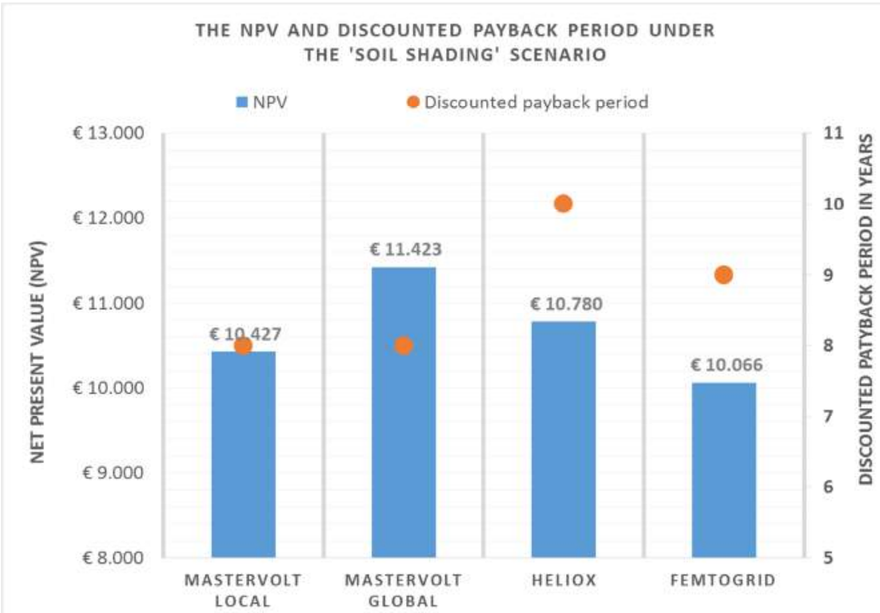

Figure 5.3: The NPV and discounted payback period under the 'soil shading' scenario.

From the static analysis we can conclude that under all shading scenarios the Mastervolt with global tracking mode on has the highest NPV. Looking to the discounted payback period, the Mastervolt global tracking solution is favored as well. Furthermore, it seems that the shading scenario does not have a big impact on the NPV in the case of the Mastervolt global tracking solution. Here the different between the shading scenarios is maximal 10%. For the Heliox and Femtogrid solution the difference is respectively 3,5% and 7%. At last, the results of the static analysis show that overall the pole shadow condition has the largest impact on the NPV and discounted payback period.

What the exact impact is of the investment cost of the inverter/MLPM solution, the replacement period and the shadow condition is not clear from this analysis. Therefore, we continue with a dynamic techno-financial analysis which makes possible to include uncertainty in the model and see what the impact is on the NPV and discounted payback period.

5.4.2 Dynamic analysis

Figure provides a comprehensive overview with the NPV and the impact of the input parameters on this NPV. Moreover, the results are presented per inverter/MLPM technology. The NPV of the string inverter (local) varies between € 4.759 and €11.668 where the average NPV is € 7.990. The range between the grey and blue dots represents the 95% confidence interval where the orange dot represents the mean. The discount rate has the largest impact and explains for 39% the NPV after 25 years. Moreover, the lower the discount rate, the higher the NPV. The shading condition determines for 29% the NPV. This can be explained due to the fairly low yearly yield of this solution in the pole shading condition (845 kWh/kWp/a). The low yield results in higher range what results in a higher impact on the NPV. Furthermore, has the electricity price change a significant impact (22%).

However, the impact of the investment in the inverter and replacement period of the inverter is minor has a significant effect (respectively 8% and 2%).

The NPV of the string inverter (global) varies between € 5.830 and € 12.077 where the average NPV is € 8.734 which is the highest among the 4 inverter/MLPM technologies. Here, the discount rate has the largest impact and explains for 55% the NPV after 25 years. Furthermore, has the electricity price change a significant impact (28%). The shading condition determines for 5% the NPV. This can be explained due to small range in annual yield between the different shading conditions (950 and 1053 kWh/kWp/a). The impact of the investment in the inverter and replacement period of the inverter is minor has a significant effect (respectively 9% and 2%).

The NPV of the micro inverter solution varies between € 5.498 and € 11.580 where the average NPV is € 8.205 which is lower than the both string inverter solutions. The discount rate has the largest impact and explains for 51% the NPV after 25 years. Furthermore, has the electricity price change a significant impact of 28%. The impact of the investment of the inverter on the NPV (16%) is higher than for the string inverter solutions this can be explained by the higher investment costs of micro inverters. The impact of the replacement period of the micro inverter and the shading condition have no significant effect on the NPV.

The NPV of the power optimizer solution varies between € 10.806 and € 4.711 where the average NPV is € 7.504 which is the lowest among the 4 inverter/MLPM technologies. The discount rate has the largest impact and explains for 51% the NPV after 25 years. Furthermore, has the electricity price change a significant impact of 29%. The investment of the string inverter and power optimizers combined explain for 14% the NPV after 25 years. Of this investment effect, 4,5% can be allocated to the investment cost of the power optimizers the other 9,5% are due to the investment cost of the string inverter. The replacement of the string inverter explains for only 1%, the NPV. Where the replacement of the power optimizers is even less than 1% and are therefore not visible in the figure. Finally, the shading scenario has no significant impact on the NPV (3%).

The most remarkable results are the small differences in the NPV among the different inverter/MLPM solutions. Overall the string inverter with global tracking is favorable, at least from the NPV perspective. The variable with the largest impact is in all cases the Discount rate. Next to the discount rate, the electricity price change has a large impact on the NPV. Together these two variables explain for about 80% the NPV after 25 years.

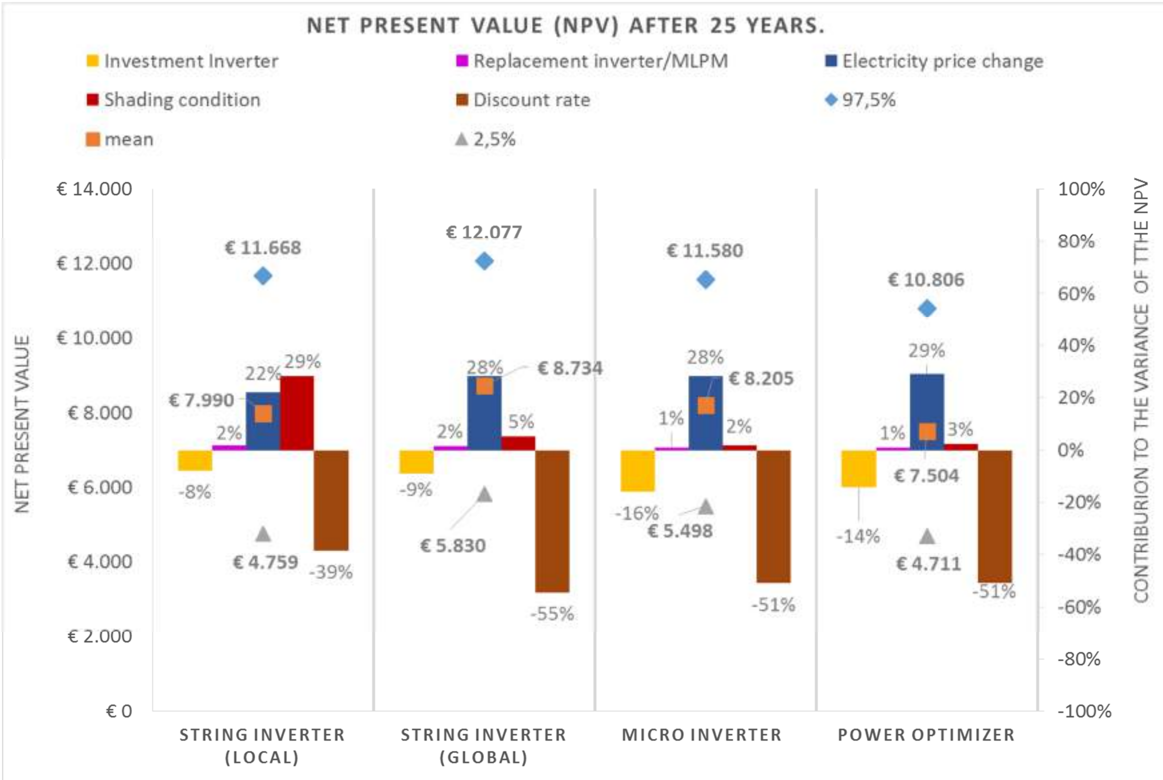

Figure 5.6: NPV after 25 years per inverter/MLPM technology.

The second outcome parameter we analyzed is the discounted payback period. Figure 5.4 reveals that the impact of the discount rate is significantly lower in comparison to the impact on the NPV. This is because the discount rate is calculated over 25 years in the case of the NPV. In the case of the discounted payback period this is between 7 and 12 years. The shading condition has a larger impact on the payback period. Furthermore, the investment of the inverter/MLPM solution has a significant effect on the discounted payback period. The payback period is within 12 years what results in no necessary additional investments in most cases due the minimum replacement period of 12 years for the inverter or MLPM system. Therefore the impact of the replacement of the inverter on the payback period can neglected. The investment for the PV modules and mounting system varies between 6% and 12% and has a significant impact here. The impact of the electricity price change varies between 5% and 8% and becomes less important when the discount rate decreases.

Based on this analysis, the string inverter (global) and the micro inverter have the most favorable discounted payback period. Between 7 and 9 years with an average payback period of 8 years. Where the string inverter with local tracking and the power optimizer solutions have an average payback period of between respectively 7 and 11 years, and 8 and 12 years. The investment of the inverter has the largest impact on the discounted payback period.

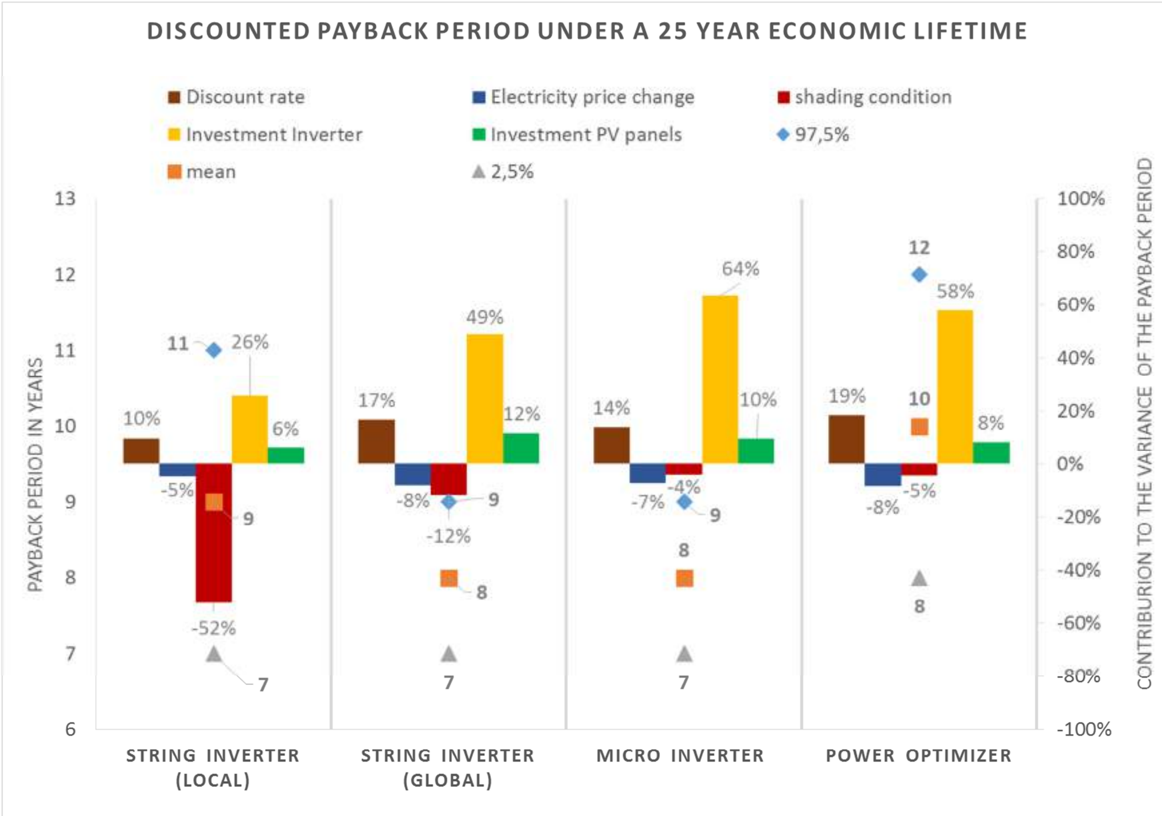

Figure 5.4: Discounted payback period per inverter/MLPM technology.

5.5 Conclusion and Discussion

We can divide the conclusion in a part focusing on the static analysis and a part focusing on the dynamic analysis. In the static analysis, we were able to directly compare the solutions of Mastervolt, Heliox and Femtogrid in financial terms. The main conclusions for the static analysis are:

- All inverter/MLPM solutions pay off financially. A typical NPV is 10.000 euro and a typical payback time 9 years. Apart from the Mastervolt inverter with local tracking, we have found a difference of about 16% between the highest and lowest NPV between all defined shading conditions.
- The presence of a pole shade in a system while using the Mastervolt inverter in local tracking mode will decrease the NPV by about 1.000 euro and will lengthen the payback time by 1 year. This is also the case for the Femtogrid solution under the horizon shading condition.
- The Mastervolt global tracking seems a very good solution to environments with partial shading. When we compare both Mastervolt configurations, the global mode always results in a higher NPV of between 200 euro in case of horizon shading and 2000 euro in case of pole shading. One has yet to be cautious with this conclusion, since the frequent bypassing of module substrings in the ‘global tracking’ mode might lead to enhanced stressing and possible failure of bypass diodes within the module. The reliability of module bypass diodes under continuous load is a topic for future research.
- In the comparison of the Mastervolt, Femtogrid and Heliox solutions, the Mastervolt with global tracking has the highest NPV after 25 years under all shading scenarios. Although the total costs for the Heliox solution is slightly lower, the performance under the different shading

conditions is lower too. An exception is the pole shading, here the Heliox micro inverter performs better than the other solutions.

- The Mastervolt solutions are favorable under all shading conditions, when the discounted payback period is key. This is due to the low initial investment costs of this solution.

In the dynamic analysis, we were able to draw more general conclusions on the comparison of micro inverter, string inverter and power optimizer technology. The main conclusions for the dynamic analysis are:

- The string inverter solution shows the highest overall financial profit. The shading scenario, investment cost inverter/MLPM and replacement period do not have a large impact on the NPV after 25 years. On average, the NPV is for about 80% determined by the electricity price and discount rate.
- The inverter/MLPM technology with the lowest NPV is the power optimizer solution. This can be explained by the high initial investment cost in combination with the replacement period of the inverter. Moreover, the relative low annual yield under the shading conditions in comparison to the other inverter/MLPM solutions plays a role.
- The technology with shortest discounted payback period is the string inverter technology. Although the difference with the other technologies is on average only one year.
- The replacement period of the inverter/MLPM system has no large impact on the payback period. The reason is that the payback period is 10 years or less and the earliest replacement period starts in year 11.
- In the case of the discounted payback period we see a larger impact of the investment cost for the string inverter (global) and micro inverter solution in comparison to the impact on the NPV. The reason is that the higher range in the initial investment in year 0 has a direct impact on the discounted payback period.
- Between de different inverter/MLPM brands, we did not find a significant impact of the replacement period of the inverter/MLPM solution on the NPV. The range of the investment costs among the different brands of a certain inverter/MLPM solution explain for between 8% and 16% the NPV after 25 years. In short, the price of an inverter does have an impact, although it is a minor one.
- If we analyze the discounted payback period, we see a large effect of the investment costs of the inverter/MLPM solution. This effect is significantly higher than that of the investment in the PV modules. The reason is the competitive pricing between different PV modules. Finally, we can conclude that the choice of inverter/MLPM brand is much more important in terms of the payback period than the choice of a certain PV module brand.

5.6 Limitations

In this study we encountered several limitations. An important limitation was the uncertainty about the replacement period of certain type of inverter. Especially for the MLPM solutions where there is no hard evidence regarding the lifetime of the system. More so because the systems simply are not long enough in operation yet.

The annual yield under the different shading conditions are based on the irradiance in the Netherlands. If shading has a larger impact in other areas in the world is not clear form this study. Moreover, has shading a larger effect on the NPV and discounted payback period in other geographical locations?

In this study we did not investigate the easiness of installment of the inverter/MLPM solutions. Micro inverters and power optimizers are attached to the panel where a string inverter often is placed in the garage or in the attic.

Finally, we limited ourselves to a 3 kWp sized residential PV system. The economic analysis will be different for commercial roofs with much larger PV capacities but also lower weighed value of electricity. A specific case of interest that is not considered in the analysis yet is a DC application such as a DC server room, as the Femtogrid solution would probably be preferable there.

Management Summary

The TKI project MLPM has generated a major boost in the knowledge position of the Netherlands on the topic of module level power management. At the same time, module level power management as an engineering solution for PV system configurations has gained more importance. The reason for this is a combination of factors: flexibility of PV system design, reduction of mismatch related yield losses, increased monitoring abilities and safety features.
The industrial and research partners in the project are now at the front line of the innovation and knowledge development in this topic. This has resulted in the launch of new products and solutions for the PV market, publications and contributions to conferences.

Heliox BV has launched a new micro inverter for the Dutch and British market. The micro inverter has been released end of 2015 and the first commercial installations have been realized. The launch of the product gained considerable attention of the International press[32].

Femtogrid BV has emerged as one of the leading DC grid solutions in the renewable energy market. After a challenging period for the company, Femtogrid now adopted a modified business strategy after the recent integration into Direct Current BV.

Mastervolt BV demonstrated that high reliability and good yield performance can be achieved by implementing a shadow mode into a string inverter mppt algorithm that can cope with many of the partially shaded scenarios of PV systems.

Solned and Proxenergy supported the other companies with their knowledge on junction box solutions and PV system data communication solutions throughout the project.

SEAC, in cooperation with HvA, investigated the system aspects of MLPM based PV system configurations. A field test was created with the highest level of accuracy and validity, resulting in a full year performance data and a new systematic approach to modelling and simulation of PV system yield under partial shading conditions.

ECN and TNO generated valuable new insights and methodologies for addressing the reliability and lifetime of mlpm components.

The project brought together five leading Dutch companies, active in PV system configuration solutions, together with the leading research institutes on the topic. Valuable knowledge was gained and shared through the project in the fields of product development, performance optimization, system monitoring, lifetime and reliability. Moreover, insights of financial aspects were gained with a static and dynamic model designed from the owner’s perspective. The project consortium exhibited excellent co-operation and professionalism despite of the turbulent times of the PV market.

[32] http://www.pv-magazine.com/news/details/beitrag/autarco-launches-made-in-europe-microinverter_100023679/